Performance of Cost-Effective Non-Proprietary UHPC in Thin-Bonded Bridge Overlays

June 2023
Final Report

Project number TR202121
MoDOT Research Report number cmr 23-011

PREPARED BY:

Kamal H. Khayat, Ph.D.

Le Teng, Ph.D.

Alfred Addai-Nimoh

Missouri University of Science and Technology

PREPARED FOR:

Missouri Department of Transportation

Construction and Materials Division, Research Section

TECHNICAL REPORT DOCUMENTATION PAGE

1. Report No.	2. Government Accession No.	3. Recipient's Catalog No.
cmr 23-011		

4. Title and Subtitle	5. Report Date
Performance of Cost-Effective Non-Proprietary UHPC in Thin-Bonded Bridge Overlays	May 2023 Published: June 2023
	6. Performing Organization Code

7. Author(s)	8. Performing Organization Report No.
Kamal H. Khayat, Ph.D., PI . http://orcid.org/0000-0003-1431-0715 Le Teng, Ph.D. Alfred Addai-Nimoh. https://orcid.org/0009-0008-4893-4247	

9. Performing Organization Name and Address	10. Work Unit No.
Department of Civil, Architectural and Environmental Engineering Missouri University of Science and Technology 1401 N. Pine St., Rolla, MO 65409	**11. Contract or Grant No.** MoDOT project # TR202121

12. Sponsoring Agency Name and Address	13. Type of Report and Period Covered
Missouri Department of Transportation (SPR-B) Construction and Materials Division P.O. Box 270 Jefferson City, MO 65102	Final Report (April 2021-May 2023) **14. Sponsoring Agency Code**

15. Supplementary Notes

Conducted in cooperation with the U.S. Department of Transportation, Federal Highway Administration. MoDOT research reports are available in the Innovation Library at https://www.modot.org/research-publications.

16. Abstract

The constructability and performance of non-proprietary thixotropic UHPC for thin bonded bridge deck overlay construction was investigated. Task 1 reviewed literature on UHPC for thin bonded overlays and non-proprietary UHPC. Crack monitoring of experimental slabs cast with UHPC thin bonded overlay (MoDOT project TR201704) and pull-off bond strength and flexural behavior for 16 composite overlay slabs cast with UHPC were determined. The overlay materials included a conventional concrete, a latex-modified concrete, and five non-proprietary UHPC mixtures made with different combinations of saturated lightweight sand (LWS) and expansive agent, fiber volumes of 2% and 3.25%, and overlay thicknesses of 1, 1.5, and 2 in. Flexural testing of the 16 overlay slabs made with substrate concrete used for bridge construction and thin bonded overlays showed that the use of UHPC overlay delayed crack opening and propagation in slab specimens. Task 2 involved fine tuning of two non-proprietary UHPC mixtures to enhance thixotropy. The effect of nanoclay, diutan and welan gums, cellulose-based viscosity-modifying admixture, anti-bleeding and segregation (ABS) admixture, styrene-butadiene rubber, and acrylic ester on key UHPC properties was evaluated. The use of 0.5% of the ABS admixture, by mass of binder, exhibited the highest thixotropy without mitigating mechanical properties of the UHPC. The effect of fiber volume was evaluated, and 3.25% volume was selected to enhance hardened properties. The robustness of the optimized UHPC was evaluated by varying the w/cm by ±10% and the sand moisture content by ±1%. These variations did not have a significant influence on rheology, shrinkage, and compressive strength. Task 3 proposed provisional performance-based specifications for the non-proprietary thixotropic UHPC for bridge overlay construction. The specifications included two proven mixture designs, batching and mixing protocols, test methods, and performance criteria for workability, mechanical properties, as well as autogenous and drying shrinkage. Recommendations were provided for minimum moist curing and compressive strength before bridge opening. Task 4 involved the implementation of the LWS17 and SRA1-3.25% mixture for the rehabilitation of two MoDOT bridge decks. A mockup slab was prepared to demonstrate the constructability of the UHPC. After 8 months of outdoor exposure, the slab did not exhibit any cracking. A field mockup test consisting of two slabs measuring 12 x 12 ft was conducted by the contractor using 1 in. twisted steel fiber instead of ½ in. microfiber. The temperature of the fresh UHPC ranged from 90 to 99 °F, which is higher than the specified value of 86°F. A curing compound, wet burlap, and plastic sheet were stipulated for 7 days before bridge opening. In-situ temperature of the UHPC dropped from 78°F at 1 day to 40°F after 2 days in the Route M overlay and to 20° F at 7 days. All compressive strength results were lower than the minimum specified values of 17,400, and 18,700 psi at 7 days and 28 days, respectively. The 2-, 7-, and 28-day compressive strengths of samples taken from the North bound lane of the Route Z Bridge are 38%, 7%, and 24%, respectively, lower than those from the South bound lane. Furthermore, samples taken from two batches along the same lane of Route Z Bridge exhibited some variation in compressive strength. The high spread in compressive strength between samples taken from different batches of the Z Bridge can be attributed to material quality control issues, especially in the case of excess water that was encountered with the saturated LWS. High strain values of -3000 and -2400 με (in compression) were recorded in the overlay at the midspan of the bridges in Route Z and M overlays, respectively.

17. Key Words	18. Distribution Statement
Ultra-High Performance Concrete; Thin bonded bridge deck overlay	No restrictions. This document is available through the National Technical Information Service, Springfield, VA 22161.

19. Security Classif. (of this report)	20. Security Classify. (of this page)	21. No. of Pages	22. Price
Unclassified.	Unclassified.	122	

Performance of Cost-Effective Non-Proprietary UHPC in Thin-Bonded Bridge Overlays

Project Number: TR202121

Final Report

Investigators

Kamal H. Khayat, Ph.D., P. Eng

Le Teng, Ph.D.

Alfred Addai-Nimoh

May 2023

COPYRIGHT PERMISSIONS

DISCLAIMER

ACKNOWLEDGMENTS

The authors would like to acknowledge the financial support of the Missouri Department of Transportation (MoDOT). The authors would like to thank Mr. Daniel Oesch, Mr. Brent Schulte, Mr. Shawn Weber of MoDOT, and Widel, Inc. for their support of this project. The help of Mr. Jason Cox, Senior Research Specialist at the Center for Infrastructure Engineering Studies (CIES) at Missouri S&T, in providing technical support for the field implementation and instrumentation of the bridge deck is greatly appreciated. The assistance of Mrs. Gayle Spitzmiller, a staff member of the CIES, and Mr. John Whitchurch of the Department of Civil, Architectural, and Environmental Engineering at Missouri S&T is highly appreciated. Special thanks to Jingjie Wei, Yucun Gu, HaoDao Li, Nima Vaziri, and Arash Aghaeipour for their assistance during the field work.

ABSTRACT

The constructability and performance of non-proprietary thixotropic UHPC for thin bonded bridge deck overlay construction was investigated. The project includes four tasks. **Task 1** involved conducting a literature review for the use of UHPC in thin bonded overlay for bridge deck rehabilitation, selection of non-proprietary UHPC including mixtures developed at Missouri S&T, as well as the monitoring of crack density, overlay-substrate bond strength, and flexural behavior for 16 composite overlay slabs cast with UHPC (MoDOT project TR201704). The slabs measured 39 × 79 in. with a depth of 6 in. and were reinforced with two mats of #4 longitudinal bars. The overlay materials included a conventional concrete (CC), a latex-modified concrete (LMC), and five non-proprietary UHPC mixtures made with different combinations of saturated lightweight sand (LWS) and expansive agent (EA), two fiber volumes of 2% and 3.25%, and overlay thicknesses of 1, 1.5, and 2 in. After approximately 33 months of outdoor exposure, no surface cracking was observed for the UHPC overlay slabs regardless of the fiber volume, overlay thickness, and use of LWS or EA. The slabs repaired with CC and LMC mixtures showed extensive surface cracking due to shrinkage. The direct pull-off bond strength ranged between 290 and 430 psi for the UHPC mixtures compared to 220 psi for the CC mixture and 290 psi for the LMC mixture. Flexural testing of overlay slabs made with substrate concrete made for bridge construction and thin bonded overlays showed that the use of UHPC overlay delayed crack opening and propagation in the slab specimens compared to the composite slabs repaired with LMC overlay. **Task 2** involved the fine tuning of two non-proprietary UHPC mixtures to enhance thixotropy, robustness, and flexural performance. The mixtures were also prepared with 17% saturated lightweight sand and 1% shrinkage-reducing admixture (LWS17 and SRA1 mixture) or only 17% saturated lightweight sand (LWS17 mixture) to reduce autogenous and drying shrinkage. The effect of nanoclay, diutan and welan gums, cellulose-based viscosity-modifying admixture (VMA), anti-bleeding and segregation (ABS) admixture, styrene-butadiene rubber, and acrylic ester on key properties was evaluated. The use of 0.5% of the ABS admixture, by mass of binder, exhibited the highest thixotropy without mitigating mechanical properties of UHPC. Furthermore, the effect of internal and external curing (3 and 7 d and continuous moist curing) on UHPC performance was evaluated. Compared to the reference UHPC mortar made without LWS and SRA, the LWS17 and SRA1 mixture exhibited 20% lower shrinkage than the reference mixture (-310 με at 56 d) and a 28-d compressive strength of 19,150 psi compared to 17,990 psi for the reference mixture. The 7-d moist curing was selected for field construction. In the third part of this task, the effect of fiber volume (2% to 3.25%) was evaluated, and 3.25% volume was selected to enhance hardened properties. The robustness of the optimized UHPC was evaluated by varying the w/cm by ±10% and sand moisture content by ±1%. These variations did not have a significant influence on rheology, shrinkage, and compressive strength. **Task 3** developed provisional performance-based specifications in collaboration with Missouri DOT (MoDOT) for the non-proprietary thixotropic UHPC for bridge overlay construction. The specifications included two proven mixture designs, batching and mixing protocols, test methods, and performance criteria for workability, mechanical properties, as well as autogenous and drying shrinkage. Recommendations were provided for minimum moist curing duration and compressive strength development before bridge opening. **Task 4** involved the implementation of the non-proprietary

thixotropic UHPC with a volume of 3.25% steel fibers (the LWS17 and SRA1-3.25% mixture) for the rehabilitation of two MoDOT bridge decks over Highway 70. A mockup slab measuring 3 × 6 ft was prepared at Missouri S&T in June 2022 to demonstrate the workability, placement, consolidation, and finishing of the UHPC. The mixture exhibited good workability with ease of placement and finishing with no sagging on a 2% sloped concrete subbase. After 8 months of outdoor exposure, the slab did not exhibit any sign of cracking. In the second phase, a field mockup test consisting of two slabs measuring 12 x 12 ft was conducted. The LWS17 and SRA1-3.25% mixture was used; however, the fiber was changed from ½ to 1 in. in length. Two UHPC mixtures were prepared with initial slump flow values of 8.5 and 6 in., and the latter was recommended for field work. Full-scale implementation of the LWS17 and SRA1-3.25% mixture to rehabilitate two bridge decks consisting of one-lane bridges measuring approximately 202 ft in length and 21 ft in width. Bridge placement took place between October 20 and November 6, 2022 at ambient temperatures of 66 to 80 °F. The temperature of the fresh UHPC at the end of mixing ranged from 90 to 99 °F, which is higher than the specified value of 86 °F to reduce the risk of cracking. The slump flow, air content, and variation of static yield stress with rest time met the performance specifications of the UHPC. A curing compound and wet burlap and plastic sheet cover were stipulated for 7 d or until the UHPC developed a compressive strength of 14,000 psi before bridge opening. However, there were problems keeping the overlay continuously moist-cured. Temperature recorded in the UHPC overlay dropped from 78°F at 1 d to 40° F after 2 d in the Route M overlay and down to 20° F after 7 d. Two sets of samples taken from the South bound lane of Route Z Bridge exhibited much higher compressive strength than two other sets of samples secured from the North bound lane that was cast 2 days earlier. For instance, the 2-, 7-, and 28-d compressive strengths of two sets of samples taken from the South bound lane were 10,580, 14,470, and 18,030 psi, respectively, compared to 7,680, 13,510, and 15,070 psi, respectively, for samples taken from the North bound lane. All compressive strength results were consistently lower than the minimum specified values of 17,400, and 18,700 psi at 7 d and 28 d, respectively. The 2-, 7-, and 28-d compressive strengths of samples taken from the North bound lane are 38%, 7%, and 24%, respectively, lower than those from the South bound lane. Furthermore, samples taken from two successive batches along the same lane of Route Z Bridge exhibited some variation in compressive strength. For example, the 2-, 7-, and 28-d compressive strength results of samples taken from the North bound lane had 18%, 8%, and 11% variation between successive batches. Lower variations of 15%, 1%, and 6%, respectively, were obtained for samples taken from the South bound lane. The high spread in compressive strength between samples taken from different batches of the Z Bridge can be attributed to material quality control issues, especially in the case of excess water that was encountered in some cases with the saturated LWS taken from the lower parts of the supersacs.

Strain values of -3000 and -2400 με (in compression) were recorded in the thin-bonded overlay at the midspan of the bridges in Route Z and M overlays, respectively. Field inspection was carried out one week and approximately 3 months following the end of construction. The West bound of Route Z Bridge had no signs of cracking after 96 d. However, approximately 25% of the North bound lane showed extensive cracking. The surface crack widths ranged from 0.01 to 0.04 in. (0.25 to 1 mm) with an average of 0.02 in. and average length of 9 in. The 2-, 7-, and 28-d compressive strengths of samples taken from the North bound lane were 38%, 7%, and 24%, respectively, lower than those from the South bound lane. Relatively high variations of compressive strength between

samples taken from different batches for the Route Z Bridge was observed. This can be attributed to material quality control issues, as indicated earlier.

The M Bridge overlay that was cast in early November 2022 exhibited cracking in approximately 45% of the bridge deck surface. The cracking can be attributed to insufficient early-age strength development and risk of microcracking resulting from the sharp drop in temperature after 3 d that was not the case for the Z Bridge. A lack of continuous moist curing for the first 7 d of age can also contribute to a higher risk of cracking.

EXECUTIVE SUMMARY

The objective of this research was to evaluate the constructability and performance of non-proprietary thixotropic ultra-high-performance concrete (UHPC) for thin bonded bridge deck overlay construction. **Task 1** reviewed literature on the use of UHPC in thin bonded overlay for bridge deck rehabilitation and the performance of non-proprietary UHPC. The task also monitored signs of cracking and bond strength between overlay and substrate slabs after 2.5 years of outdoor exposure. The flexural behavior of 16 overlay slabs cast in MoDOT project TR201704 was determined to select candidate mixtures for bridge deck rehabilitation. **Figure 1(a)** showed that UHPC overlay slabs exhibited 35% to 75% higher flexural load capacity compared to slabs repaired with latex-modified concrete and conventional concrete. The increase of overlay thickness from 1 to 2 in. enhanced flexural load capacity by 30% to 40%, as shown in **Figure 1(b)**.

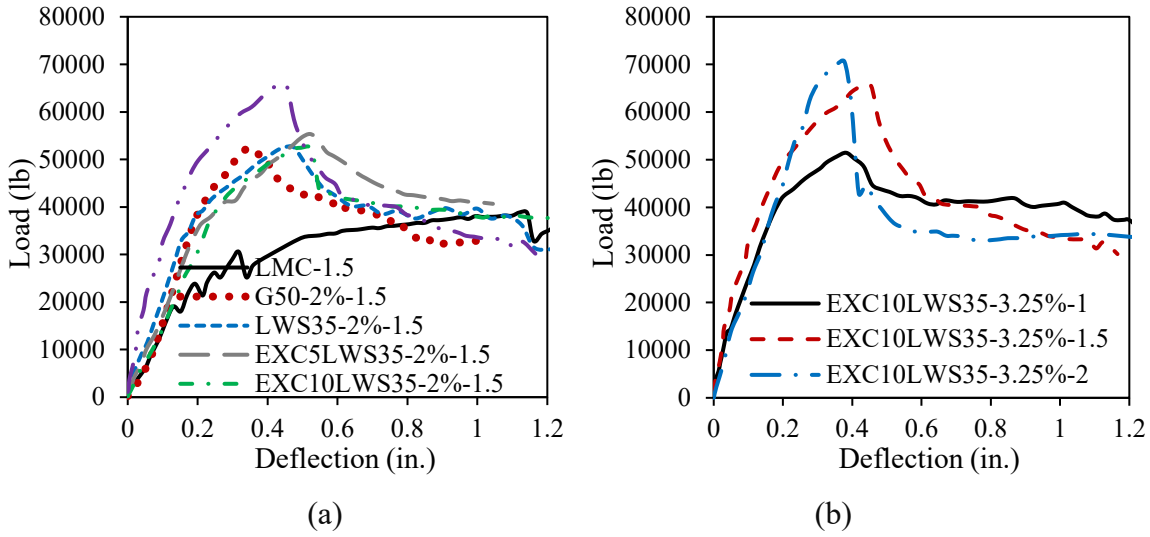

Figure 1 Load-deflection curves of UHPC overlay slab mixtures

Task 2 involved the fine-tuning of the non-proprietary UHPC mixture by enhancing thixotropy shrinkage performance. The effect of nanoclay (NC), welan gum (WG), diutan gum (DG), cellulose-based VMA (CE), anti-bleeding and segregation (ABS) admixture, styrene-butadiene rubber (SBR), and acrylic ester (AE) on key fresh and hardened properties was evaluated. The ABS admixture was most effective to enhance thixotropy. The effect of shrinkage-reducing admixture (SRA) and saturated lightweight sand (LWS) on shrinkage and the potential to reduce external moist curing duration was evaluated. The LWS17 and LWS17SRA1 UHPC mixtures shown in **Figure 2** were finally selected given their superior overall performance. External moist curing of 7 d was recommended. The effect of fiber volume ranging between 2% and 3.25% on UHPC performance was also evaluated. The upper value was selected given 30% reduction in restrained shrinkage and 30% increase in flexural load capacity compared to UHPC made with 2% fiber, as shown in **Figure 3**. The robustness of the optimized UHPC was also evaluated. The investigated parameters included small changes in w/cm, sand moisture content, and superplasticizer (SP) dosage. Test results showed that the variations of w/cm by ±10% and sand moisture content by ±1% did not have a significant influence on rheology, shrinkage, and compressive strength of the selected UHPC.

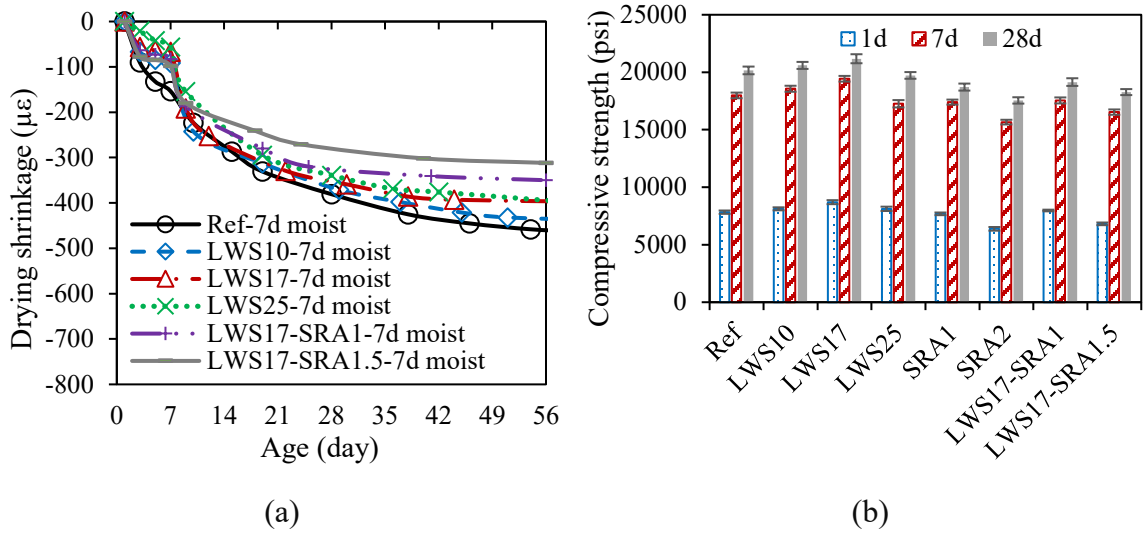

(a) (b)

Figure 2 Influence of LWS and SRA on (a) drying shrinkage and (b) compressive strength for samples subjected to 7 d of moist curing

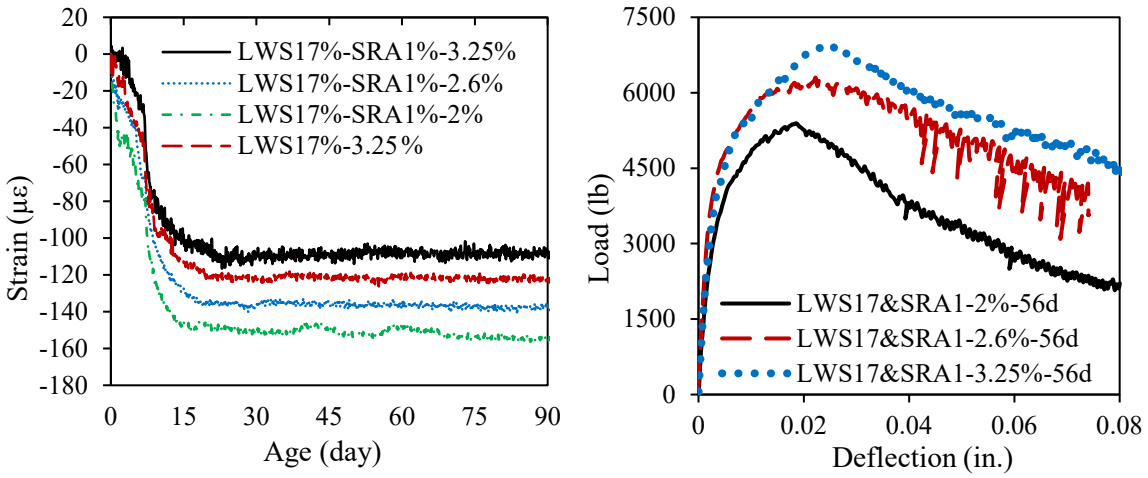

(a) (b)

Figure 3 Influence of fiber volume on (a) restrained shrinkage and (b) flexural performance

In **Task 3**, provisional performance-based specifications for the non-proprietary thixotropic UHPC were developed. The specifications included two proven mixture designs, batching and mixing protocols, test methods, and performance specifications for workability, mechanical properties, and shrinkage. Recommendations were provided for minimum moist curing duration.

In **Task 4**, two Missouri DOT bridges were rehabilitated between October 20 and November 6, 2022 using the LWS17 and SRA1-3.25% UHPC. A laboratory mockup was performed to demonstrate the constructability of the mixture. No signs of cracking were observed after 7-d moist curing and 8 months of outdoor exposure. A field mockup test was conducted to verify the constructability of the mixture on site using materials selected by the contractor, including a 1-in. long twisted steel fiber instead of 0.5-in. long straight microfiber. Two single-lane bridge decks measuring approximately 203 ft in length and 21 ft in width were rehabilitated using 1.5 in. thin bonded overlays.

The compressive strength of samples taken from six batches from the UHPC repair material used for Route Z and M overlays were consistently lower than the minimum specified values of 17,400, and 18,700 psi at 7 d and 28 d, respectively. The reduction of 7- and 28-d compressive strengths ranged from 17% to 25% and 5% to 19%, compared to the specified values of 17,400 and 18,700 psi, respectively. Route Z and M Bridges were inspected after 96 and 81 d, respectively. A maximum strain of -3000 and -2400 με (in compression) was recorded at the midspan of the bridges in Route Z and M overlays, respectively. A visual inspection was carried out 7 d after the construction of Route Z Bridge and indicated no surface cracking; Route M Bridge was covered by snow at 7 d. The South bound of Route Z Bridge had no signs of cracking after 96 d. However, approximately 25% of the North bound lane showed extensive cracking. The surface crack widths after 96 and 81 d ranged from 0.01 to 0.04 in. (0.25 to 1 mm) with an average of 0.02 in. and average length of 9 in. The 2-, 7-, and 28-d compressive strengths of samples taken from the North bound lane were 38%, 7%, and 24%, respectively, lower than those from the South bound lane. Relatively high variations of compressive strength between samples taken from different batches for the Route Z Bridge was observed. This can be attributed to material quality control issues, especially in the case of excess water that was encountered in some cases with the saturated LWS in the lower parts of the supersacs. The top part of the supersacs may have dried out, thus resulting in further variations in the moisture content of the LWS. The M Bridge overlay that was cast in early November 2022 exhibited cracking in approximately 45% of the bridge deck surface. The cracking can be attributed to insufficient early-age strength development and risk of microcracking resulting from the sharp drop in temperature after 3 d that was not the case for the Z Bridge. A lack of continuous moist curing for the first 7 d of age can also contribute to a higher risk of cracking. A summary of key performance-based criteria for the UHPC is presented in **Table 1**.

Table 1 Summary of performance-based specifications for non-proprietary thixotropic UHPC

Test methods	Range
Initial slump flow before jolting (ASTM C230)	4-6 in.
Initial slump flow after 25 cycles of jolting (ASTM C230)	6-7 in.
Air content (ASTM C138)	< 2.5%
UHPC temperature after mixing	< 86 °F
Static yield stress at 5 min (Portable vane)	> 0.1 psi
Increase rate of static yield stress from 5 to 30 min	> 0.01 psi/min
1-d compressive strength (ASTM C109)	> 7,700 psi
7-d compressive strength (ASTM C109)	> 17,400 psi
Minimum period of moist curing	7 d or time to reach 14 ksi
Strength at bridge opening	> 14,000 psi
28-d compressive strength (ASTM C109)	> 18,700 psi
28-d flexural stress at first crack (ASTM 1609)	> 1,500 psi
28-d flexural strength (ASTM C1609)	> 2900 psi
28-d flexural tension ratio (peak to first crack)	> 1.25
28-d flexural toughness (ASTM C1609)	> 350 lb.in.
28-d tensile strength	> 720 psi
28-d autogenous shrinkage	< 450 με
56-d drying shrinkage after 7-d of moist curing (ASTM C157)	< 500 με

Table of Contents

List of Figures

List of Tables

Chapter 1: Introduction

Missouri has the seventh-largest state highway system in the U.S. totaling 33,856 miles, which includes 10,385 bridges. Missouri Department of Transportation (MoDOT) reports that the number of structures in good condition is declining, which adds to the number of structures in fair or poor condition. Bridge decks are highly prone to deterioration, which can be caused by a combination of various factors including vehicle loading, freeze-thaw degradation, cracking, or corrosion of internal reinforcement. One promising approach to rehabilitate bridge decks is the use of thin bonded ultra-high-performance concrete (UHPC) overlays. Thin bonded UHPC overlays can reduce dead weight and secure superior durability and mechanical properties. This includes tensile and flexural strengths, bond to the substrate, resistance to cracking, and strain-hardening and ductility characteristics compared to conventional overlay materials, such as latex-modified concrete (LMC) and fiber-reinforced concrete (FRC).

Haber et al. (2017) of the Federal Highway Administration (FHWA) compared different overlay materials that can be used for thin bonded overlay. As summarized in **Table 1-1**, proprietary UHPC overlay materials with a thickness of 1 to 2 in. can have a unit cost ranging from \$9 to \$18/ft^2 of overlay surface compared to \$18 to \$39/ft^2 for LMC and \$13 to \$19/ft^2 for low slump concrete. Non-proprietary UHPC has the lowest unit cost compared to other overlay materials.

UHPC thin overlays can reduce dead weight compared to conventional thicker overlays or LMC. The use of UHPC for thin bonded overlay for bridge deck rehabilitation has been successfully used, although on a limited scale in the U.S., including some pilot studies in Iowa, Delaware, and New York (Brühwiler et al., 2015). Such novel material can enable the construction of thin bonded overlays of 1 to 2 in. thickness for the rehabilitation of bridge decks and restoration of the structural capacity of bridges.

Table 1-1 Comparison of different overlay materials (Haber et al., 2017)

Overlay type	Overlay thickness (in.)	Cost (\$/ft^2)
High performance concrete	1.0 – 5.0	17 – 25
Low slump concrete	1.5 – 4.0	13 – 19
Latex-modified concrete	1.0 – 5.0	18 – 39
Asphalt with membrane	1.5 – 4.0	3 – 8
Polymer-based	0.13 – 6.0	10 – 17
Non-proprietary UHPC	1.0 – 2.0	3 – 6 (a)
Proprietary UHPC	1.0 – 2.0	9 – 18 (b)
Structural rehabilitation of Chillon Viaduct using proprietary UHPC	1.6	20 (c)

Note: (a): Price reflects materials cost only, assumes cost of \$1,000 per cubic yard; (b): Price reflects materials cost only, assumes cost of \$3,000 per cubic yard; (c): Price reflects cost of material and installation

A new class of cost-effective, non-proprietary UHPC mixtures that are self-consolidating to facilitate placement and finishing has been developed. These formulations were prepared with

conventional riverbed concrete sand, masonry sand, and different combinations of supplementary cementitious materials (SCMs) selected to reduce superplasticizer demand, plastic viscosity, autogenous shrinkage, and unit cost (Meng et al., 2017). As shown in **Table 1-2**, the performance of four non-proprietary UHPC mixtures proposed from that study is compared to that of a proprietary UHPC proportioned with 25% undensified silica fume (SF) and fine quartz sand with a maximum diameter of 600 μm. The non-proprietary UHPC mixtures included two binary binders, a 50% cement replacement with slag (G) and another one with 60% class C fly ash (FA), by volume of binder. Two mixtures with ternary binders were also developed, 50% G and 5% SF as well as 40% FA and 5% SF, by volume of binder. These non-proprietary mixtures were prepared with widely available concrete river sand and finer masonry sand at 70% and 30% volume ratios to achieve high packing density.

The non-proprietary UHPC mixtures developed approximate compressive strengths of 18,000 psi at 28 d under standard moist curing condition and presented approximately 50% cost savings compared to the proprietary UHPC that had compressive strengths of 19,600 and 23,900 psi under moist and steam curing, respectively.

Table 1-2 Performance of a proprietary and four non-proprietary UHPC mixtures

Code	Curing regime	Unit cost ($/ft^3/psi)	28-d f_c (psi)	28-d f_f (psi)	28-d E_s (ksi)	Drying shrinkage** at 100 d (με)	Rapid Cl^- permeability (Coulomb)	Scaling mass loss (lb/ft^2)
Ductal	®	1,300	23,930	2,900	7,800	-555	360	None
	*	1,560	19,580	2,855	7,600	-600	-	None
G50SF5	*	940	18,130	2,930	7,200	-430	-	None
G50	*	820	17,985	3,305	7,200	-55	-	None
FA40SF5	*	840	17,980	3,090	7,500	-465	20	None
FA60	*	760	17,405	2,915	6,700	-500	-	None

Note: f_c: compressive strength; E_s: elastic modulus; f_f: flexural strength; ® 48-h steam curing at 140 °F followed by air curing; *: 28-d moist curing; **: positive and negative length changes denote expansion and shrinkage, respectively

Under MoDOT projects TR201701(Khayat et al., 2018) and TR201704 (Khayat et al., 2018), non-proprietary UHPC mixtures with low shrinkage, which is of special interest to overlay construction, were developed. Shrinkage mitigating approaches included the use of saturated lightweight sand (LWS), CaO- and MgO-based expansive agents (EXC and EXM), and shrinkage-reducing admixture (SRA). Test results showed that the use of 25% LWS (by volume of river sand) led to 30% increase in compressive strength and 35% reduction in autogenous shrinkage. Furthermore, the combined use of EXC and LWS resulted in an early-age expansion that compensated for subsequent autogenous and drying shrinkage. In general, the SRA3LWS60 mixture made with 3% SRA and 60% LWS (expressed as replacement of normal weight sand, or 42% of the total sand volume) exhibited the highest overall performance with compressive strength of 18,100 psi at 28 d, -20 με autogenous shrinkage at 28 d, and -320 με drying shrinkage at 91 d.

As shown in **Table 1-3**, some of the optimized UHPC mixtures were selected to cast thin bonded overlays in the laboratory at Missouri S&T (Teng et al., 2022). In total, 16 composite slabs with a dimension of 39 x 79 x 6 in. in thickness were cast with a MoDOT bridge concrete mixture. The

UHPC mixtures were prepared with either 2% or 3.25% fiber volume using ½ in. straight fibers. The composite slabs were stored outdoors and monitored for signs of cracking for 2.5 years. Direct tensile bond pull-off tests were carried out at 185, 350, and 500 d of age. Test results indicated that the non-proprietary UHPC mixtures with low shrinkage characteristics exhibited high resistance to cracking and high direct pull-off bond strength to the substrate material. On the other hand, overlays made with low slump concrete or LMC exhibited cracking and delamination within 6 months and had a bond strength of 290 psi to the substrate concrete compared to 290 and 430 psi for the UHPC mixtures.

Table 1-3 Compressive strength and shrinkage values of non-proprietary UHPC mixtures made with saturated lightweight sand and shrinkage mitigating admixtures

Code	28-d f'_c (psi) *	28-d autogenous shrinkage (με)	91-d drying shrinkage (με) *
G50	13,930	-520	-520
G50-LWS60	19,150	-75	-750
G50-EXC7.5	13,490	-50	-415
G50-EXC7.5LWS25	16,250	-195	-525
G50-EXC7.5LWS40	16,680	+30	-550
G50-EXC7.5LWS60	17,120	+270	-620
G50-EXC5LWS60	17,410	+225	-565
G50-EXC10LWS60	15,520	+785	-395
G50-EXM5LWS60	16,250	-25	-600
G50-EXM7.5LWS60	15,520	+215	-545
SRA1.5LWS60	18,130	-180	-555
SRA3LWS60	17,700	-20	-315

Note: * refers to 3 d of moist curing; positive and negative length changes denote expansion and shrinkage, respectively

The investigated UHPC mixtures had a self-consolidating consistency with an approximate slump flow of 11 in., without any jolting on the flow table, to facilitate placement of UHPC in repair applications (e.g., repair of columns and girders). However, these highly flowable mixtures are not suitable for bridge deck overlay construction given the sloped bridge deck surface that can vary from 2% to 7% (Sritharan et al., 2018). Such sloping surfaces necessitate the reduction of the initial flowability of the UHPC to resist sagging. Yet, sufficient workability is needed to facilitate the mixing, placement, consolidation, and finishing of the UHPC. The mixtures for overlay construction are therefore designed to enhance thixotropy where the UHPC can flow readily when sheared during mixing, placement, and consolidation (i.e., structural breakdown) followed by rapid gain in static yield stress at rest after consolidation (i.e., structural build-up) to resist flow on sloped surfaces. Field demonstration of the constructability and performance of these non-proprietary thixotropic UHPC mixtures is critical for further acceptance of this novel construction material.

1.1 Research Objectives

The main objective of this research was to evaluate the constructability and performance of non-proprietary thixotropic UHPC for thin bonded bridge deck overlay construction. The specific objectives of the project that is elaborated in this report are as follows:

1. Fine-tune non-proprietary UHPC mixtures to enhance structural build-up characteristics at rest to enable the rehabilitation of bridge decks with sloped surfaces.

2. Carry out field implementation of thin bonded overlay measuring 1.5 in. in thickness to rehabilitate bridges with the collaboration of MoDOT and evaluate the constructability, mechanical properties autogenous and drying shrinkage of the non-proprietary UHPC.

3. Monitor in-situ properties of thin overlays including variations in strain, temperature, and relative humidity with time, and signs of distress in the overlay.

4. Propose candidate mixtures for bridge deck rehabilitation and develop performance-based specifications and guidelines for mixing, placement, and curing of the UHPC.

1.2 Research Approach

The work plan was grouped into the following tasks: (1) selection of cost-effective non-proprietary UHPC; (2) fine-tuning of the mixture to enhance the performance of thixotropic UHPC; (3) develop performance-based specifications for non-proprietary thixotropic UHPC for bridge overlays and provide recommendations and guidelines for UHPC overlay construction; and (4) carry out field implementation using a thixotropic UHPC for bridge deck overlay construction and fine-tune the performance-based specifications.

Task 1 Selection of cost-effective non-proprietary thixotropic UHPC

In this task, a thorough review of the available literature, specifications, and field performance of cost-effective non-proprietary UHPC for bridge deck overlay construction was conducted. The mixture proportioning and key fresh and hardened material properties of candidate UHPC mixtures were compared. The review also focused on strategies that could be used to secure thixotropic UHPC mixtures to prevent flow of the concrete after placement and consolidation. Key hardened performance of UHPC overlay materials including tensile and flexural properties, autogenous and drying shrinkage, and bond strength between overlay and substrate were reviewed. Test methods for quality control were reviewed and summarized in this task.

The performance of the 16 experimental overlay slabs cast at Missouri S&T (MoDOT project TR201704) was summarized in terms of cracking resistance and direct pull-off bond to the concrete substrate. Flexural testing of the 16 composite overlay slabs was conducted to determine flexural strength, the extent of cracking, and flexural toughness. The information generated in Task 1 was used to finalize the candidate UHPC mixtures for the design of non-proprietary thixotropic UHPC for bridge deck rehabilitation.

Task 2 Fine-tuning of mixture design

Task 2 was carried out in four parts. The effect of various specialty admixtures on UHPC mortars was evaluated. Furthermore, the effect of internal and external curing on UHPC performance was investigated. In the third phase, the effect of fiber volume ranging between 2% and 3.25% on UHPC performance was studied, and finally, the robustness of the optimized UHPC mixture was investigated.

Task 3 Develop performance-based specifications

Based on Tasks 1 and 2, recommendations and guidelines about the use of non-proprietary thixotropic UHPC overlay to rehabilitate the bridge deck were developed. This included:

i. Performance-based specifications of thixotropic UHPC for bridge deck overlay construction.

ii. Field-oriented test methods and acceptance criteria to evaluate workability and thixotropy of UHPC.

iii. Acceptable criteria for hardened properties including shrinkage.

iv. Guidelines for proportioning and mixing of thixotropic UHPC mixtures.

v. Recommendations for batching, mixing, placement, consolidation, and curing of UHPC overlay materials.

Task 4 Field implementation

The research team from Missouri S&T and MoDOT engineers conducted a field implementation to construct thin bonded bridge deck overlay prepared one of the two proposed non-proprietary thixotropic UHPC mixtures developed in Task 2. The field implementation was divided into the following parts:

i. Carry out laboratory mockup test at Missouri S&T using the materials and mixing equipment used in Task 2.

ii. Carry out field mockup test using the materials and mixer proposed by the contractor.

iii. Cast and evaluate the performance of bridge deck overlays for two MoDOT bridges using the same UHPC mixture and two surface preparation methods (hydrodemolition and scarification by diamond grinding).

iv. Fine-tune the performance specifications presented in Task 3.

Chapter 2: Selection of Non-Proprietary Thixotropic UHPC

2.1 Literature Review

The purpose of this task was to conduct a thorough review of available literature, specifications, and field performance of UHPC that can be used for bridge deck overlay rehabilitation. **Table 2-1** summarizes the characteristics of three UHPC bridge deck overlay field projects with overlay thicknesses varying between 1.25 and 1.75 in. The 1.25-in. overlay was used for waterproofing, whereas the thicker overlay (≥ 1.5 in.) was cast with reinforcing bars to enhance the structural integrity of the bridge deck. Given sloping surfaces of bridge deck that can vary between 2% and 7%, the UHPC mixture is formulated to be thixotropic to prevent flow and sagging of the repair overlay after casting and consolidation. Haber et al. (2017) recommended limiting the slump flow of thixotropic UHPC to 7 in. after jolting, based on the mortar flow table test (ASTM C1437).

Table 2-1 Summary of UHPC bridge deck overlay field application projects (all these mixtures ae prepared with 0.5 in. fibers)

Location	Bridge name	UHPC	Overlay thickness (in.)	Reinforcement	Bridge slope	Substrate surface preparation
Switzerland	Chillon Viaduct	Ductal	1.75	Reinforcing bars	7%	Hydrodemolition
Buchanan Country, Iowa	Mud Creek Bridge	Ductal	1.50	Wire mesh over pier location	5%	Scarification
Switzerland	Cudrex Viaduct	Ductal	1.25 (1.75 structural sidewalks)	None	N/A	N/A

Typical properties of UHPC mixtures from published literature are shown in **Table 2-2**. The proprietary UHPC is the Ductal NaG3 TX mixture. The non-proprietary mixtures were developed at Missouri S&T by the PI using high volume replacement of the cement with supplementary cementitious materials. Such an approach, coupled with the use of concrete river sand and fine masonry sand as a replacement for the fine quartz sand, enabled the reduction of unit cost and shrinkage of the non-proprietary UHPC. The non-proprietary mixtures were prepared with a water-to-cementitious material ratio (w/cm) of 0.20 and 0.5 in. fibers.

The field-cast proprietary UHPC shown in **Table 2-2** included 3.25% micro steel fibers, by volume, and measuring 0.5 in. in length, to ensure high resistance to cracking when used for thin bonded overlays. The non-proprietary UHPC mixtures shown in **Table 2-2** were developed for casting self-consolidating UHPC for structural applications and proportioned with 2% micro steel fibers. The proprietary field-cast UHPC mixtures and non-proprietary UHPC mixtures had similar hardened properties under moist-curing conditions. UHPC can develop high autogenous shrinkage due to its low w/cm and use of SCMs, especially SF. Such shrinkage can lead to high shear stress at the interface between overlay and substrate, which can cause cracking and delamination. The substrate material can restrain shrinkage of the UHPC, which can result in the development of

tensile stresses at early-age leading to cracking in the overlay material. In MoDOT projects TR201701 and TR201704 carried out by the PI, non-proprietary UHPC mixtures with low autogenous and drying shrinkage were developed using various shrinkage mitigating approaches including the use of saturated LWS, EXC, EXM, and SRAs.

Table 2-2 Performance of field-cast proprietary and three non-proprietary UHPC mixtures

Property	Proprietary	Non-proprietary		
	Field-cast (Wibowo et al., 2018)	FAC40SF5 (Meng et al., 2017)	FAC60 (Meng et al., 2017)	G50 (Meng et al., 2017)
28-d compressive strength (psi)	18,000	17,980	17,410	17,990
28-d elastic modulus (ksi)	6,530	7,540	6,700	7,200
28-d tensile strength (psi)	1,300*	1,740**	1,450**	1,740**
Drying shrinkage at 90 d after 7-d moist curing (με)	-500	-465	-500	-55
Diffusion coefficient of Cl^- at 90 d (ft^2/s)	$\leq 1.1\times10^{-12}$	$\leq 1.0\times10^{-12}$	$\leq 1.0\times10^{-12}$	$\leq 1.0\times10^{-12}$

Note: * refers to results measured by direct tensile test using dogbone specimens; ** refers to results measured by splitting tensile test using cylinder specimens

Key characteristics of these mixtures are summarized in **Table 2-3**. The LWS35 mixture refers to the mixture made with a replacement of 35% of the total sand by pre-saturated LWS that was used for internal curing. The EXC5LWS35 and EXC10LWS35 mixtures had 5% and 10% EXC, respectively, combined with 35% LWS. The fiber volume of UHPC varied from 2% to 3.25%. Test results showed that the use of 25% LWS (by volume of river sand) led to 35% reduction in autogenous shrinkage and 30% increase in compressive strength. Furthermore, the combined use of EXC and LWS resulted in early-age expansion that partially compensated autogenous and drying shrinkage. In general, the SRA3LWS60 mixture made with 3% SRA and 60% LWS (expressed as replacement of normal weight sand or 42% of the total sand volume) exhibited the highest overall performance with 28-d compressive strength of 18,100 psi, 28-d autogenous shrinkage of 20 με (expansion), and 91-d drying shrinkage of 315 με.

In the Mud Creek Bridge deck overlay project (Wibowo et al., 2018), the concrete surface was ground and grooved to expose coarse aggregate and create a target surface roughness of 1/8 in. The substrate surfaces were water sprayed before casting the UHPC overlay. A vibrating truss screed was used to consolidate the UHPC and maintain a thickness of 1.5 in. The curing compound was applied to the UHPC immediately after placement. Traffic was allowed on the bridge when the compressive strength of the UHPC reached 11,600 psi, which was obtained after 4 d of age. The direct tensile pull-off strength conducted on the overlay was 335 psi. The failure location was in the adhesive layer between the metallic disc and UHPC overlay, thus indicating that the bond strength between the substrate and overlay was greater than 335 psi.

Table 2-3 Hardened properties of non-proprietary UHPC mixtures (MoDOT TR201704)

Code	28-d compressive strength (psi)	28-d autogenous shrinkage (με)	91-d drying shrinkage (με)*
FA40SF5	17,980**	-500	-565
FA40SF5-LWS25	22,920**	-330	N/A
FA40SF5-LWS50	20,310**	-265	-465
G50-LWS60	19,150*	-75	-750
G50-EXC7.5	13,490*	-50	-415
G50-EXC7.5LWS25	16,250*	-195	-525
G50-EXC7.5LWS40	16,680*	+30	-550
G50-EXC7.5LWS60	17,120*	+270	-620
G50-EXC5LWS60	17,410*	+225	-565
G50-EXC10LWS60	15,520*	+785	-395
G50-EXM5LWS60	16,250*	-25	-600
G50-EXM7.5LWS60	15,520*	+215	-545
SRA1.5LWS60	18,130*	-180	-555
SRA3LWS60	17,700*	-20	-315

Note: * refers to 3 d of moist curing; ** refers to 28 d of moist curing

Graybeal and Haber (Haber et al., 2017) investigated the effect of substrate surface preparation using the hydrodemolition and scarification methods on the overlay-substrate bond of UHPC. The hydrodemolition method necessitated the removal of approximately 1/2 in. of concrete bridge deck substrate compared to 3/8 in. for the scarification method. The results showed that the use of hydrodemolition led to tensile pull-off strength of 495 psi where the failure location was within the substrate material. On the other hand, the pull-off strength was limited to 115 psi for the scarification method, and the failure location was at the overlay-substrate interface. Such low overlay-substrate bond strength can be attributed to the fact that excessive scarification can introduce microcracking on the substrate material.

2.2 Performance of Composite Overlay Slabs

2.2.1 Cracking and Bond Performance

Surface cracking, direct pull-off testing, and flexural performance of the 16 composite overlay slabs that were cast as part of MoDOT project TR201704 were determined. This included the evaluation of variations of in-situ strain, temperature, and internal relative humidity (IRH) as well as the cracking density and overlay-substrate bond strength, as shown in **Figure 2.1**. The slabs included five non-proprietary UHPC mixtures and one LMC mixture used to cast thin bonded overlays with thicknesses of 1, 1.5, and 2 in. The G50 mixture described earlier was taken as the reference UHPC mixture and was prepared without any shrinkage mitigating materials.

Conventional concrete with 28-d compressive strength of 5,800 psi was used to cast the substrate slabs. The slabs measured 39×79 in. and 6 in. in depth, as shown in **Figure. 2.2**. All substrate slabs were reinforced using a mat made with two-layer of #4 bars measuring 0.5 in. diameter. The top and bottom reinforcing bars were located at 1 and 2 in. from the top and bottom of the slab,

respectively. The reinforcing bars were spaced at 6 in. center to center in both directions. The coarse aggregate at the top surfaces was exposed before casting the overlay to enhance bond with the substrate. The roughness level of the bonded surface corresponds to CSP10 of the ICRI concrete surface profile classification, which is the highest classification for surface roughness. Unlike the base slab, no rebar was installed in the overlay material.

(a) (b) (c)

Figure 2.1 (a) Overview of overlay slab specimens, (b) cracking of slab specimens repaired with UHPC overlay, and (c) direct tensile pull-off bond test

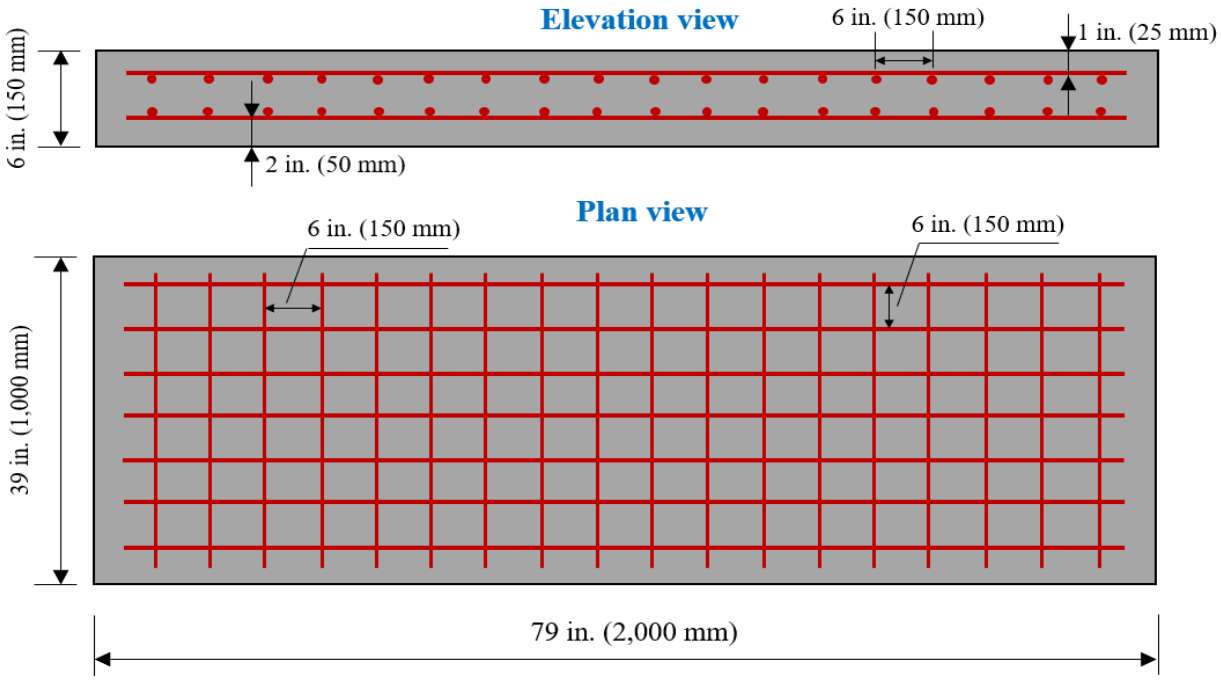

Figure 2.2 Reinforcement details of substrate slab

Table 2-4 summarizes the characteristics of the investigated overlay materials, fiber volume, thicknesses, as well as the 28-d compressive strength and 90-d drying shrinkage results of samples

obtained during the casting of the various overlay materials. All mixtures were proportioned with straight microsteel fibers measuring 0.5 in. in length.

The slab specimens were stored indoors after casting for approximately 6 months then moved outdoors in the winter of 2018. Structural health monitoring was determined as part of this subtask after approximately 2.5 years of outdoor exposure. The overlay materials included a conventional concrete (CC), an LMC, and five non-proprietary UHPC mixtures made with different combinations of saturated LWS and EXC. Temperature variations of the 1.5-in. thick overlay slab specimen made with the EXC10LWS35 mixture are shown in **Figure 2.3**. Similar results were observed in other overlay slab specimens.

Table 2-4 Characteristics of overlay systems

No.	Code	Thickness (in.)	Fiber vol. (%)	28-d compressive strength (psi)*	90-drying shrinkage (με)**
1	LMC-38	1.5	0	6,670	-395
2	LMC-50	2.0	0		
3	G50-38-2	1.5	2	16,100	-845
4	LWS35-38-2	1.5	2	19,580	-455
5	EXC5LWS35-25-2%	1.0	2	17,410	-250
6	EXC5LWS35-38-2%	1.5	2		
7	EXC10LWS35-25-2%	1.0	2	15,230	175
8	EXC10LWS35-38-2%	1.5	2		
9	EXC10LWS35-50-2%	2.0	2		
10	EXC10LWS35-25-3.25%	1.0	3.25	17,410	175
11	EXC10LWS35-38-3.25%	1.5	3.25		
12	EXC10LWS35-50-3.25%	2.0	3.25		

Note: * UHPC was tested using 4×8 in cylinders; ** 7 d of moist curing followed by dry curing at 73 ± 2 °F until testing age

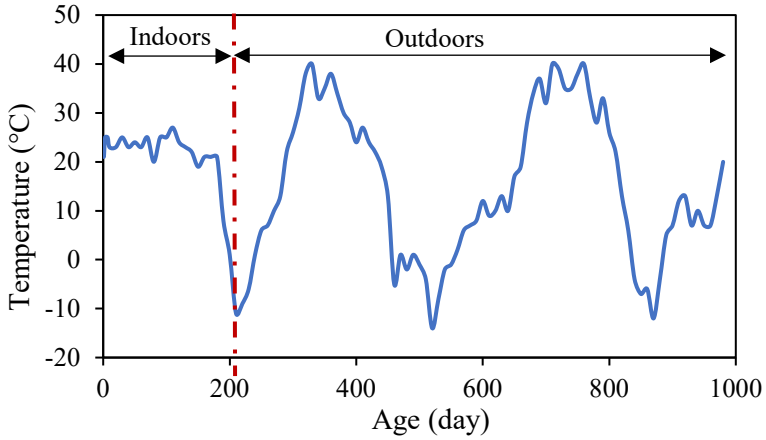

Figure 2.3 Temperature variation of EXC10LWS35 mixture for 1.5-in. thick overlay

Figure 2.4(a) presents typical variations of IRH determined for various overlay materials cast at 1.5 in. thickness measured during the indoor curing period. The drop in IRH of the G50 mixture after 7 d of moist curing was sharper than that of the other mixtures, which is due to the self-desiccation of the material in the absence of saturated LWS. Unlike the G50 mixture, no drop in IRH was observed for the LWS35 mixture within the first 30 d of age. Such UHPC exhibited 20% greater IRH at 180 d than the G50 mixture. The use of EA accelerated the rate of moisture loss given the hydration of the EXC (CaO-based material). Similar results were observed for the 1- and 2-in. thick overlay specimens prepared with different overlay materials. **Figure 2.4(b)** shows the effect of overlay thickness on the variation of IRH of the EXC10LWS35 overlay slab. As expected, the decrease in overlay thickness from 2 to 1 in. increased the rate of moisture loss. Similar results were observed for the other overlay specimens.

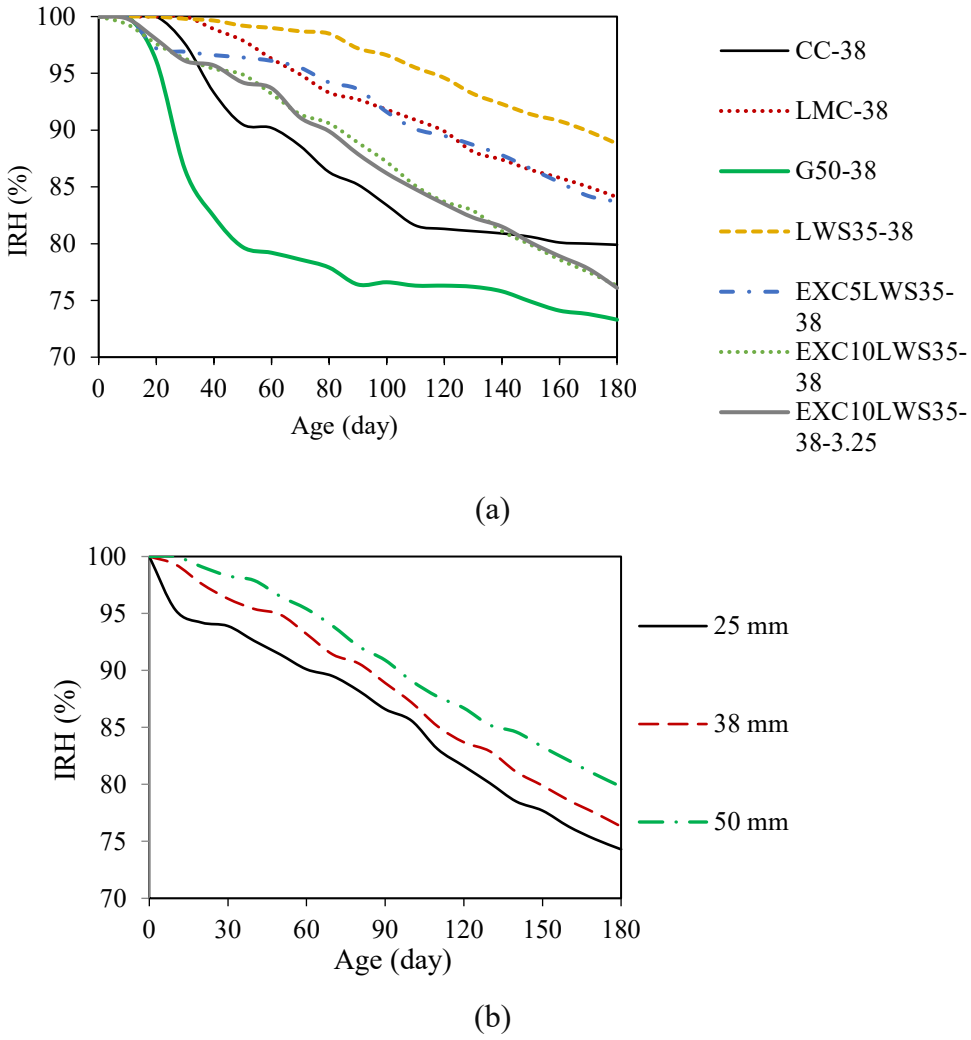

Figure 2.4 Variation of IRH of(a) repair materials used in 1.5-in. thick overlay and (b) EXC10LWS35 mixture used at overlay thickness of 1, 1.5, and 2 in.

Figure 2.5 compares the in-situ strain results of the various repair materials used in bonded overlay slab specimens. Positive and negative strain values represent expansion and shrinkage, respectively. In the first 185 d (indoor exposure), the in-situ strain decreased gradually. A drop in

strain was observed when the specimens were moved outdoors, and the concrete temperature dropped from 77 to -14°F. In-situ strain varied thereafter with daily temperatures. The in-situ strain of the CC and LMC specimens was interrupted after approximately 250 and 400 d, respectively, due to cracking of the overlay material that resulted in damage to the embedded strain gauges. The incorporation of EXC significantly increased the early-age expansion of the UHPC overlay. For example, the combined use of 10% EXC and 35% LWS led to a high in-situ strain of 850 με at 7 d.

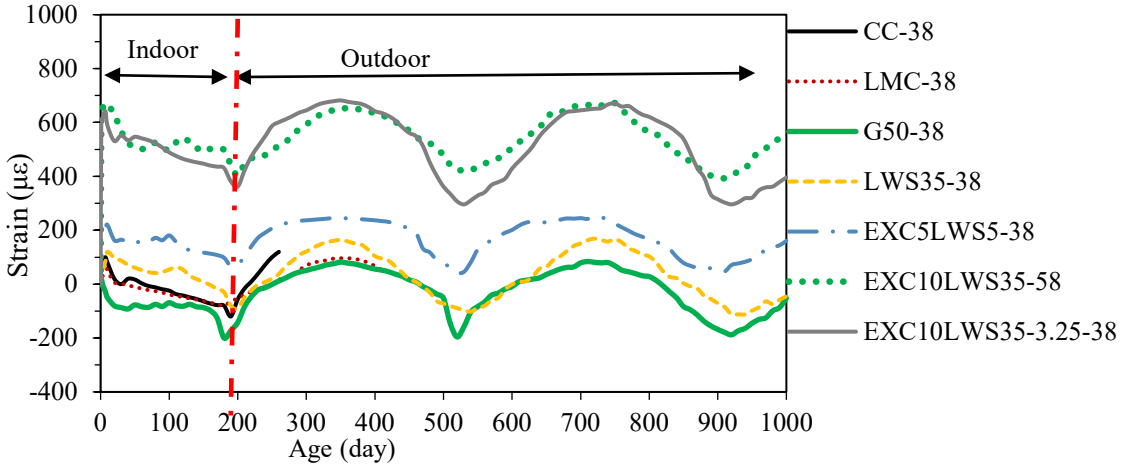

Figure 2.5 Variation of in-situ strain of 1.5-in. overlay slabs

Unlike the CC and LMC mixtures, no surface cracking was observed for the UHPC overlay specimens during the testing period of approximately 1000 d. The evolution of the crack density of the CC and LMC overlay slabs is shown in **Figure 2.6**. For a given overlay thickness, the LMC overlay slab specimens had less surface cracking compared to CC slabs. For example, the relative area of surface cracking in the 1.5- and 2-in. thick CC overlays were 7% and 16% greater than those made with LMC, respectively. The increase in overlay thickness reduced the density of surface cracking. For example, the increase in LMC thickness from 1 to 2 in. led to 50% decrease in the relative crack area at 1000 d.

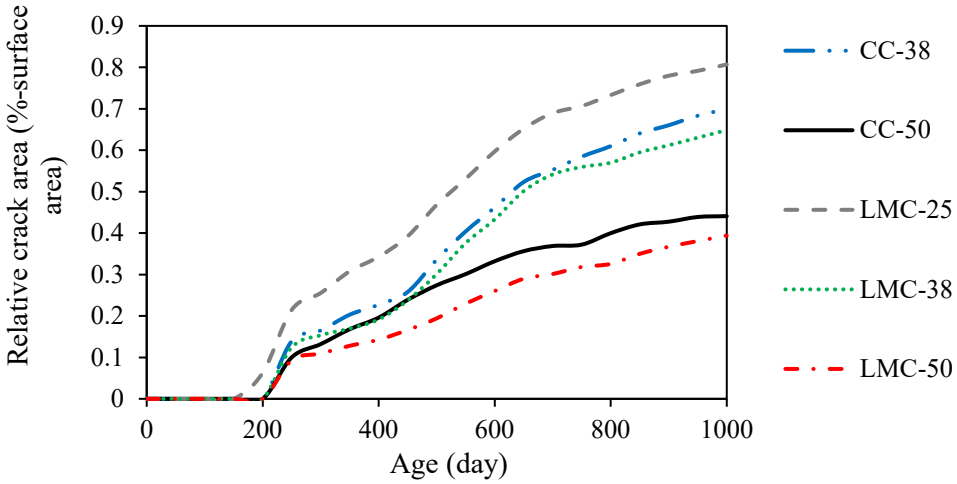

Figure 2.6 Relative crack area with time of CC and LMC overlay specimens

Table 2-5 presents the results of the direct pull-off test bond strength at 185, 350, and 500 d. The mean bond strength of three samples, coefficient of variation (COV) values, and failure mode are reported. The average bond strength was 220 psi for the CC mixture and 290 psi for the LMC mixture. The failure location of the CC and LMC mixtures was systematically observed at the overlay-substrate interface, thus indicating that bond strength was lower than the tensile strength of the CC substrate. On the other hand, the failure location of the UHPC overlay occurred within the substrate, regardless of the testing age. The mean direct pull-off strength ranged between 290 and 430 psi.

Table 2-5 Bond strength of overlay specimens

Test	185 d		350 d		500 d		Failure location
	Mean (psi)	COV (%)	Mean (psi)	COV (%)	Mean (psi)	COV (%)	
CC-38	220	27.1	235	15.6	220	23.2	Interface
CC-50	245	31.2	200	11.3	175	17.8	Interface
LMC-25	335	21.4	230	19.6	310	20.3	Interface
LMC-38	305	17.9	350	32.8	250	11.1	Interface
LMC-50	260	19.8	305	24.7	220	22.9	Interface
G50-38	365	24.1	235	23.8	275	34.5	Substrate
LWS35-38	310	22.1	350	22.2	305	9.2	Substrate
EXC5LWS35-25	405	20.5	400	37.2	370	21.7	Substrate
EXC5LWS35-38	390	19.7	380	14.5	280	26.8	Substrate
EXC10LWS35-25	390	26.4	360	19.0	355	17.3	Substrate
EXC10LWS35-25R	375	27.1	420	26.2	335	16.4	Substrate
EXC10LWS35-38	365	16.8	365	28.9	360	32.1	Substrate
EXC10LWS35-50	430	17.3	410	21.7	380	18.8	Substrate
EXC10LWS35-25-3.25	390	19.2	365	18.6	360	29.9	Substrate
EXC10LWS35-38-3.25	550	23.3	385	17.8	385	19.5	Substrate
EXC10LWS35-50-3.25	395	27.9	290	15.6	320	21.3	Substrate

2.2.2 Flexural Performance of Composite Slabs

The flexural behavior of 12 experimental slabs repaired using thin bonded UHPC overlay was investigated. The composite slabs made with the CC-38, CC-50, and LMC-25 mixtures were not tested since they had developed substantial amount or cracking during the 2.5 years of outdoor exposure. The EXC10LWS25 mixture was used to cast two composite slabs. Only one slab was tested in flexure. The slabs were tested and analyzed with respect to failure modes, load-deflection response, and load-compressive strain response. The four-point bending test was carried out to

evaluate the flexural performance of the overlay slabs, as shown in **Figure 2.7**. The span of the slabs was 70 in., and the area subjected to pure bending moment was 30 in. in length.

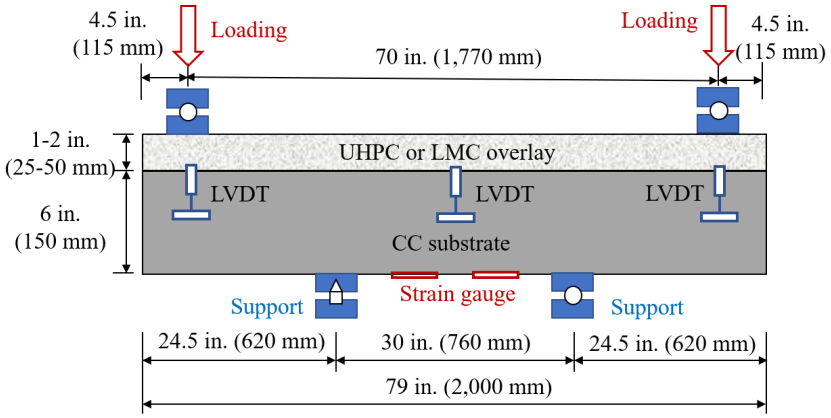

Figure 2.7 Test setup and instrumentation

Six linear vertical displacement transformers (LVDTs) were installed at mid-span and the edges of the slabs to monitor deflection, as shown in **Figures 2.8(a)** and **(b)**. Four concrete strain gauges were installed at the bottom of the overlay slabs to monitor strain variations in the compressive region, as presented in **Figure 2.8(c)**. The loading rate was set at 0.1 in./min.

(a) 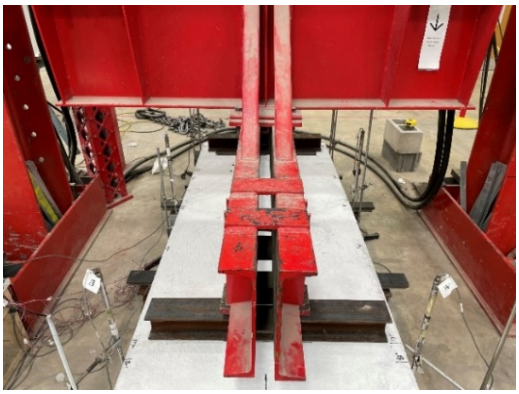

(b) 

(c) 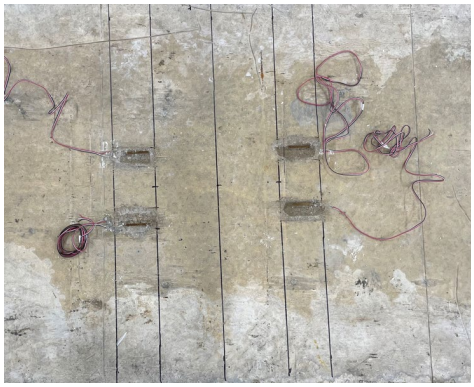

Figure 2.8 Experimental photos of (a) flexural test setup, (b) instrumentation using LVDT, and (c) strain gauges installed at the bottom of overlay slabs

Figure 2.9 shows typical failure modes for the LMC and UHPC overlay slab specimens. For the LMC overlay, several cracks occurred on the overlay in the pure bending region after the applied loading exceeded the LMC cracking loading. As the loading further increased, the cracks became wide and propagated along the depth towards the bottom of the slab. However, the change of crack amount was limited. At the failure stage, the LMC overlay exhibited four main cracks with the crack width ranging between 0.12 and 0.31 in.

In the case of UHPC overlay, the cracks also initiated in the pure bending moment region. As the loading increased, many new micro-cracks occurred at that region, but the change in crack width was limited. After reaching peak loading, no new cracks occurred, and one of the cracks developed as the main crack. At the failure stage, the UHPC overlay specimens exhibited one main crack and 15 to 25 fine cracks. The width of the main crack was greater than 0.4 in., while the width of the other cracks was limited to 0.04 in.

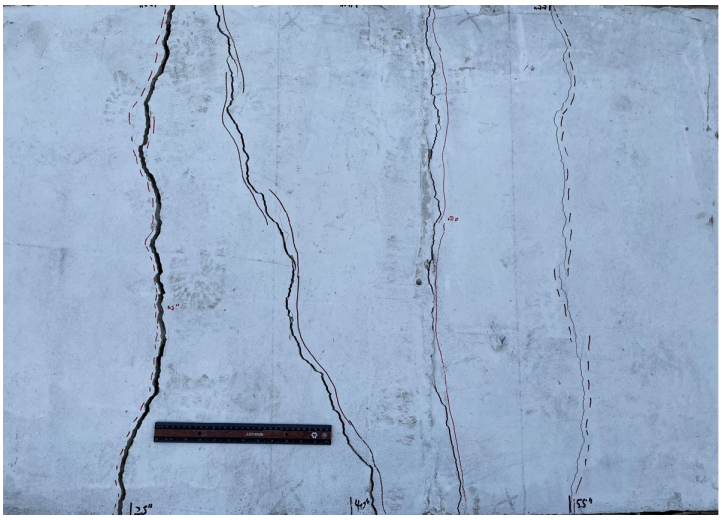

(a)

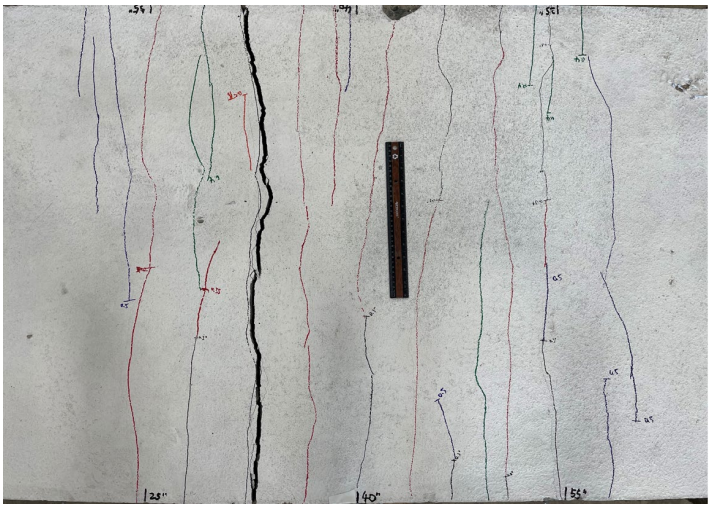

(b)

Figure 2.9 Typical failure modes of slab repaired using (a) 1.5 in. LMC overlay and (b) 1.5 in. EXC10 LWS35-3.25 overlay

Figure 2.10 compares the load-deflection curves of slabs strengthened with various overlay materials. The thickness of the overlay was 1.5 in. The flexural response included three stages. The first stage is the elastic stage where the loading linearly increased with the deflection. The second one is the cracking stage where the overlay slab specimens started cracking, but the longitude rebar did not yield. In this stage, the load increased with the deflection with a decreasing slope. The last stage corresponds to the yield of the longitude rebar. The UHPC and LMC overlay slabs exhibited different load-deflection responses in this stage. For the UHPC overlay, the load decreased with the increase of deflection. In the case of LMC overlay, the load increased slowly with a significant increase in deflection.

UHPC overlay slabs exhibited a higher load capacity in the first and second stages compared to the LMC overlay slab due to the cracking-bridging effect of the fibers. For example, the peak load of the G50 overlay slab was 51,410 lb compared to the 27,650 lb for the LMC overlay slab.

The increase of the volume of the 0.5-in. long microfibers from 2% to 3.25% was shown to enhance the maximum load capacity from 53,930 to 65,535 lb. However, the loading deflection response of UHPC overlay slabs became similar to that of LMC overlay slabs after the peak loading was reached. This is attributed to the fact that the fibers were pulled out and could not effectively bridge the cracks.

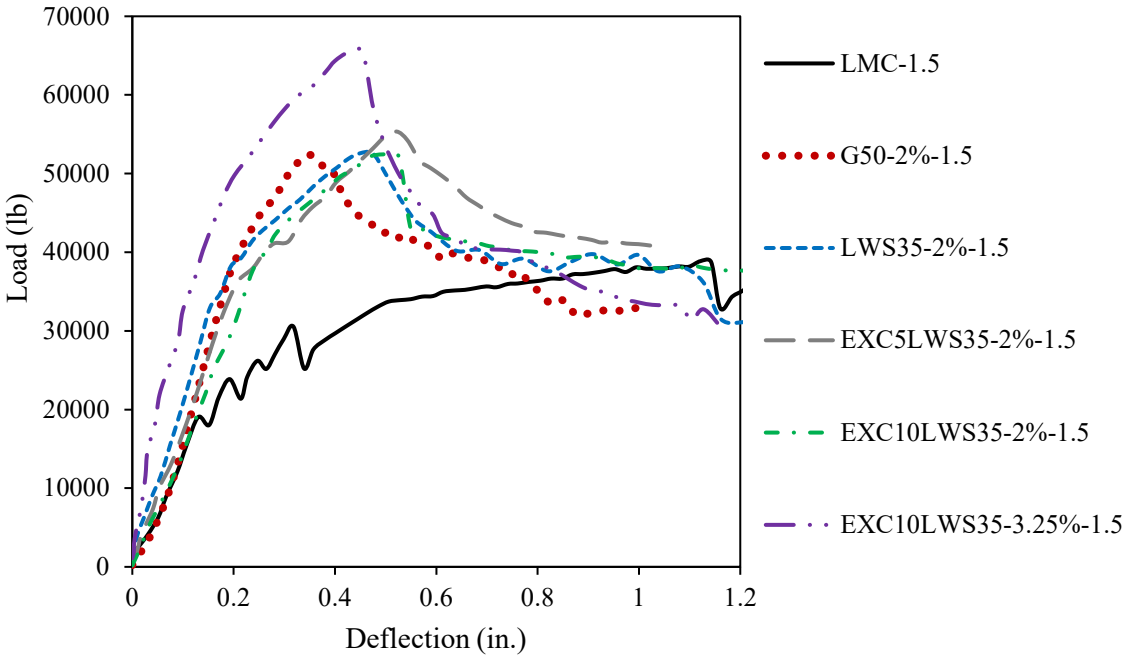

Figure 2.10 Effect of overlay materials on load-deflection curves

Figure 2.11 presents the effect of overlay thickness on the load-deflection curves of overlay slabs. In general, the increase of overlay thickness led to higher peak load capacity. However, the slabs strengthened using a thicker overlay exhibited sharper reduction in load capacity after the peak of loading was reached. In general, the load-deflection response became similar after the deflection exceeded 0.5 in. for slab strengthened using different overlay thicknesses.

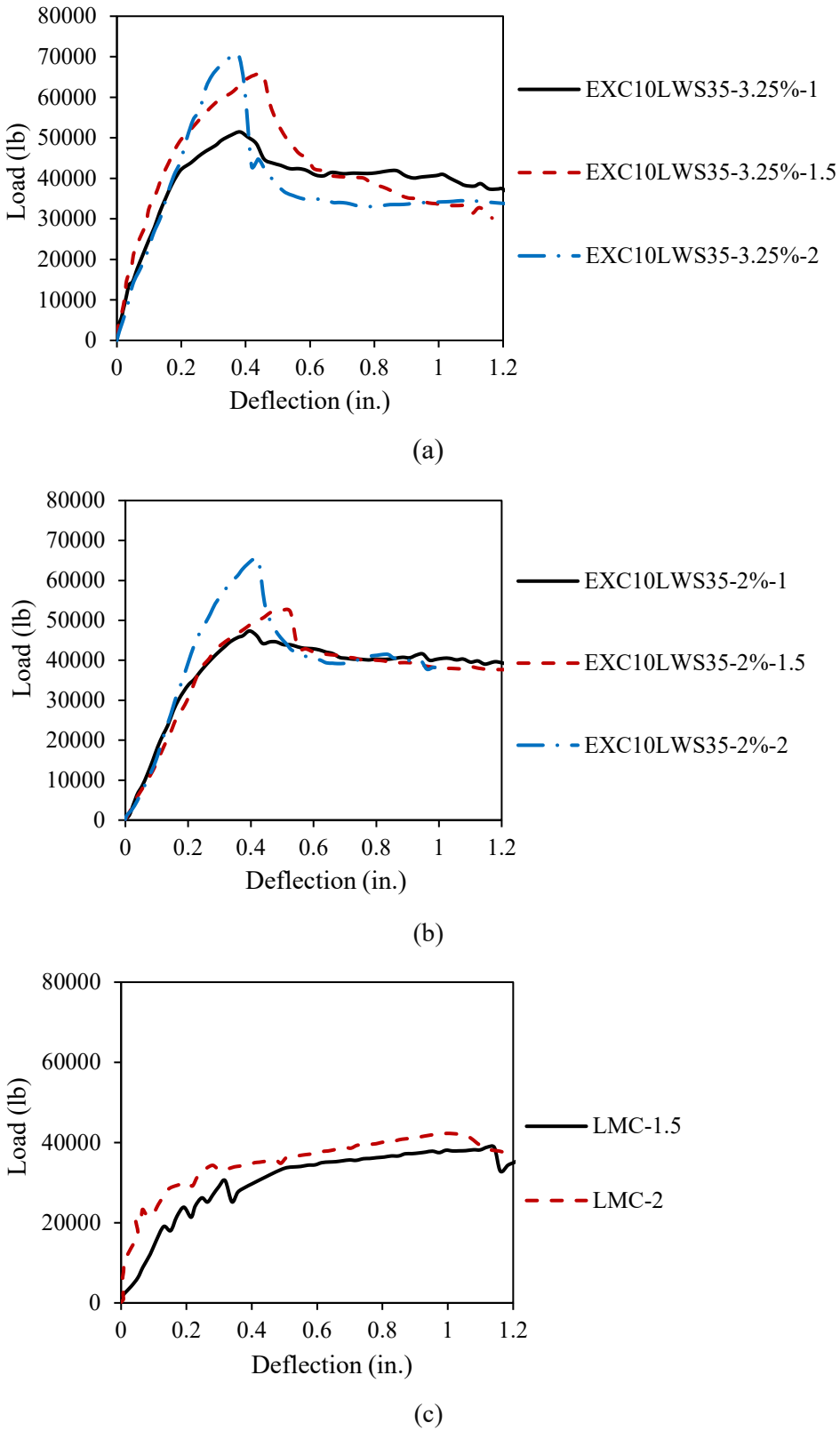

Figure 2.11 Effect of overlay thickness on load deflection of (a)EXC10LWS35-3.25% overlay, (b) EXC5LWS35-2% overlay slab, and (c) LMC overlay slab

Table 2-6 summarizes the key parameters of flexural loading-deflection response at different stages for the investigated overlay slab specimens. In the cracking stage, the deflection (Δ_{cr}) and loading (P_{cr}) at first cracking occurred in the overlay slabs. The cracking width (W_p), loading (P_p), and toughness (T_p) at the start of the yield stage (also known as peak state) are reported. The parameters (W_u, P_u, and T_u) at the end of the yield stage (ultimate state) are also investigated. The T_p is defined as the area within the flexural load-deflection curve between deflection values of 0 and values corresponding to the peak of loading. The T_u is defined as the area between the deflection values of 0 and 1.2 in. The results show that the use of UHPC overlay enhanced the cracking and peak loading and delayed the formation and development of cracking compared to the LMC overlay. The UHPC overlay slabs exhibited 185% to 270% higher T_p and 15% to 35% greater T_u compared to the LMC overlay slab. The highest load capacity was obtained when the cracking width propagated to approximately 0.02 to 0.05 in. for the UHPC overlay slabs. The increase of UHPC overlay thickness from 1 to 2 in. enhanced P_p by 30% to 40% and T_p by 15% to 25%. Such levels of improvement were 5% to 10% and 10% to 30% when the fiber content increased from 2% to 3.25%.

Table 2-6 Summary of flexural test results for all overlay slab specimens

Specimen	Cracking state		Peak/yield state			Ultimate state		
	Δ_{cr} (in.)	P_{cr} (lb)	W_p (in.)	P_p (lb)	T_p (lb·in.)	W_u (in.)	P_u (lb)	T_u (lb·in.)
LMC-38	0.130	8,745	0.138	38,873	5,705	0.287	35,219	36,030
LMC-50	0.146	11,432	0.157	42,285	7,608	0.319	37,139	39,477
G50-38-2%	0.193	30,660	0.035	52,343	16,412	0.622	32,692	42,397
LWS35-38-2%	0.183	35,239	0.022	52,579	17,062	0.539	31,042	46,105
EXC5LWS35-25-2%	0.141	32,782	0.031	41,944	11,665	0.516	31,284	42,047
EXC5LWS35-38-2%	0.198	36,601	0.033	55,347	18,297	0.421	40,667	46,016
EXC10LWS35-25-2%	0.185	35,924	0.027	47,354	12,642	0.520	39,482	44,145
EXC10LWS35-38-2%	0.209	38,799	0.029	52,446	16,331	0.480	36,539	45,513
EXC10LWS35-50-2%	0.240	49,666	0.016	65,282	14,890	0.465	38,243	47,700
EXC10LWS35-25-3.25	0.187	35,718	0.020	51,453	13,498	0.646	36,901	46,857
EXC10LWS35-38-3.25	0.201	46,273	0.014	65,533	21,055	0.602	32,747	49,226
EXC10LWS35-50-3.25	0.256	55,841	0.030	70,562	16,894	0.465	34,516	46,321

Figure 2.12 compares the load-compressive strain curves of slabs strengthened with various overlay materials. The thickness of the overlay was 1.5 in. The increase in loading led to a lower compressive strain level in UHPC overlay slabs compared to that of the LMC slab. When the applied loading was approximately 30,000 lb, the EXC10LWS35-2% overlay slab exhibited 780 με in compression compared to 915 με for the LMC overlay slab.

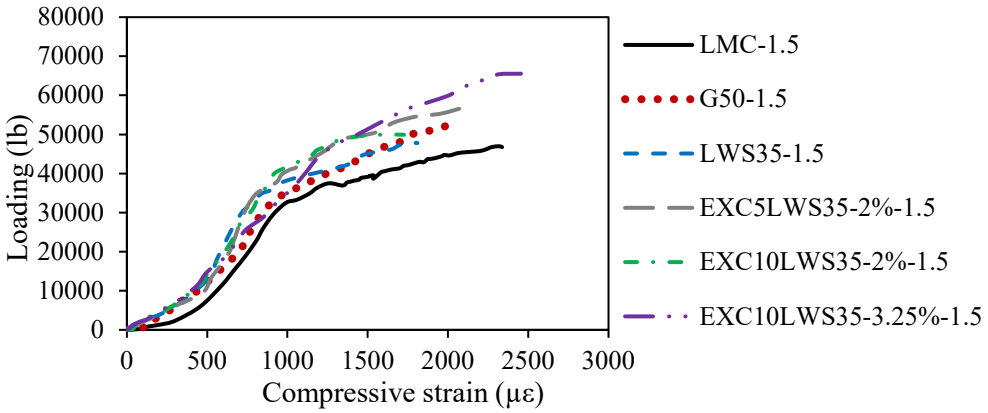

Figure 2.12 Effect of overlay material on load compressive strain curves

Figure 2.13 presents the effect of overlay thickness on load-compressive strain curves of UHPC overlay slabs. The increase in overlay thickness led to a slightly lower compressive strain in the subbase slab. When the applied loading reached approximately 40,000 lb, the increase of overlay thickness from 1 to 2 in. reduced the compressive strain from 1,115 to 990 με for the EXC10LWS35-3.25% slab.

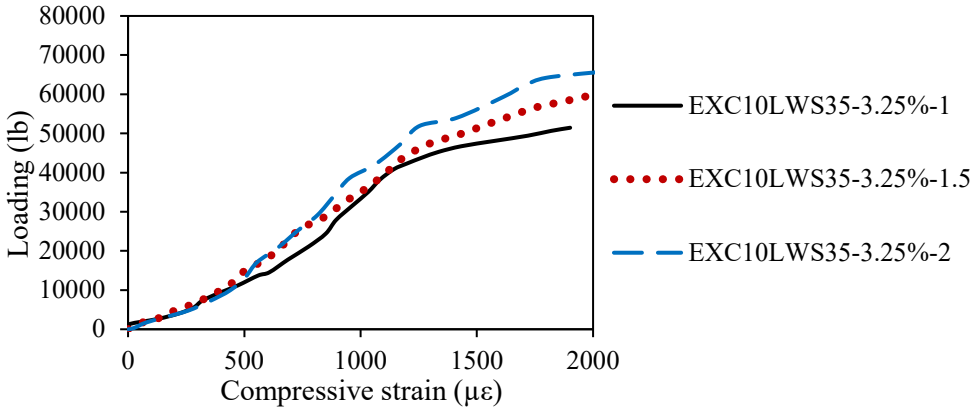

(a)

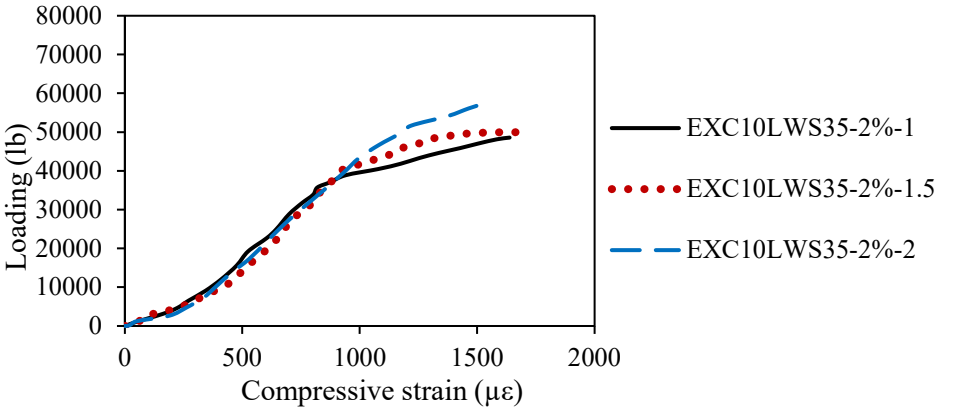

(b)

Figure 2.13 Load compressive strain curves for (a)EXC10LWS35-3.25 and (b) EXC10LWS35

2.3 Summary

In this task, a thorough review of the available literature and field performance of non-proprietary UHPC that can be used for bridge deck overlay construction was conducted. The direct pull-off bond strength, as well as the monitoring of temperature, IRH, and in-situ strain of 16 composite slabs repaired with CC, LMC, and UHPC mixtures were conducted. Furthermore, the flexural testing of the 16 composite slabs cast was determined. The major findings of this task are summarized below.

1. The non-proprietary UHPC mixtures exhibited high bond strength (290 to 430 psi within substrate) compared to the composite slabs repaired with CC (220 psi at interface) and LMC (290 psi at interface) mixtures. Furthermore, the incorporation of saturated LWS in the UHPC mixtures reduced the sharp drop in IRH by up to 20% compared to the mixtures made without any LWS.

2. The use of UHPC overlay delayed the crack opening and propagation in slab specimens compared to LMC overlay. UHPC overlay slabs made with 3.25% steel fiber volume exhibited 95% and 270% higher flexural load capacity and toughness, respectively, compared to the LMC overlay slabs at a crack width of 0.04 in.

3. At a maximum crack width of 0.04 in., the flexural load capacity of slabs made with UHPC overlay increased by 35% with the increase of overlay thickness from 1 to 2 in. for UHPC prepared with 3.25% fiber volume. In the case of slabs with a lower UHPC overlay thickness of 1.5 in., the increase of fiber volume from 2% to 3.25% led to 25% enhancement in flexural load capacity at a crack width of 0.04 in.

4. In general, the investigated non-proprietary UHPC mixtures exhibited no cracking after approximately 2.5 years of outdoor exposure (without mechanical loading) regardless of the fiber content and overlay thickness. The UHPC made with 0.5-in. long steel microfiber used at a volume of 3.25% is recommended. The cracking and flexural performance of the 1.5- and 2-in. thick UHPC overlays were similar. The use of the 2-in. thick overlay is more conservative to reduce the potential of cracking and crack propagation and extend service life.

Chapter 3: Design and Performance of Thixotropic UHPC for Thin Bonded Overlay Construction

3.1 Materials and Mixture Proportion

In this study, a proven non-proprietary UHPC mortar derived from the FAC40SF5 mixture described in Chapter 2 was chosen as the base mixture. The investigated mixture had a self-consolidating consistency that is not suitable for casting bridge deck overlays. The mixture proportioning of the non-fibrous mortar is shown in **Table 3-1**. The binder combination consisted of 5% silica fume and 40% Class C fly ash used to replace 45% of a Type III cement, by volume. The w/cm was fixed 0.20, by mass. A 70% concrete river sand and a 30% masonry sand, by volume, were used to enhance the packing density of the aggregate. The binder-to-sand volume ratio was fixed at 1.

Table 3-1 Mixture design (kg/m^3)

Type III cement	Silica fume	Class C fly ash	Water	Masonry sand	River sand
649	41	405	219	302	688

The objective of this first part was to use specialty admixtures to enhance the thixotropy of flowable UHPC as well as bond strength to the substrate in the case of latex-modified admixture. As shown in **Table 3-2**, seven chemical admixtures were used to enhance thixotropy. The dosage of the superplasticizer (SP) was adjusted to maintain a fixed initial slump flow of 7.5 ± 0.5 in. for ease of placement. This investigation was conducted using non-fibrous mortar. A polyether-based air detraining admixture (ADA) was employed to reduce the volume of entrapped air.

Table 3-2 Specialty chemical admixtures

Type		Content (% of binder, by mass)
Nanomaterial	Nanoclay (NC)	0, 0.25, 0.5, 1
Viscosity-modifying admixture	Welan gum (WG)	0.09, 0.18, 0.27
	Diutan gum (DG)	0.0015, 0.003, 0.0075, 0.015
	Cellulose-based VMA (CE)	0.25, 0.5, 1, 1.5
	EUCON anti-bleeding, and segregation (ABS)	0.1, 0.25, 0.5, 1
Latex-modified admixture	Styrene-butadiene rubber (SBR)	0.9, 1.8
	Acrylic ester (AE)	0.45, 0.9

The objective of the second part was to select an optimum curing protocol to reduce shrinkage and enhance the mechanical performance of thixotropic UHPC. The investigated mixtures were prepared with 2% steel microfibers measuring 0.5 in. in length. **Table 3-3** presents the various curing scenarios that were implemented; mainly, external moist curing of 3 and 7 d combined with internal curing using four different contents of saturated LWS. Furthermore, 56-d moist curing was applied as the reference curing regime. In addition to using saturated LWS to mitigate shrinkage, the UHPC made with 17% LWS was prepared with 1% or 1.5% SRA.

Table 3-3 Shrinkage mitigation methods for UHPC

Mixture	Saturated LWS content (% of total sand, by volume)	SRA content (% of binder, by mass)
Ref	0	0
LWS10	10	0
LWS17	17	0
LWS25	25	0
SRA1	0	1
SRA2	0	2
LWS17 and SRA1	17	1
LWS17 and SRA1.5	17	1.5

Note: * All mixtures were subjected to 3-, 7-, and 56-d moist curing

The objective of the third part was to investigate the influence of fiber content on key fresh and hardened properties, as well as autogenous, drying, and restrained shrinkage of UHPC. Two UHPC mixtures, one containing only 17% LWS and the other one containing a combination of 17% LWS, and 1% SRA were studied. The investigated fiber contents ranged between 2% and 3.25%, by volume. The mixture proportions are shown in **Table 3-4**.

Table 3-4 Investigated UHPC mixtures

Mixture	2% steel fiber	2.6% steel fiber	3.25% steel fiber
LWS17	x	x	x
LWS17 and SRA1			x

The objective of the fourth part was to evaluate the robustness of the optimized UHPC mixtures that were proportioned with 17% LWS, 1% SRA, and 3.25% steel microfibers. Robustness is considered the ability of the material to tolerate small changes in mixture parameters without undergoing considerable changes in performance. **Table 3-5** summarizes the investigated parameters, including the w/cm, moisture content of the sand, and SP dosage that deviated from the optimized values. The SP dosage was varied with the w/cm and sand moisture to maintain an initial slump flow of 7 ± 0.5 in. The effect of these parameters on key fresh and hardened properties including autogenous and drying shrinkage was evaluated.

Table 3-5 Parameters to determine the robustness of non-proprietary UHPC

Parameters	w/cm	Moisture of sand	SP dosage
Variation	±10%	±1%	±10%

3.2 Experimental Program

Flow properties of the UHPC were determined using the slump test in accordance with ASTM C230. Unit weight was determined in accordance with ASTM C138. The Contec 5 coaxial cylinder rheometer was employed to determine the plastic viscosity of the investigated mortar mixtures based on the steady-flow measurement protocol. The measurement started at the end of the mixing.

The samples were pre-sheared at 0.5 rad per second (rps) for 25 s followed by a reduction of rotational velocity from 0.5 to 0.025 rps in 10 steps. The data points at a rotational velocity of 0.5 and 0.45 rps were removed after checking the signs of equilibrium. The plastic viscosity was calculated using the Bingham model, as shown in Eqs. 1-2.

$$T = G + H \cdot N \tag{1}$$

$$\mu = \frac{\left(\frac{1}{R_i^2} - \frac{1}{R_0^2}\right)}{8\pi^2 h} H \tag{2}$$

where T (N·m) is the torque, G (N·m) is the intercept of the flow curves, H (N·m/s) is the slope of the flow curves, N (m/s) is the rotational velocity, μ (Pa·s) is the plastic viscosity, R_i (m) is the radius of coaxial cylinders, R_0 (m) is the radius of the container, and h (m) is the height of the inner cylinder submerged in the materials tested in the rheometer.

The static yield stress of UHPC mortar was evaluated after rest periods of 5, 15, and 30 min with the mortar placed in the rheometer, which corresponds to 5, 20, and 50 min after the end of mixing, respectively. The mortar was subjected to a very low rotational velocity of 0.05 rps for 120 s without any pre-shear. The resulting torque was progressively increased with time to a peak value, then it decreased to an equilibrium value.

The static yield stress(τs) was calculated as follows:

$$t_s = \frac{T_{max}}{2\pi h R_i^2}$$

where Tmax (N·m) is the peak torque in the process of testing.

The undisturbed slump spread (USS) and disturbed slump spread (DSS) shown in **Figure 3.1** was used to evaluate thixotropy. Cylindrical specimens measuring 4x8 in. were employed to conduct the test. The USS test method involved filling UHPC in four moulds at the end of mixing. The moulds were removed consequently after rest periods of 5, 10, and 15 min, and the diameter of the spread was determined. In parallel, the UHPC was remixed after conducting the USS test using a Hobart mixer for 1 min, and the diameter of spread was measured. This is known as the disturbed slump spread. The difference between the undisturbed and disturbed spread diameters can be used to quantify thixotropy.

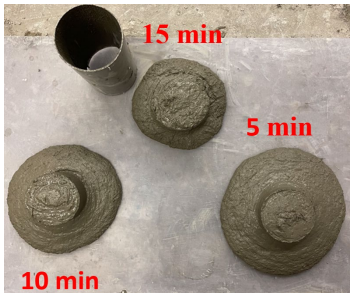

Figure 3.1 Undisturbed and disturbed slump spread test

The portable vane (Omran et al., 2009) is a simple and reliable field-oriented method to evaluate the thixotropy of concrete, as shown in **Figure 3.2**. Three vanes measuring 3 in. in diameter and various heights of 8, 6, and 4 in. were used to conduct the test after three periods of 5, 15, and 30 min, respectively. The vane was rotated under the applied slow shear rate for 10 to 15 s, and the maximum torque T was measured. The static yield stress was calculated as follows:

$$\tau_{sy} = T/K$$

where $K = 2\pi r^2(h + 1/3r)$, and h and r are the filling height and radius of the vane (m), respectively.

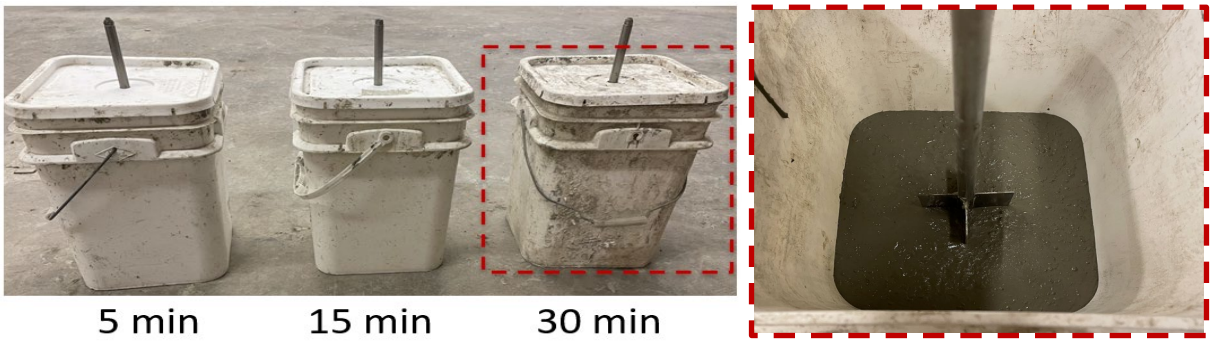

Figure 3.2 Portable vane test

The compressive strength of concrete was determined using 2-in. cubic samples. The flexural properties of UHPC were determined using prismatic specimens measuring 16×3×3 in. in compliance with ASTM C1609 and ASTM C1856. The loading rate was set at 0.1 mm/min. The area under the load-deflection curve between deflection values of 0 to 0.08 in. was used to determine the flexural toughness. For each mixture, an average of two beams were tested.

The autogenous shrinkage of UHPC mortar (without fiber) was evaluated in accordance with ASTM C 1698 using samples in corrugated plastic tubes and stored immediately after casting at 70 ± 0.5 °F and 50% ± 2% RH. The first measurement is taken as final setting. The second measurement is taken at 12 h after final setting. Other measurements are carried out daily within the first week, and then, weekly until 28 d after final setting.

The autogenous shrinkage of fiber-reinforced UHPC was tested using sealed specimens with embedded vibrating strain gauges as shown in **Figure 3.3**. Data acquisition was used to collect data at a 5-min interval.

Figure 3.3 Autogenous shrinkage test of sealed prismatic samples

The restrained shrinkage was tested using the ring test method (ASTM C1581). As shown in **Figure 3.4**, the deformation of the inner steel ring was measured using strain gauges. The data acquisition system was used to test the strain at a 6-min interval after the final setting time.

Figure 3.4 Restrained shrinkage test

3.3 Results and Discussion

3.3.1 Effect of Specialty Admixtures

Figure 3.5 shows the effect of various chemical admixtures on plastic viscosity and SP demand of UHPC mortar prepared with a fixed initial slump flow of 7.5 ± 0.5 in. Given the constant slump flow, the yield stress measured approximately 40 Pa (0.0058 psi) for the investigated mixtures. The use of VMA had a greater effect on the increase of plastic viscosity compared to the NC and polymer latex admixtures (AE and SBR). For example, the increase of WG content from 0 to 0.18% increased plastic viscosity from 7 to 60 Pa·s. On the other hand, the maximum value of plastic viscosity was limited to 12 Pa·s for the mixtures made with NC and 19 Pa·s for those made with the SBR. Furthermore, the increase in VMA and NC contents led to a significant increase in SP demand. For example, the use of 0.015% DG increased the SP demand by 265% compared with the reference mixture made without any thixotropy-enhancing admixture. Furthermore, the incorporation of SBR and AE latex had a limited influence on SP demand.

The variation of the static yield stress of the reference mixture with rest time is shown in **Figure 3.6** The static yield stress increased more rapidly in the first 5 min of rest, followed by a linear increase with rest time. Two thixotropic indices were used to describe the evolution of static yield

stress. The τ_{floc} (Pa or psi) refers to the initial increase of yield stress due to particle flocculation after a short time of rest (in this case taken as 5 min). The other index is the A_{thix} (Pa/min or psi/min) which refers to the slope of the linear growth of static yield stress with rest time.

Figure 3.7 compares the effect of various admixtures on the thixotropy of UHPC mortar with a slump flow of 7.5 ± 0.5 in. In general, the use of DG and ABS had the highest effect on thixotropy, followed by WG, CE, as well as SBR and AE latex. The use of NC had a limited effect on the increase of thixotropy. This can be related to the increase in SP demand that affects thixotropy.

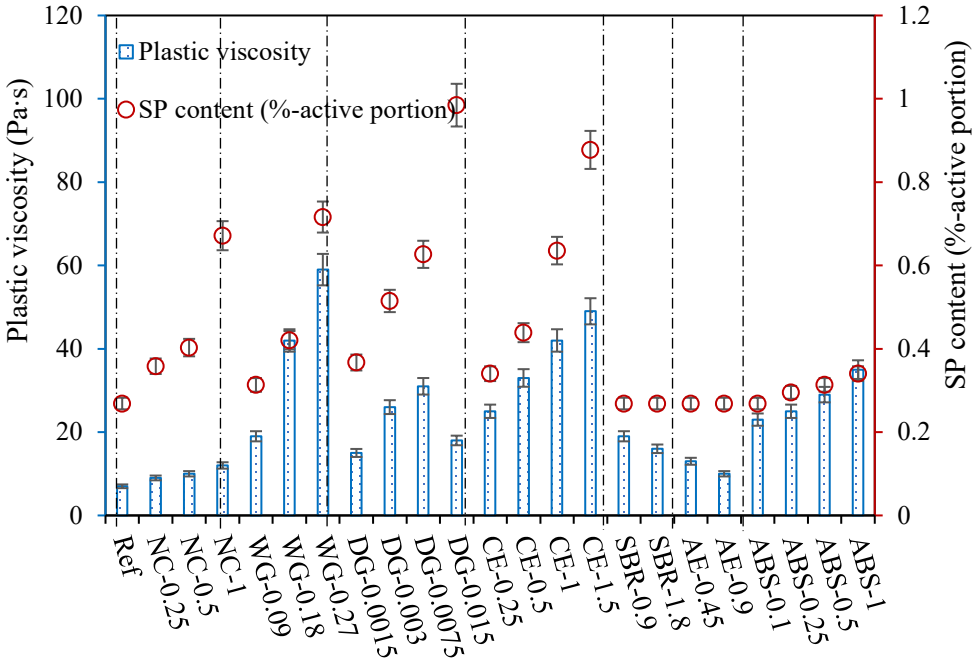

Figure 3.5 Effect of different admixture contents on plastic viscosity and SP demand of UHPC mortar with slump flow of 7.5 ± 0.5 in. (1Pa=0.000145 psi)

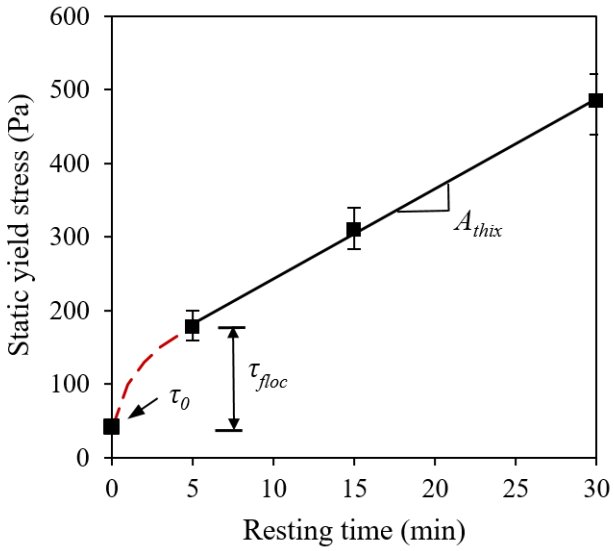

Figure 3.6 Example of evolution of static yield stress of the reference mixture with rest time

The compressive strength of the investigated mortars is shown in **Figure 3.8**. The increase of NC content from 0 to 1% led to a 6% increase in compressive strength at 28 d (17,120 to 18,280 psi). The compressive strength decreased by 15% with the incorporation of VMA. For example, the increase of WG from 0 to 0.27% reduced the 28-d compressive strength from 17,120 to 15,090 psi. A significant drop of 40% to 70% compressive strength was observed in mixtures made with SBR and AE compared to the reference UHPC mixture.

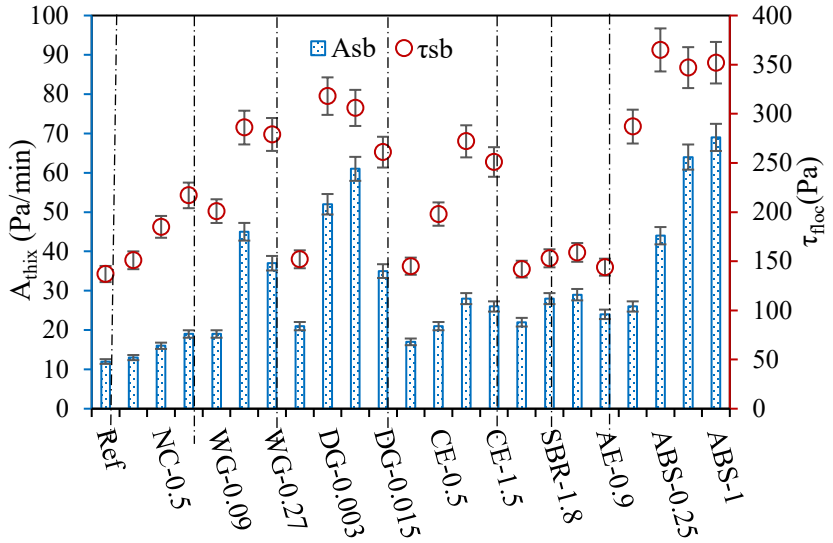

Figure 3.7 Effect of various admixtures on A_{thix} and τ_{floc} of UHPC mortar with a slump flow of 7.5 ± 0.5 in. (1 Pa = 0.000145 psi)

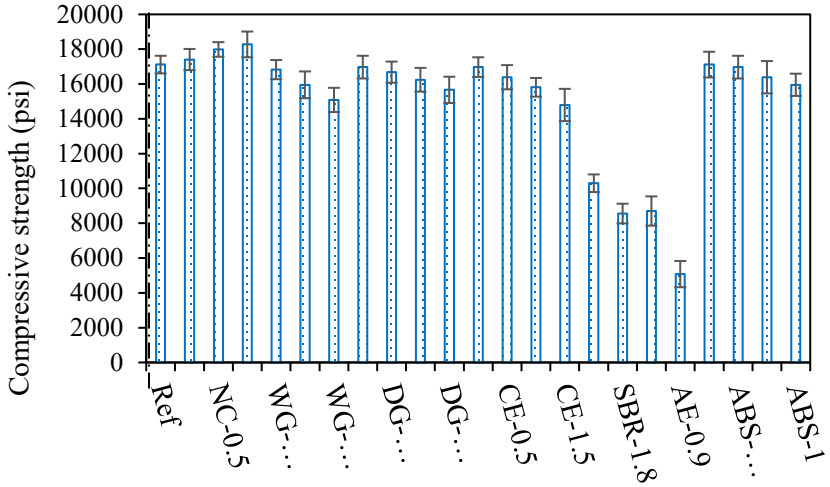

Figure 3.8 Influence of specialty admixtures on 28-d compressive strength of UHPC mortar with a slump flow of 7.5 ± 0.5 in.

The variation of autogenous shrinkage of UHPC mortar made with NC, WG, and DG admixtures is shown in **Figure 3.9**. For example, the increase in NC content from 0 to 1% increased the 28-d autogenous shrinkage from -555 to -630 με. The mortar made with 0.27% WG exhibited a lower autogenous shrinkage of -485 με at 28 d compared to -555 με for the reference mixture.

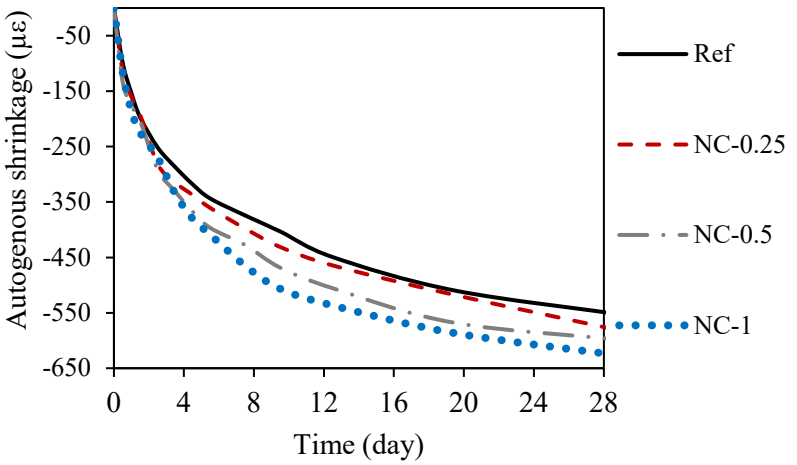

(a)

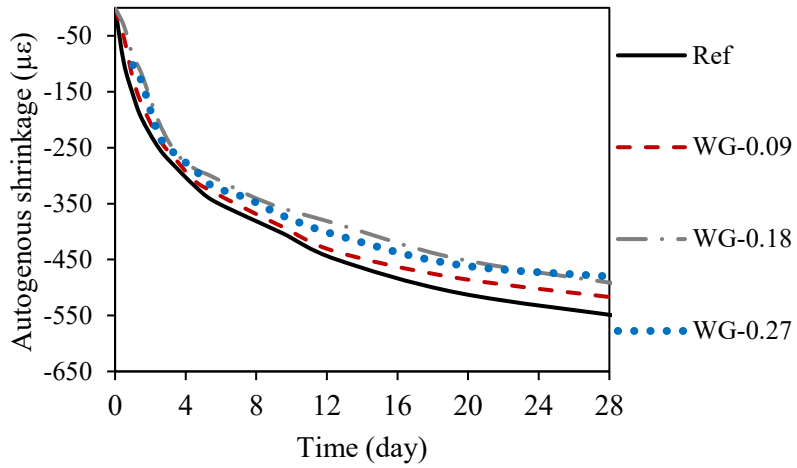

(b)

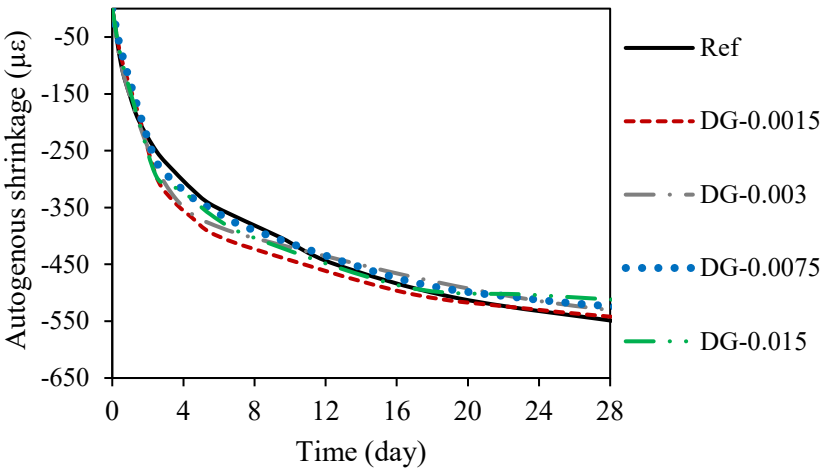

(c)

Figure 3.9 Variation of autogenous shrinkage with (a) NC, (b) WG, and (c) DG

The variation of autogenous shrinkage of UHPC mortar made with CE, AE, and ABS admixtures is shown in **Figure 3.10**. For example, the increase of SBR content from 0 to 1.8% reduced slightly the 28-d autogenous shrinkage from -550 to -490 με.

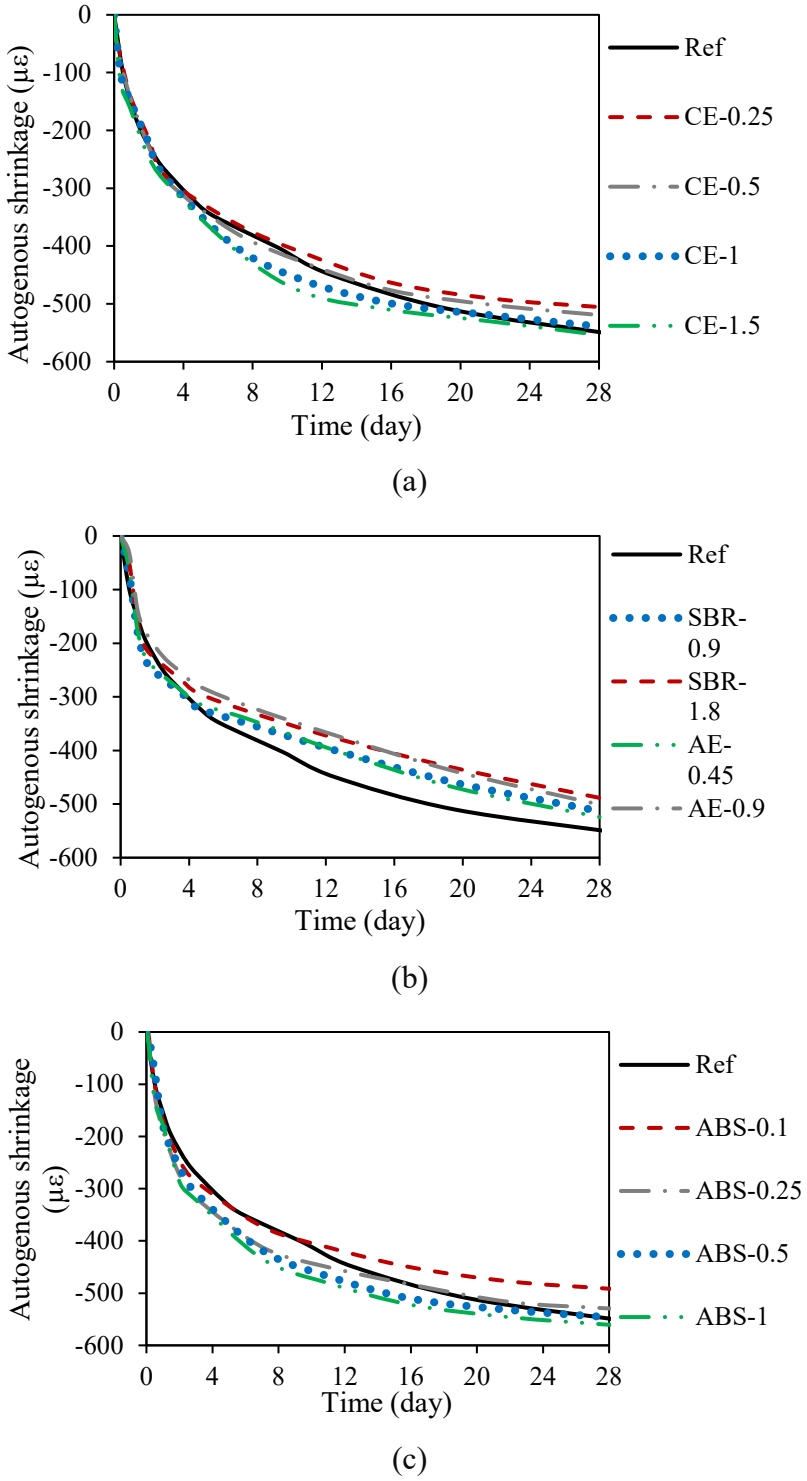

Figure 3.10 Variation of autogenous shrinkage with (a) CE, (b) latex admixture (SBR and AE), and (c) ABS admixtures

Based on the results, the ABS admixture with 0.5%, by mass of binder, was selected and used in the subsequent subtask which involved investigating the effect of LWS and SRA.

3.3.2 Effect of LWS and SRA

The temperature and the unit weight and calculated air content of the mixtures made with LWS and SRA are presented in **Table 3-6**. The air content was reduced by 15% for the mortar made with 17% LWS and increased by 15% for that prepared with 2% SRA. UHPC made with 17% LWS and 1% or 1.5% SRA had a similar air content compared to the reference UHPC.

Table 3-7 presents the effect of LWS and SRA on the variation of slump flow of UHPC with rest time. The slump flow test was conducted with and without 25 cycles of jolting. In general, the use of LWS accelerated the loss of workability, whereas the loss of workability was retarded using SRA.

Table 3-6 Unit weight, air content, and temperature of fresh UHPC

Mixture	Unit weight (lb/ft^3)	Air content (%)	Temperature (°F)
Ref	151	2.4	85.6
LWS10	150	2.0	84.6
LWS17	148	2.1	86.2
LWS25	146	2.1	86.7
SRA1	151	2.5	87.6
SRA2	150	2.8	87.1
LWS17 and SRA1	148	2.3	84.4
LWS17 and SRA1.5	147	2.5	87.8

Table 3-7 Variation of slump flow with a rest time of UHPC

Mixture	Slump flow before jolting (in.)				Slump flow after 25 jolts (in.)			
	0 min	5 min	15 min	30 min	0 min	5 min	15 min	30 min
Ref	7.7	5.9	4.7	4.3	9.5	8.1	7.3	5.9
LWS10	7.9	5.7	4.5	4.1	9.8	7.9	7.3	5.9
LWS17	7.1	5.1	4.3	4.0	9.3	7.0	6.4	5.5
LWS25	7.3	5.1	4.1	4.0	9.1	6.9	6.3	5.5
SRA1	7.5	6.1	4.9	4.2	9.1	8.1	7.3	6.3
SRA2	7.4	6.3	5.0	4.3	9.2	8.3	7.3	6.5
LWS17 and SRA1	7.6	5.7	4.7	4.2	9.1	7.7	7.1	6.2
LWS17 and SRA1.5	7.8	6.2	4.9	4.2	9.1	8.1	7.2	6.3

The effect of LWS and SRA on SP demand to maintain a fixed slump flow of 7.5 ± 0.5 in. is shown in **Figure 3.11**. The increase of LWS content from 0 to 25% led to 30% reduction in SP dosage. The incorporation of SRA had a limited influence on SP demand.

The effect of LWS and SRA on yield stress and plastic viscosity of UHPC is presented in **Figure 3.12**. The yield stress ranged between 75 and 95 Pa (0.011 and 0.014 psi). The plastic viscosity ranged from 10 to 15 Pa·s (0.0014 to 0.0022 psi·s) reflecting the limited effect of LWS and SRA on viscosity.

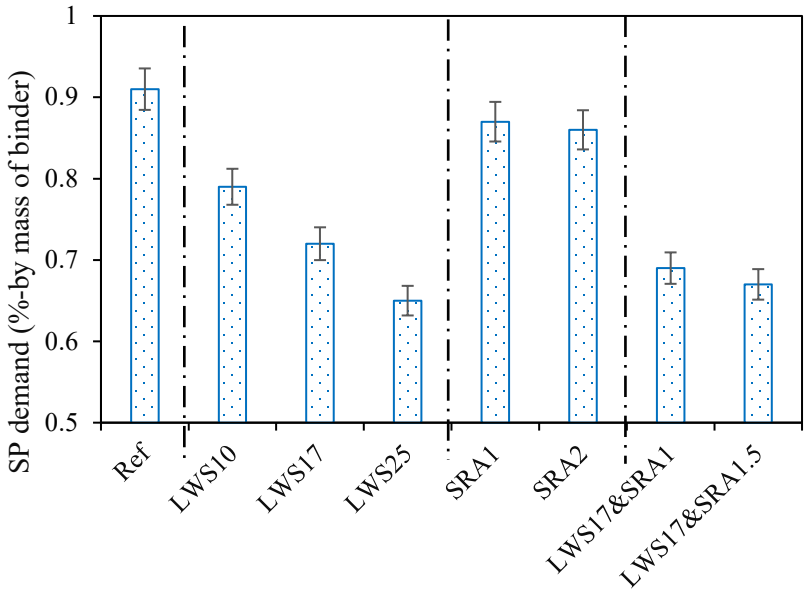

Figure 3.11 Influence of LWS and SRA on SP demand (slump flow of 7.5 ± 0.5 in.)

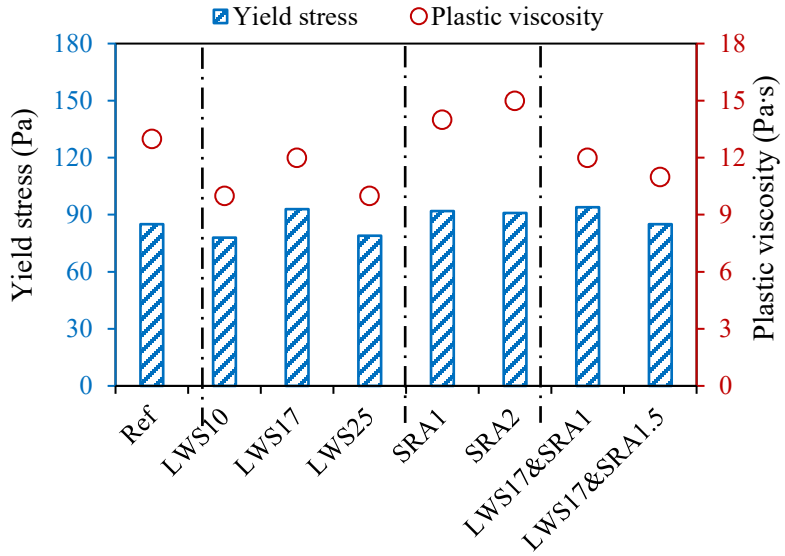

Figure 3.12 Influence of LWS and SRA on rheological properties of UHPC with slump flow of 7.5 ± 0.5 in.

Figure 3.13 presents the τ_{floc} and A_{thix} of UHPC made with LWS and SRA. The increase of LWS from 0 to 25% led to 25% and 30% increase in τ_{floc} and A_{thix}, respectively. However, UHPC made with 2% SRA exhibited 15% and 10% lower τ_{floc} and A_{thix}, respectively, compared to the reference

UHPC made without any SRA and LWS. UHPC made with 17% LWS and 1% or 1.5% SRA exhibited similar τ_{flo} and A_{thix} compared with UHPC made without any LWS and SRA.

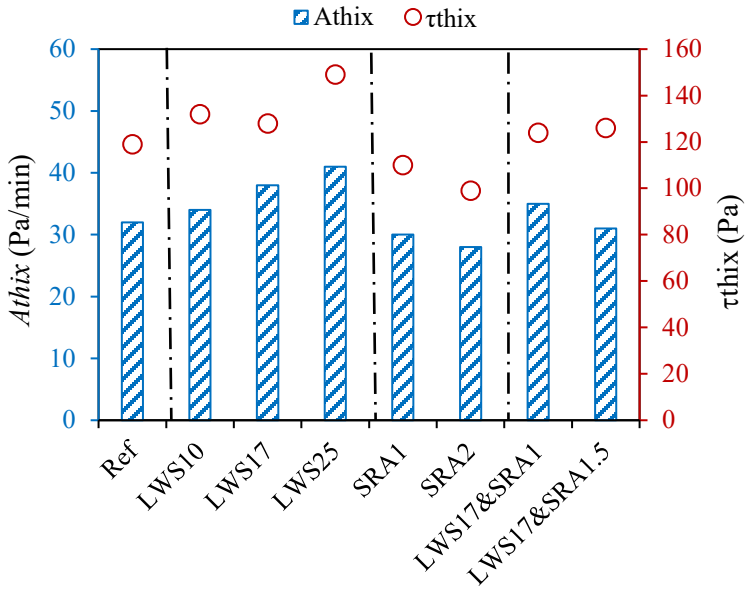

Figure 3.13 Influence of LWS and SRA on A_{thix} and τ_{thix} of UHPC

Examples of linear increase in static yield stress with a rest time of UHPC made with different LWS contents are shown in **Figure 3.14(a)**. The slope of the curve is used as a thixotropic index of $A_{thix.PV}$ (Pa/min or psi/min). **Figure 3.14(b)** presents the variation of $A_{thix.PV}$ of UHPC made with LWS and SRA. The increase of LWS from 0 to 25% led to 55% increase in $A_{thix.PV}$. However, $A_{thix.PV}$ was reduced by 30% using 2% SRA compared to reference UHPC made without any SRA and LWS.

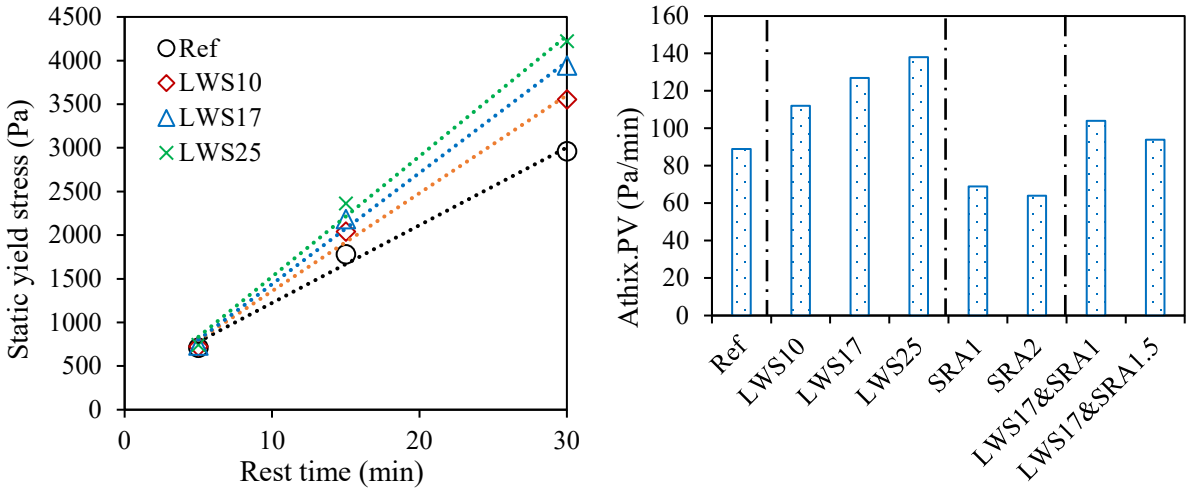

Figure 3.14 (a) Examples of variations of static yield stress with rest time for UHPC made with different LWS contents and (b) influence of LWS and SRA on $A_{thix.PV}$ of UHPC (1 Pa = 0.000145 psi)

As reported in **Table 3-8**, the use of LWS accelerated the loss of spread for both USS and DSS tests, whereas the spread loss was retarded using SRA. This agrees with the results of the portable vane and Contec 5 rheometer tests.

Table 3-8 Variations of USS and DSS with a rest time of UHPC

Mixture	USS (in.)				DSS (in.)			
	0 min	5min	10 min	15 min	0 min	5 min	15 min	30 min
Ref	12.5	9.5	7.4	5.8	12.5	10.5	10.0	9.5
LWS10	13.0	9.4	5.1	4.0	13.0	10.3	9.5	7.5
LWS17	13.0	8.7	4.2	4.0	13.0	10.0	9.0	7.0
LWS25	12.5	8.2	4.0	4.0	12.5	9.5	8.0	6.5
SRA1	13.0	9.8	8.2	6.5	13.0	11.5	10.8	10.5
SRA2	13.0	11.0	8.9	7.1	13.0	13.0	12.5	12.0
LWS17 and SRA1	12.0	8.0	5.2	4.0	12.0	10.5	10.3	10.0
LWS17 and SRA1.5	13.0	9.5	6.8	6.0	13.0	11.0	10.5	10.3

The effect of saturated LWS, SRA, and curing time on the length change of UHPC is shown in **Figure 3.15**. The moist curing had the greatest effect on reducing shrinkage, followed by SRA and LWS. For example, the increase of moist curing from 3 to 56 d reduced the 56-d shrinkage from -520 to -260 με for the reference UHPC made without any saturated LWS and SRA. The use of 2% SRA reduced the 56-d shrinkage from -520 to -350 με for the mortar subjected to 3-d moist curing. The combined use of 17% LWS and 1.5% SRA exhibited the lowest shrinkage regardless of the moist curing duration.

The compressive strength of UHPC made with saturated LWS and SRA is presented in **Figure 3.16**. UHPC made with 17% LWS exhibited the highest compressive strength regardless of the curing type. The compressive strength was increased with the extension of the curing age. For example, the increase of curing age from 3 to 28 d led to 10% enhancement in 28-d compressive strength of the reference UHPC mixture. The use of SRA reduced compressive strength. The 28-d compressive strength of UHPC subjected to 7-d moist curing was reduced by approximately 15% when incorporating 2% SRA. The use of 17% LWS and 1% SRA exhibited similar compressive strength compared to reference UHPC prepared without any LWS and SRA.

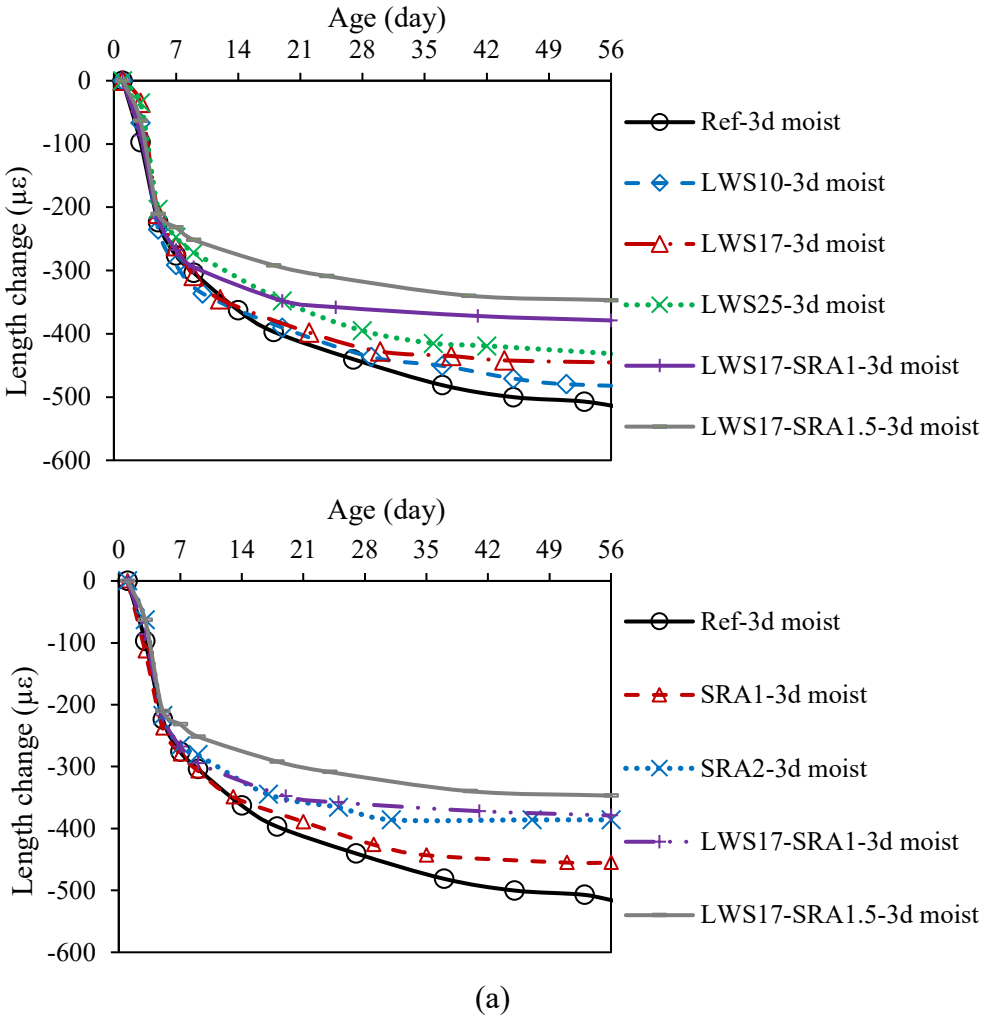
Age (day)
0
7
14
21
28
35
42
49
56
0
-100
-200
-300
-400
-500
-600
Length change (με)
Ref-3d moist
LWS10-3d moist
LWS17-3d moist
LWS25-3d moist
LWS17-SRA1-3d moist
LWS17-SRA1.5-3d moist
Age (day)
0
7
14
21
28
35
42
49
56
0
-100
-200
-300
-400
-500
-600
Length change (με)
Ref-3d moist
SRA1-3d moist
SRA2-3d moist
LWS17-SRA1-3d moist
LWS17-SRA1.5-3d moist

(a)

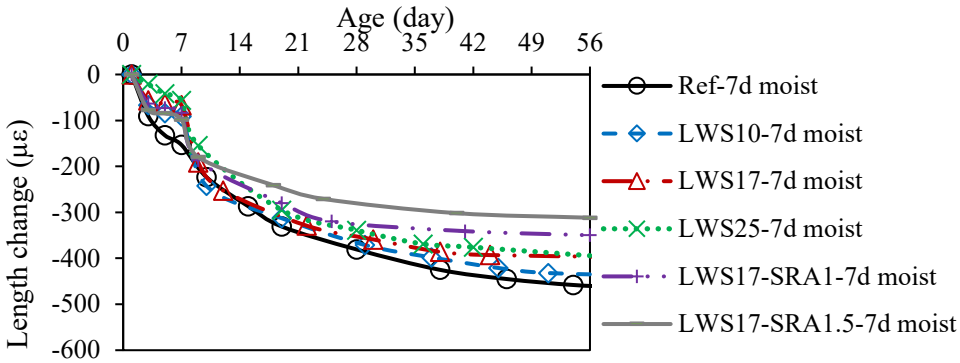
Age (day)
0
7
14
21
28
35
42
49
56
0
-100
-200
-300
-400
-500
-600
Length change (με)
Ref-7d moist
LWS10-7d moist
LWS17-7d moist
LWS25-7d moist
LWS17-SRA1-7d moist
LWS17-SRA1.5-7d moist

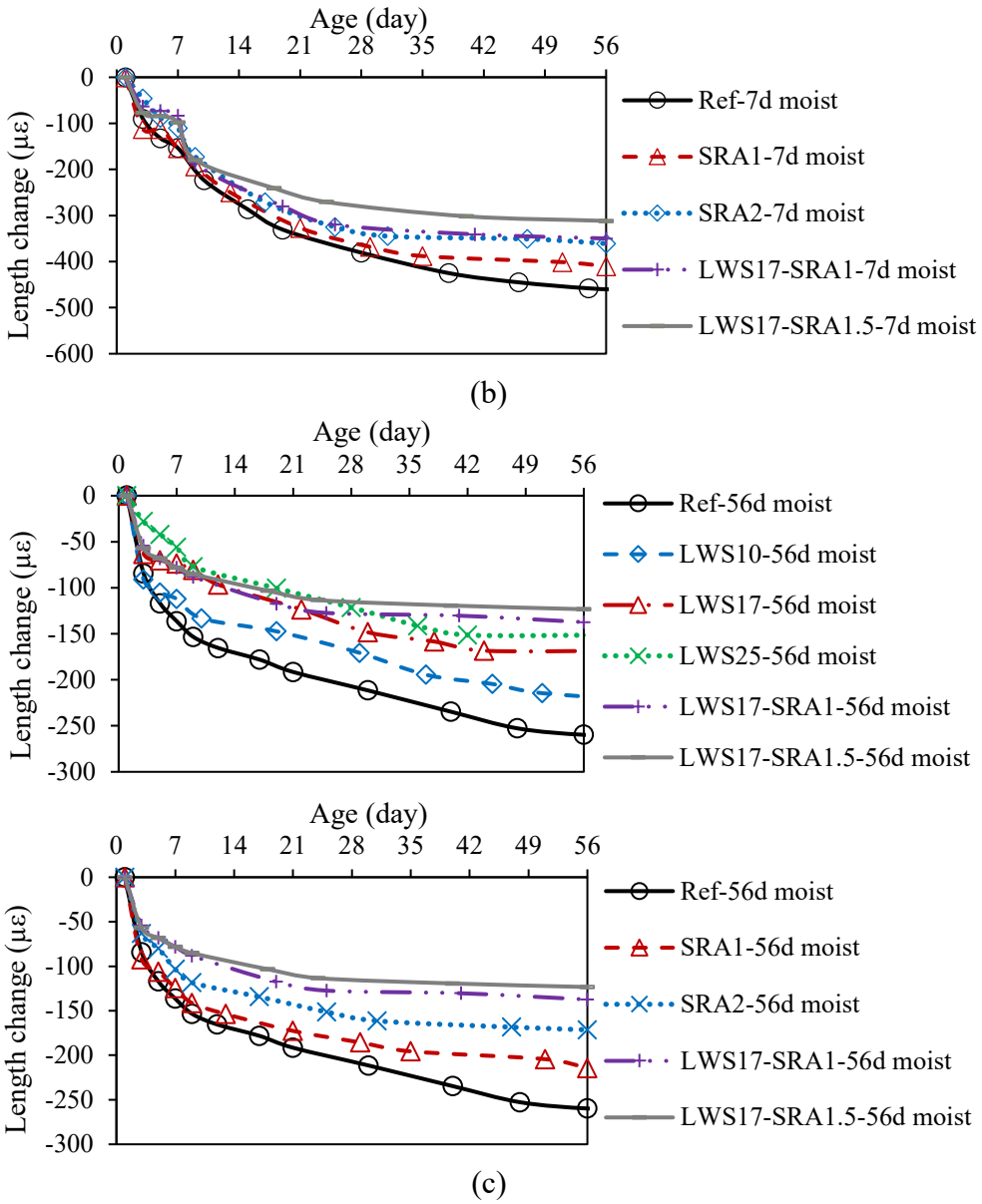

Figure 3.15 Influence of LWS & SRA on shrinkage of UHPC at (a) 3 d, (b) 28 d, and (c) 56 d

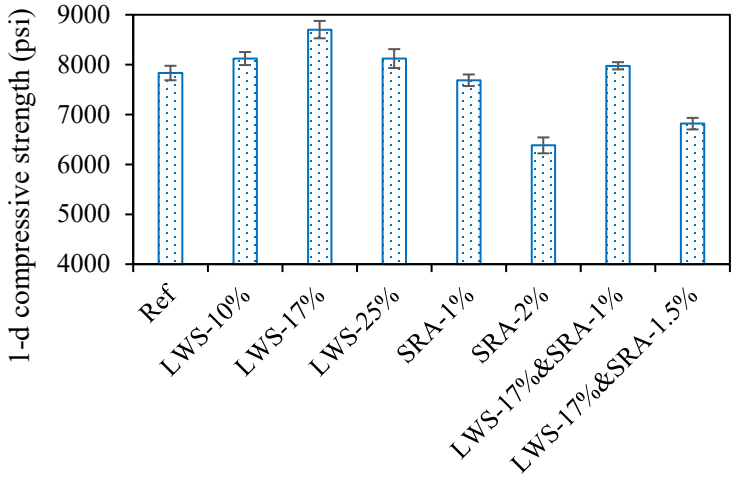
1-d compressive strength (psi)
9000
8000
7000
6000
5000
4000
Ref
LWS-10%
LWS-17%
LWS-25%
SRA-1%
SRA-2%
LWS-17%&SRA-1%
LWS-17%&SRA-1.5%

(a)

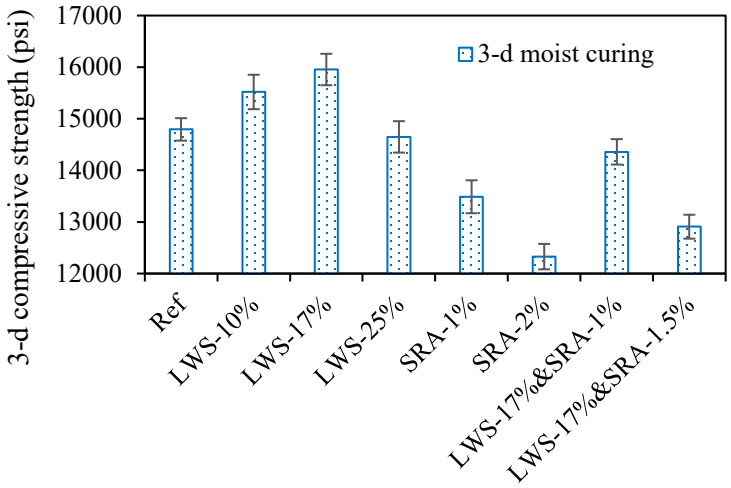
3-d compressive strength (psi)
17000
16000
15000
14000
13000
12000
3-d moist curing
Ref
LWS-10%
LWS-17%
LWS-25%
SRA-1%
SRA-2%
LWS-17%&SRA-1%
LWS-17%&SRA-1.5%

(b)

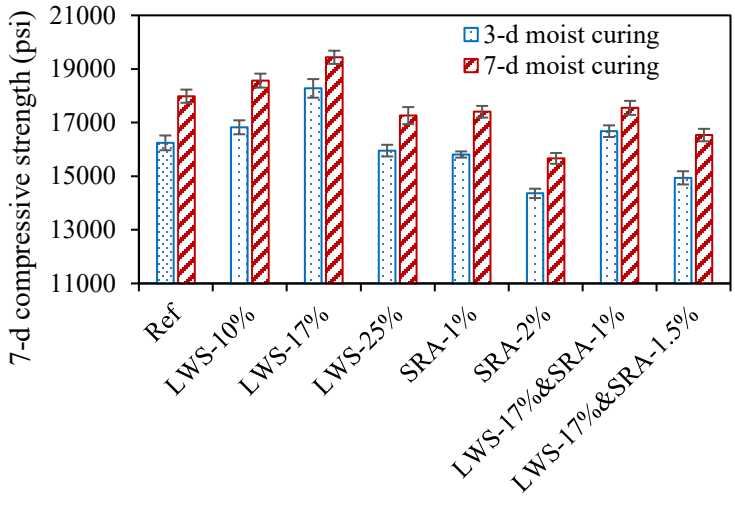
7-d compressive strength (psi)
21000
19000
17000
15000
13000
11000
3-d moist curing
7-d moist curing
Ref
LWS-10%
LWS-17%
LWS-25%
SRA-1%
SRA-2%
LWS-17%&SRA-1%
LWS-17%&SRA-1.5%

(c)

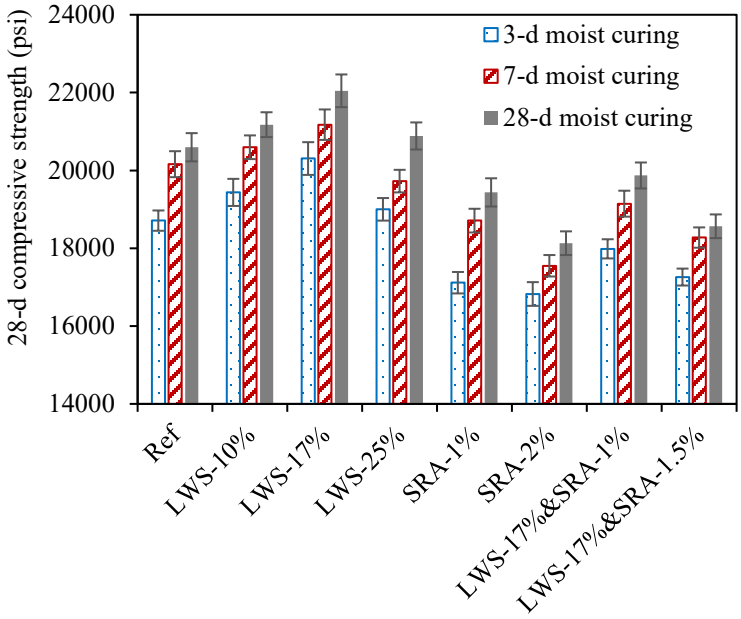

(d)

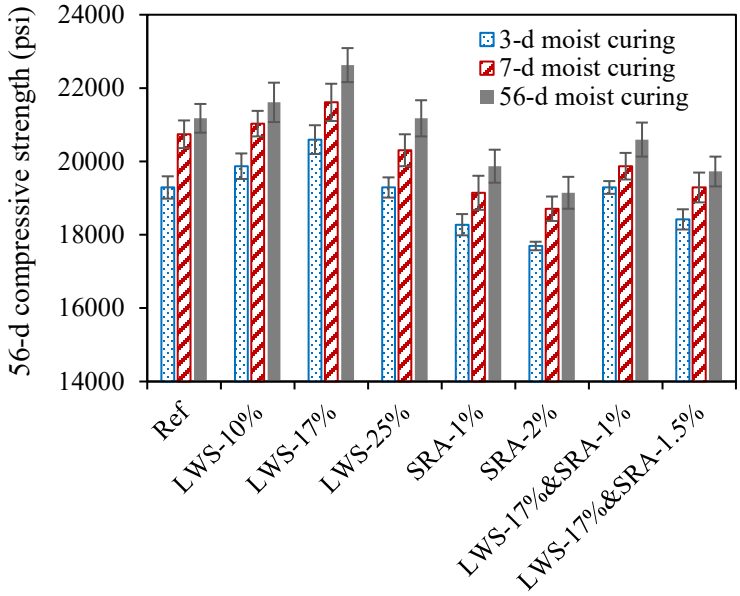

(e)

Figure 3.16 Influence of LWS, SRA, and curing age on compressive strength of UHPC at (a) 1 d, (b) 3 d, (c) 7 d, (d) 28 d, and (e) 56 d

In general, the increase of autogenous shrinkage slowed down after 7 d. The incorporation of LWS and SRA was effective in reducing the autogenous shrinkage as shown in **Figure 3.17**. For example, 14-d autogenous shrinkage was reduced by 25% using 25% LWS or 30% using 2% SRA. The combined use of 17% LWS and 1% SRA exhibited a low autogenous shrinkage of -315 με at

14 d. The LWS17 and SRA1.5 mixture exhibited a similar autogenous shrinkage compared to the LWS17 and SRA1 mixture.

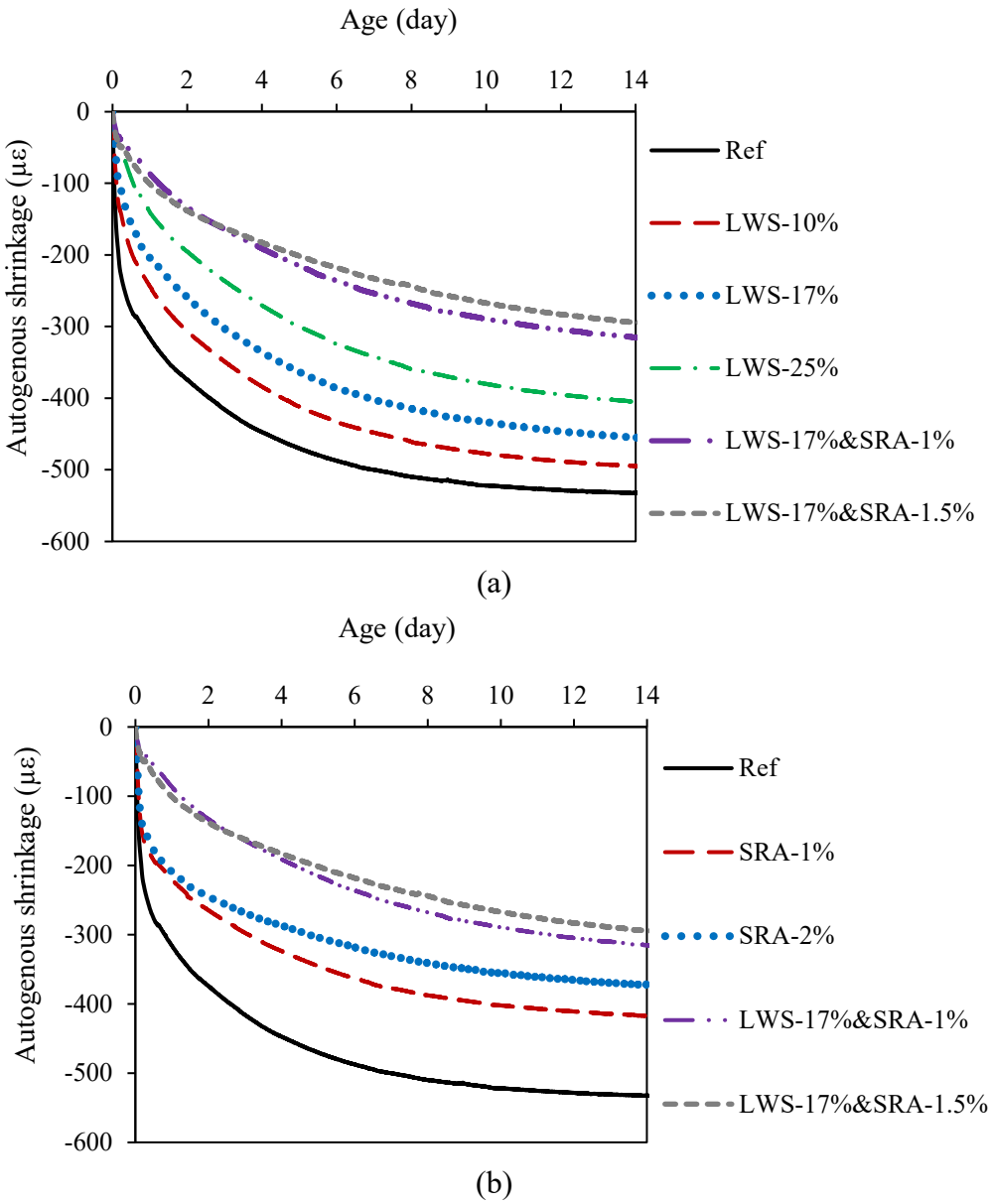

Figure 3.17 Influence of LWS and SRA on autogenous shrinkage of UHPC

3.3.3 Effect of Fiber Content

The unit weight, air content, and temperature of UHPC made with LWS and SRA is presented in **Table 3-9**. In general, the increase of fiber content from 2% to 3.25% increased the unit weight from 148 to 153 lb/ft^3 for the LWS17 and LWS17 and SRA1 mixtures. The air content was slightly reduced with the increase in fiber content.

The effect of fiber content on SP demand to maintain a fixed slump flow of 7.5 ± 0.5 in. is shown in **Figure 3.18**. The increase of fiber content from 2% to 3.25% led to 10% increase in SP content for the LWS17 and LWS17 and SRA1 mixtures.

Table 3-9 Unit weight, air content, and temperature of fresh UHPC

Mixture	Unit weight (lb/ft^3)	Air content (%)	Temperature (°F)
LWS17-2%	148	2.1	86.2
LWS17-3.25%	153	0.9	86.4
LWS17 and SRA1-2%	148	2.3	84.4
LWS17 and SRA1-2.6%	150	1.7	85.8
LWS17 and SRA1-3.25%	153	1.0	86.0

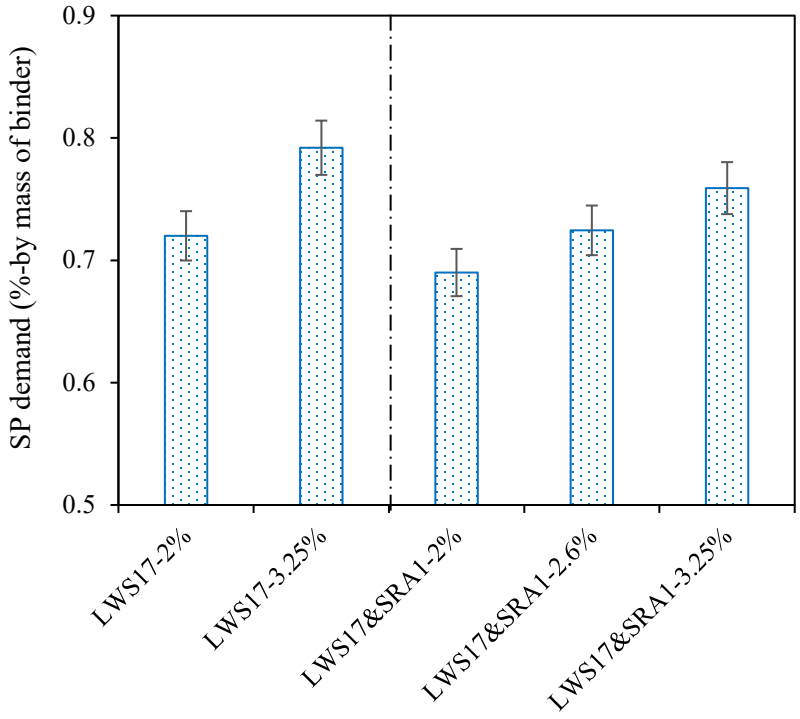

Figure 3.18 Variation of SP demand with LWS and SRA (slump flow of 7.5 ± 0.5 in.)

Table 3-10 presents the effect of fiber content on the variation of slump flow of UHPC with rest time. In general, the UHPC made with higher fiber content showed a lower level of fluidity.

The effect of fiber content on yield stress and plastic viscosity of UHPC is presented in **Figure 3.19**. The increase in fiber content from 2% to 3.25% led to an increase of yield stress from 95 to 130 Pa (0.0138 to 0.0189 psi) and plastic viscosity from 10 to 20 Pa·s (0.0014 to 0.0029 psi·s).

Table 3-10 Variation of slump flow with a rest time of UHPC

Mixture	Slump flow before jolting (in.)				Slump flow after 25 jolts (in.)			
	0 min	5 min	15 min	30 min	0 min	5 min	15 min	30 min
LWS17-2%	7.1	5.1	4.3	4.0	9.3	7.0	6.4	5.5
LWS17-3.25%	6.7	4.8	4.0	4.0	8.3	6.9	6.1	5.2
LWS17 and SRA1-2%	7.6	5.7	4.7	4.2	9.1	7.7	7.1	6.2
LWS17 and SRA1-2.6%	7.2	5.7	4.6	4.0	8.6	7.5	6.5	5.9
LWS17 and SRA1-3.25%	6.9	5.6	4.6	4.0	8.2	7.2	6.1	5.4

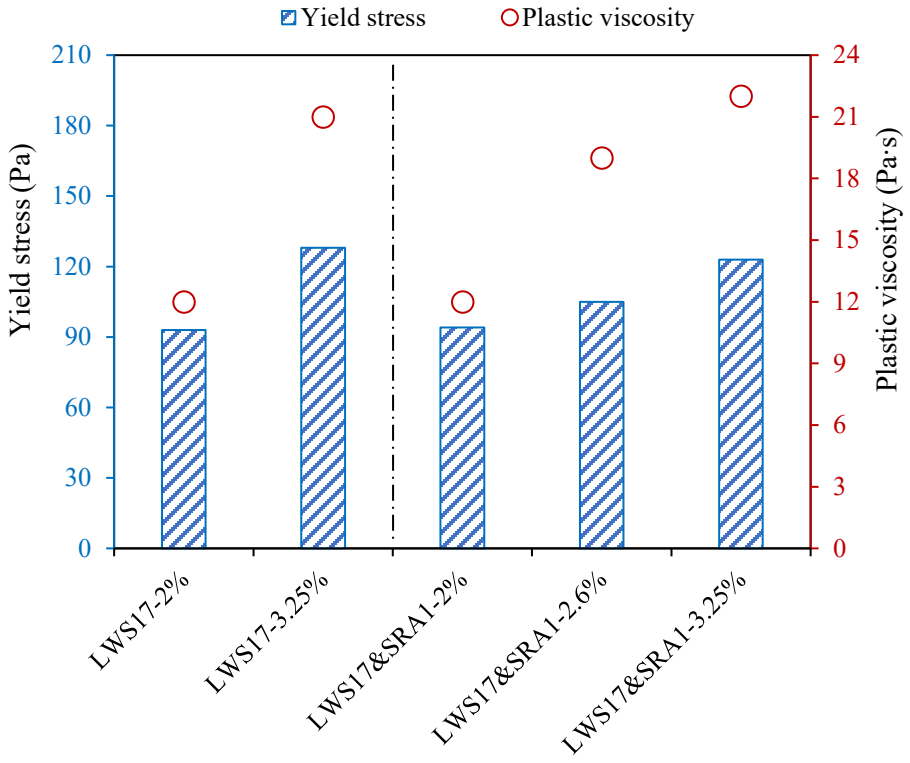

Figure 3.19 Influence of LWS and SRA on yield stress and plastic viscosity of UHPC

Figure 3.20 presents the variations of τ_{thix} and A_{thix} of UHPC made with different fiber contents. For the LWS17 and SRA1 mixture, the increase of fiber content from 2% to 3.25% led to 100%

and 45% increase in τ_{thix} and A_{thix}, respectively. Such increase was 140% and 50% for τ_{thix} and A_{thix}, respectively, for the LWS17 mixture.

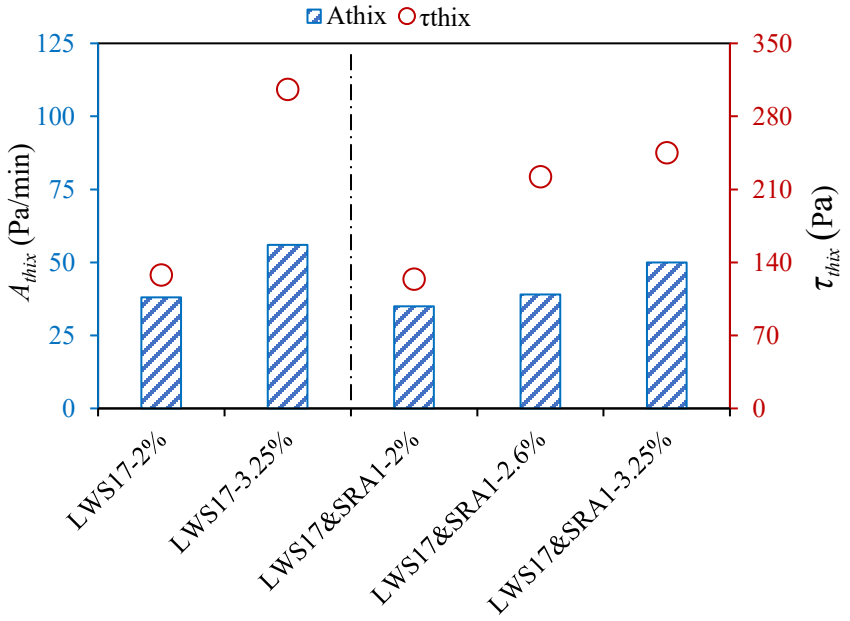

Figure 3.20 Influence of fiber content on τ_{thix} and A_{thix} of UHPC

As shown in **Figure 3.21**, $A_{thix.PV}$ was enhanced with the increase of fiber content. For example, for the LWS17 and SRA1 mixture, the increase of fiber content from 2% to 3.25% led to an increase of $A_{thix.PV}$ from 105 to 120 Pa/min (0.015 to 0.017 psi/min).

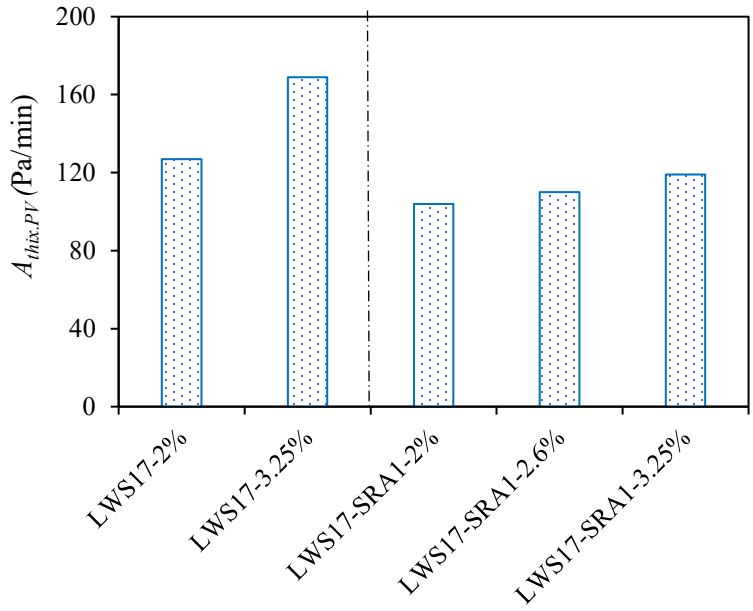

Figure 3.21 Influence of fiber content on $A_{thix.PV}$ of UHPC (1 Pa = 0.000145 psi)

Table 3-11 depicts the effect of fiber content on the variations of USS and DSS of UHPC. The increase of fiber content accelerated the loss of spread for both USS and DSS tests.

Table 3-11 Variations of USS and DSS with a rest time of UHPC with different fiber contents

Mixture	USS (in.)				DSS (in.)			
	0 min	5 min	10 min	15 min	0 min	5 min	15 min	30 min
LWS17-2%	13.0	8.7	4.2	4.0	13.0	10.0	9.0	7.0
LWS17-3.25%	10.2	7.3	4.0	4.0	10.2	8.5	7.5	7.2
LWS17 and SRA1-2%	12.0	8.0	5.2	4.0	12.0	10.5	10.3	10.0
LWS17 and SRA1-2.6%	10.5	7.5	5.4	4.0	10.5	9	8.0	7.6
LWS17 and SRA1-3.25%	10.1	7.3	4.5	4.0	10.1	8.7	7.4	7.0

The variation of autogenous shrinkage of UHPC made with different fiber contents is shown in **Figure 3.22**. The increase of fiber content had a limited effect on the autogenous shrinkage of UHPC. For example, the increase of fiber content from 2% to 3.25% reduced the 28-d autogenous shrinkage by 7% and 9% for the LWS17 and LWS17 and SRA1 mixtures, respectively.

Drying shrinkage was monitored after demolding at 1 d of age. The specimens were subjected to initial moist curing of 7 d in lime-saturated water at 68 ± 5 °F followed by air curing at 68 ± 5 °F and 50% ± 4% relative humidity until the age of 56 d. The effect of fiber content on the shrinkage of UHPC is presented in **Figure 3.23.** The increase of fiber content slightly decreased shrinkage. For UHPC made with 17% LWS and 1% SRA, the increase in fiber content from 2% to 3.25% reduced the 56-d shrinkage from -350 to -300 με. Such reduction was from -400 to -380 με for the UHPC made with 17% LWS.

Figure 3.24 shows the variations of the strain of the inner steel ring with time. The negative value indicates compressive strain. Shrinkage of UHPC led to compressive stress in the steel ring. In general, the strain decreased gradually at first 7 d, followed by a rapid drop at 7 d due to the change of moist curing to the beginning of the drying shrinkage (air curing). Then the rate of reduction slowed down. Limited strain variation in shrinkage was found after 30 d. An increase of steel fiber volume reduced shrinkage, resulting in lower compressive stress in the steel ring. For example, the increase of fiber content from 2% to 3.25% of the UHPC prepared with 17% LWS and 1% SRA reduced the compressive strain from 155 to 110 με at 90 d.

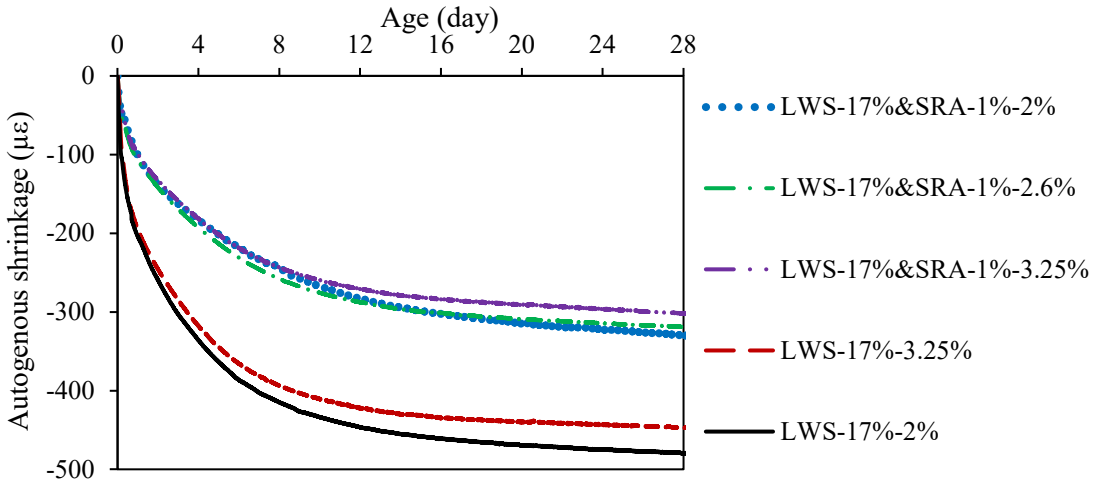

Figure 3.22 Influence of fiber content on autogenous shrinkage of UHPC

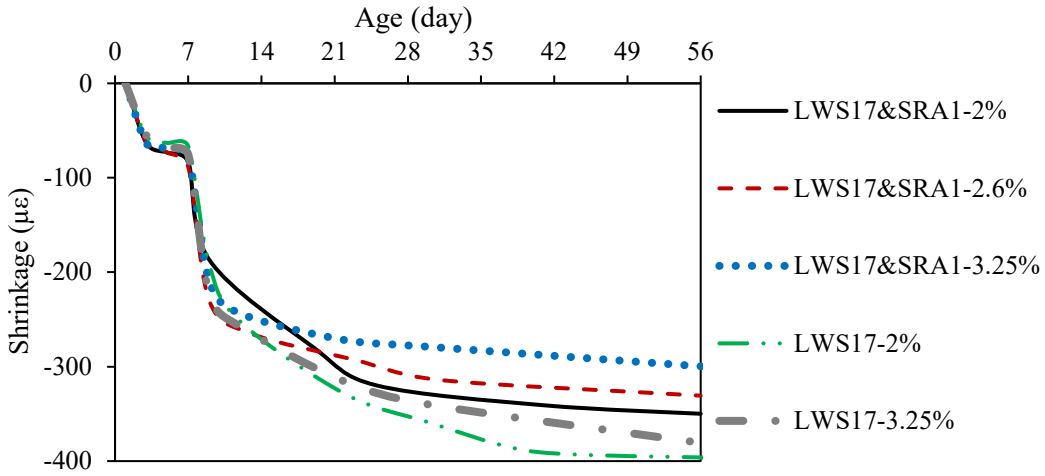

Figure 3.23 Influence of fiber content on drying shrinkage of UHPC mortar

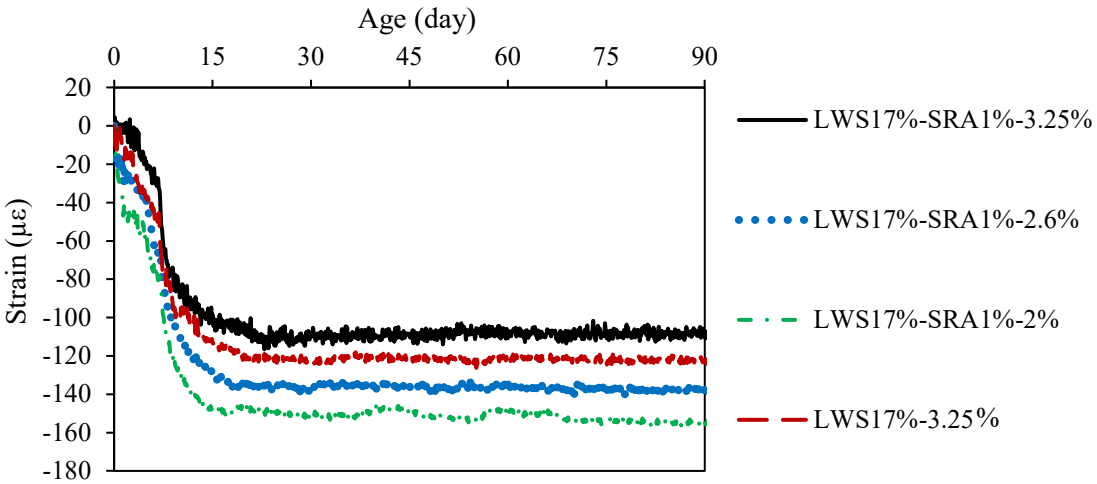

Figure 3.24 Effect of fiber content on restrained shrinkage

The compressive strength of UHPC made with different fiber contents is presented in **Figure 3.25**. All mixtures were subjected to 3, 7, and 56 d of moist curing. The increase of fiber content enhanced compressive strength. For example, the 28-d compressive strength of the LWS17 and SRA1 mixture was enhanced by 10% with the increase of fiber volume from 2% to 3.25%.

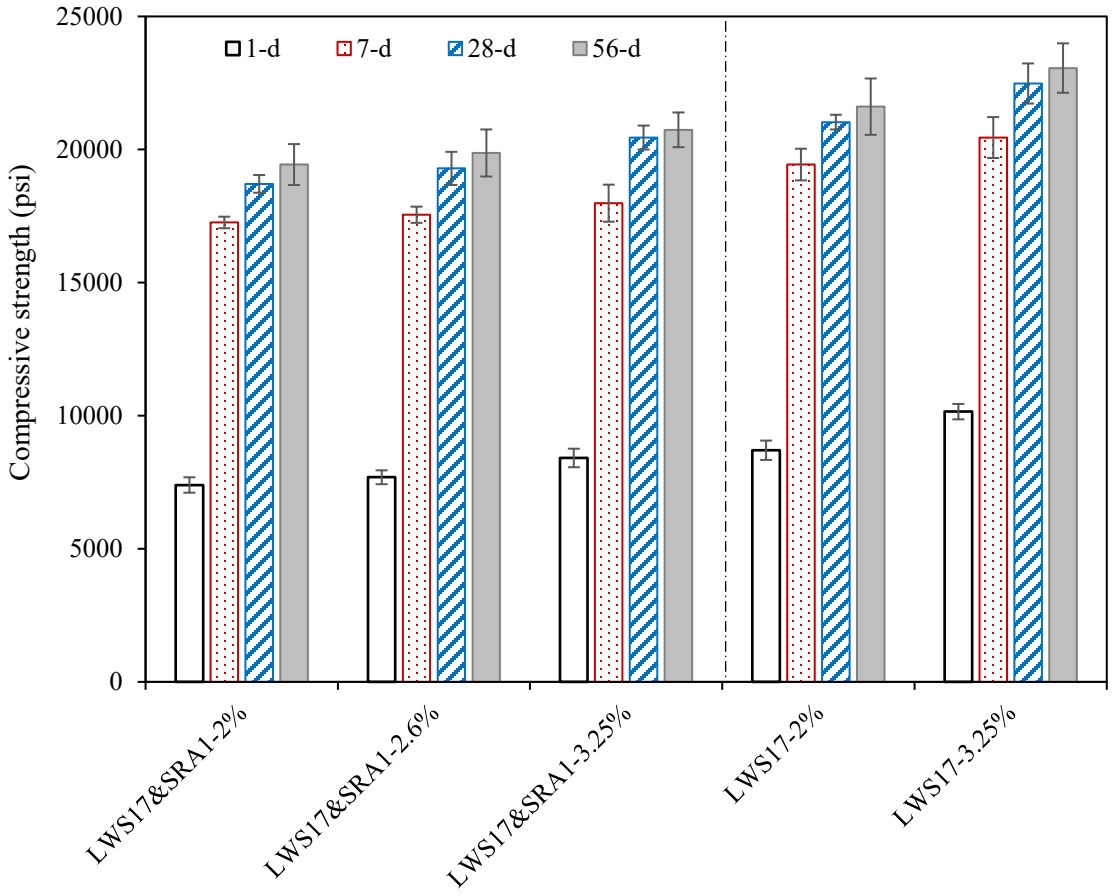

Figure 3.25 Influence of fiber content on compressive strength of UHPC

The effect of fiber content on flexural performance is shown in **Figure 3.26**. Three stages were observed in the load-deflection curves, including the elastic stage (linear increase), the deflection-hardening stage (non-linear increase), and the deflection-softening stage (non-linear decrease).

Figure 3.27 shows the variations of flexural strength and toughness of UHPC. The latter one is defined as the area within the flexural load-deflection curve between deflection values of 0 and L/150 (L is the span of the beam, and is equal to 12 in.) The increase of fiber content enhanced flexural strength and toughness. For example, the 28-d flexural strength and toughness of the LWS17 and SRA1 mixture increased by 30% and 35%, respectively, with the increase of fiber volume.

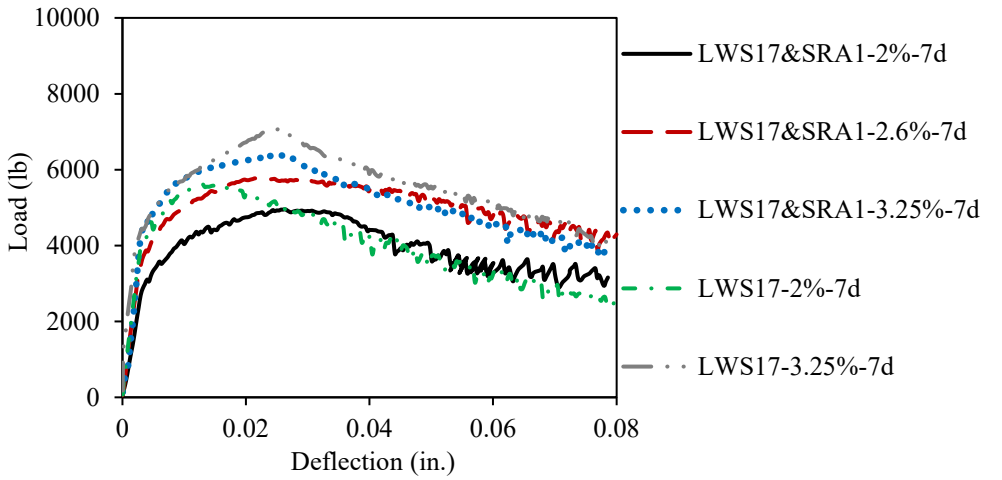

(a)

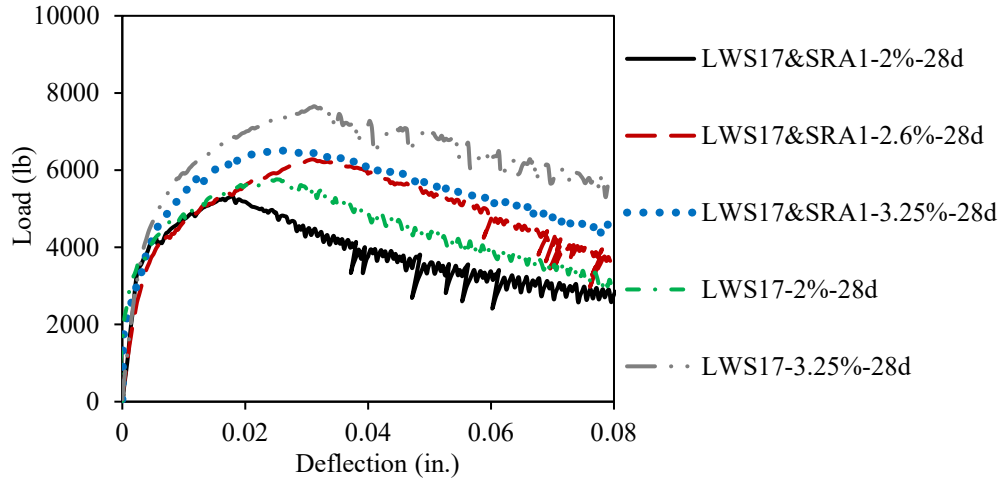

(b)

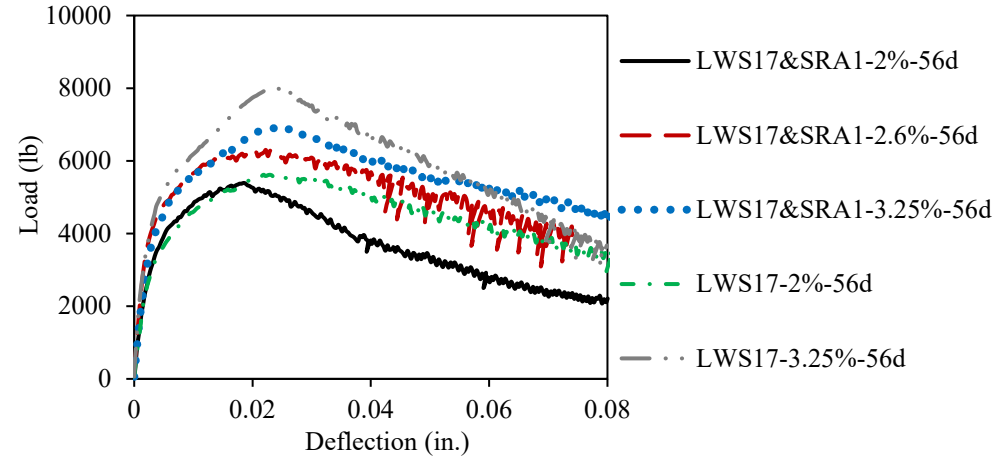

(c)

Figure 3.26 Influence of fiber content on load-deflection curve of UHPC at (a) 7 d, (b) 28 d, and (c) 56 d

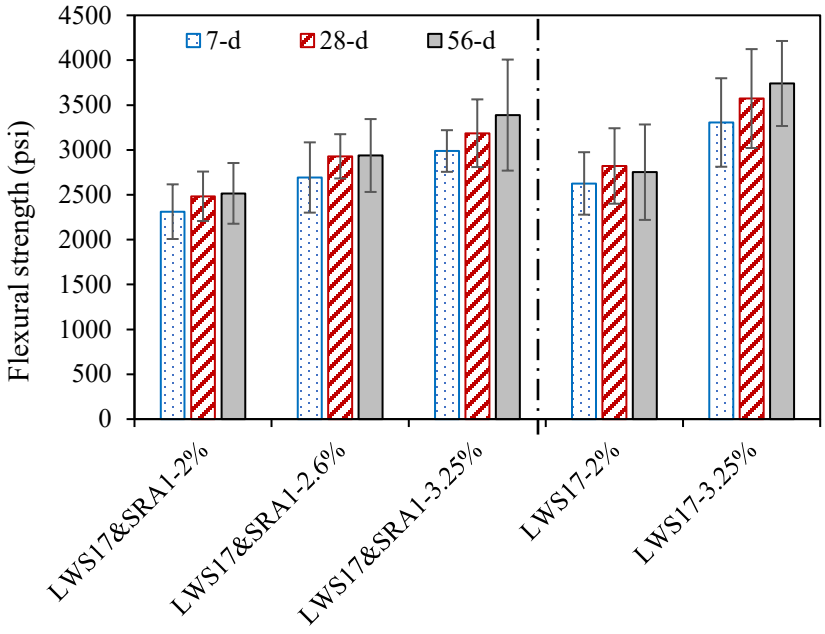

(a)

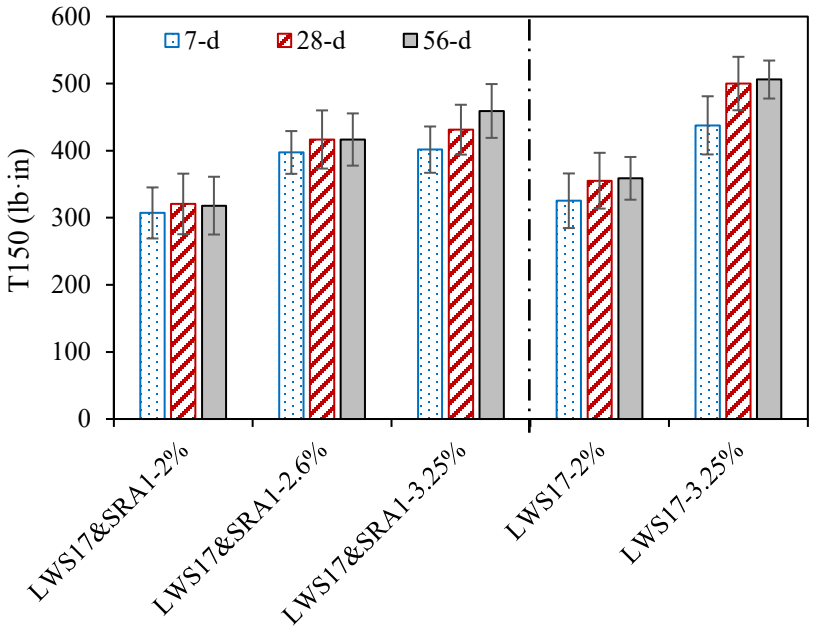

(b)

Figure 3.27 Influence of fiber content on (a) flexural strength and (b) toughness

3.3.4 Robustness of UHPC - Effect of Small Variation of W/CM, Sand Moisture Content, and SP Dosage on Performance

The variations of unit weight and calculated air content and temperature of the investigated UHPC mixtures with w/cm, sand moisture content, and SP dosage are shown in **Table 3-12**. The decrease in w/cm from 0.2 to 0.18 increased unit weight from 153 to 160 lb/ft^3 and air content from 1% to

2.7%. The variation in sand moisture by ±1 and SP dosage by ±10% had an insignificant effect on unit weight, air content, and temperature.

Table 3-12 Unit weight, air content, and temperature of fresh UHPC

Parameter	Variation	Unit weight (lb/ft^3)	Air content (%)	Temperature (°F)
w/cm	0.18	160	2.7	89
	0.20	153	1.0	86
	0.22	154	1.2	82
Sand moisture	-1%	156	0.6	86
	0	153	1.0	86
	+1%	152	1.3	88
SP dosage	-10%	154	0.85	83
	0	153	1.0	86
	+10%	155	0.3	81

The effect of w/cm and sand moisture on SP demand to maintain a fixed slump flow of 7.5 ± 0.5 in. is shown in **Figure 3.28**. The decrease in w/cm from 0.2 to 0.18 led to a 40% increase in SP demand. Furthermore, the decrease in sand moisture content by -1% led to 20% reduction in SP demand. The increase in sand moisture content by +1% showed an insignificant effect on SP demand.

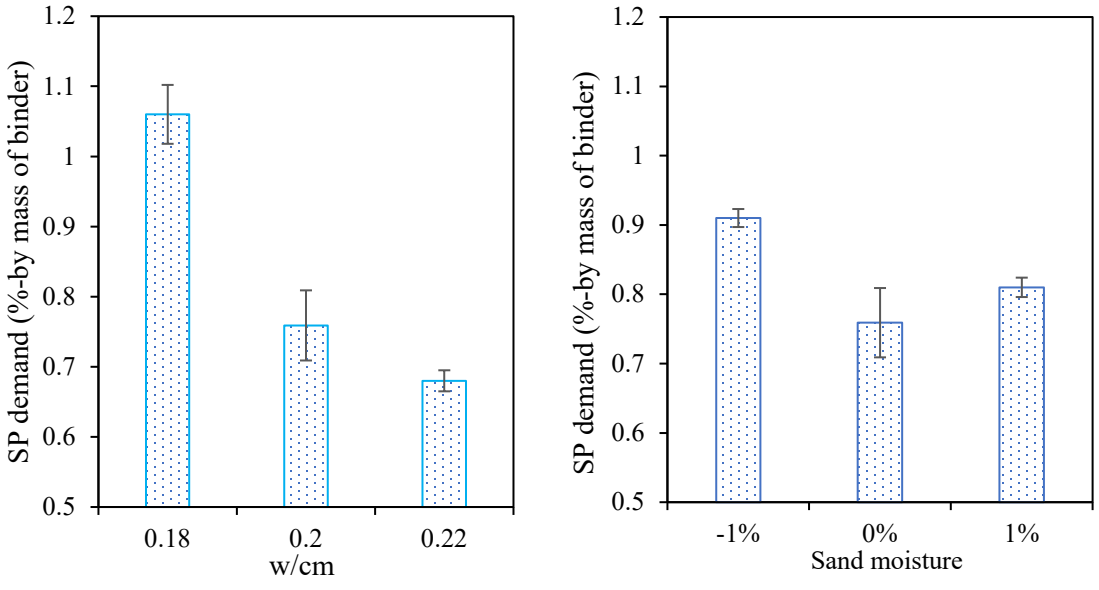

Figure 3.28 Variations of SP demand with (a) w/cm and (b) sand moisture

Table 3-13 presents the effect of w/cm, sand moisture, and SP dosage on the slump flow of UHPC with rest time. The slump flow test was conducted before and after 25 jolting cycles. The reduction in SP dosage by 10% reduced the initial slump flow and accelerated the loss of slump flow of the UHPC. The changes in sand moisture and w/cm had a limited effect on the variation of slump flow with time because additional SP was added to maintain slump flow.

Table 3-13 Variation of slump flow with a rest time of UHPC

Parameters	Variation	Slump flow before jolting (in.)				Slump flow after 25 jolts (in.)			
		0 min	5 min	15 min	30 min	0 min	5 min	15 min	30 min
w/cm	0.18	7.0	6.0	5.1	4.8	9.5	7.6	7.4	7.3
	0.20	6.9	5.6	4.6	4.0	8.2	7.2	6.1	5.4
	0.22	7.0	5.3	4.8	4.4	8.8	7.9	7.4	6.7
Sand moisture	-1%	7.3	5.9	5.3	4.8	9.8	7.8	7.5	6.4
	0	6.9	5.6	4.6	4.0	8.2	7.2	6.1	5.4
	+1%	7.6	5.7	4.7	4.2	9.1	7.7	7.1	6.2
SP dosage	-10%	4.5	3.5	3.0	3.0	6.0	5.5	5.0	4.5
	0	6.9	5.6	4.6	4.0	8.2	7.2	6.1	5.4
	+10%	6.5	5.8	5.5	5.0	8.0	7.5	6.5	6.0

The effect of w/cm, sand moisture content and SP dosage on the yield stress, plastic viscosity, and thixotropy (τ_{thix} and A_{thix}) of the UHPC is presented in **Figures 3.29-3.30**. The yield stress, plastic viscosity, τ_{thix} and A_{thix} increased by 460%, 40%, 160%, and 130% respectively with the increase in SP dosage by 10%. Furthermore, the decrease in w/cm by 10% increased yield stress, plastic viscosity, τ_{thix} and A_{thix} by 80%, 40%, 40%, and 20% respectively.The increase in w/cm and sand moisture content by 10% and 1% respectively had limited influence on the rheological properties of UHPC.

Figure 3.31 presents the variation of $A_{thix.PV}$ with w/cm, sand moisture, and SP dosage. The $A_{thix.PV}$ was determined using a portable vane. The decrease in SP dosage by 10% increased $A_{thix.PV}$ by 40%. Similarly, the decrease in w/cm from 0.2 to 0.18 increased $A_{thix.PV}$ by 40%. The variation in sand moisture content by ±1% had an insignificant effect on $A_{thix.PV}$.

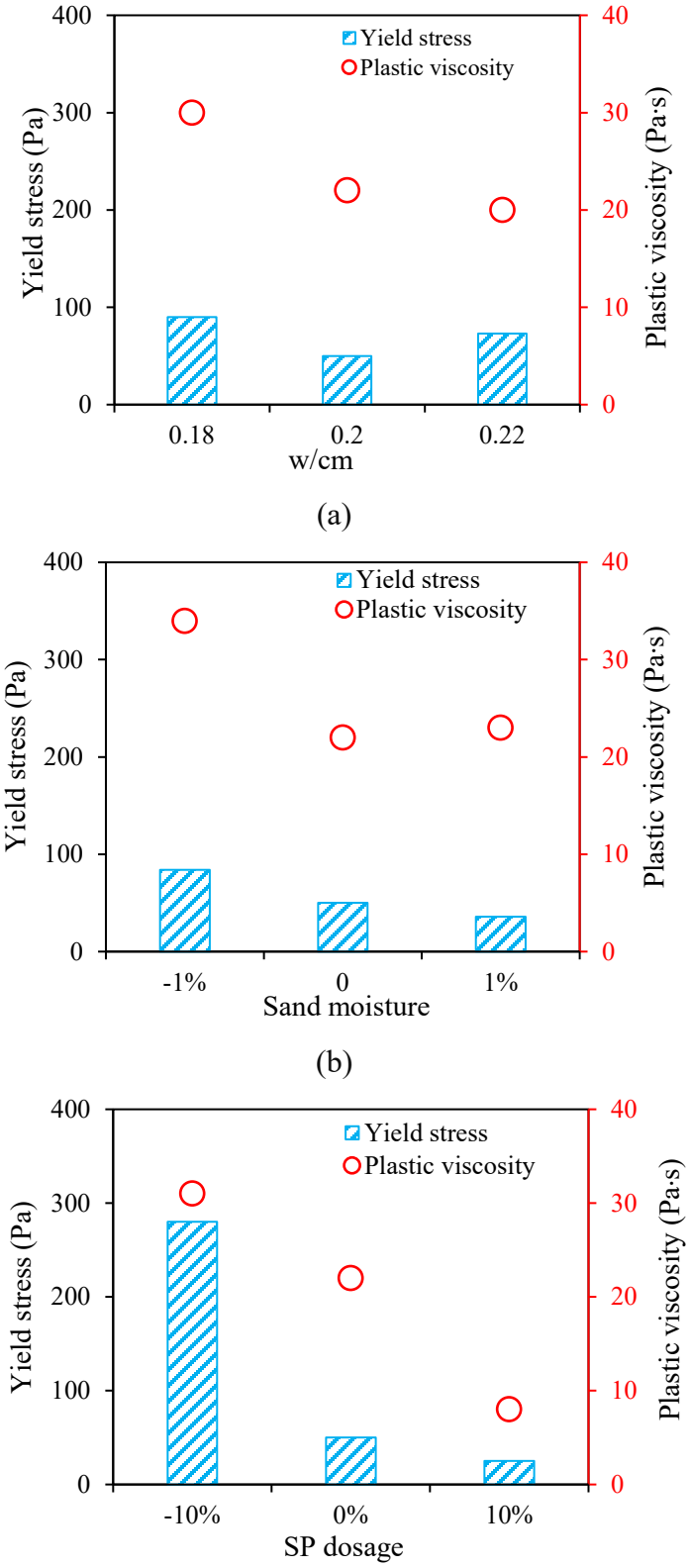

Figure 3.29 Variations of rheological properties with (a) w/cm, (b) sand moisture, and (c) SP dosage

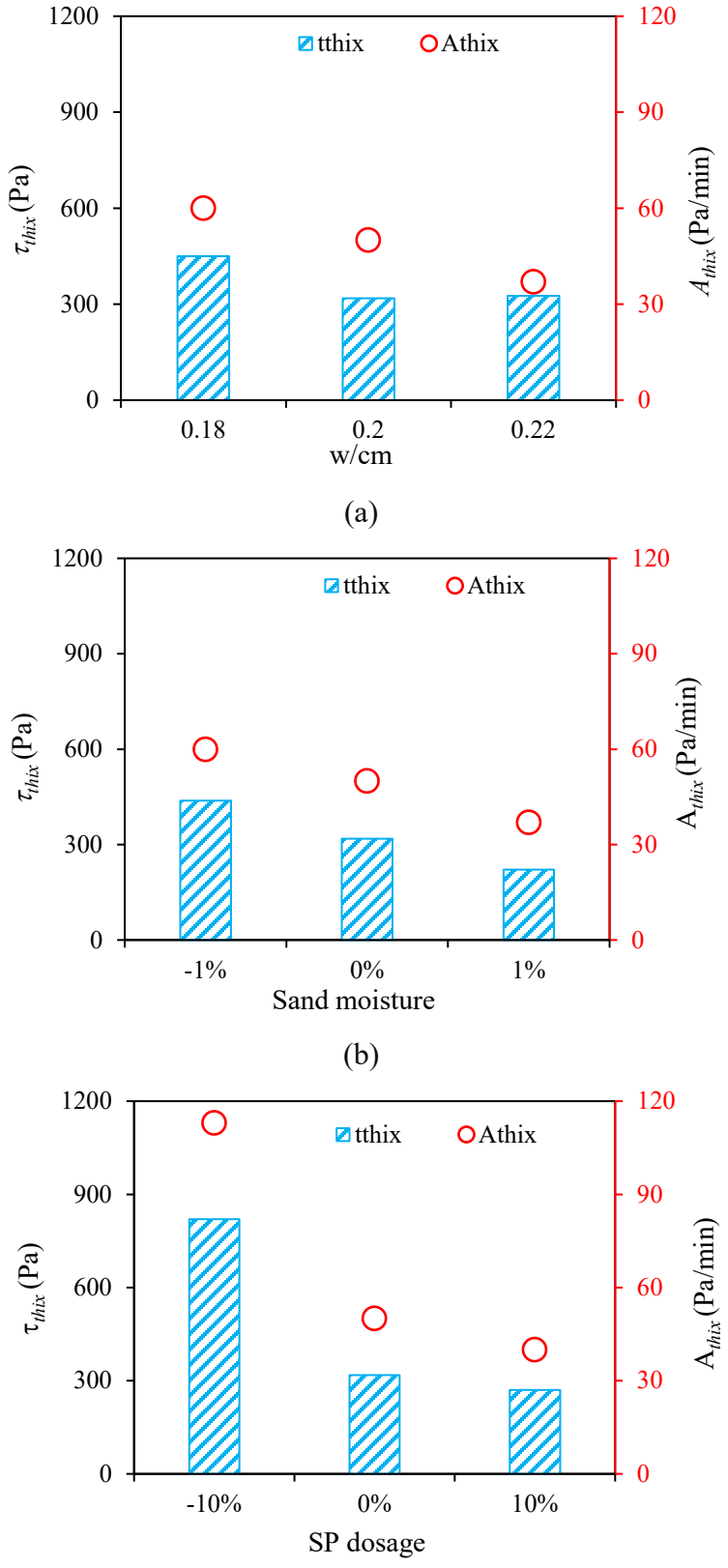

Figure 3.30 Variations of τ_{thix} and A_{thix} with (a) w/cm, (b) sand moisture, and (c) SP dosage

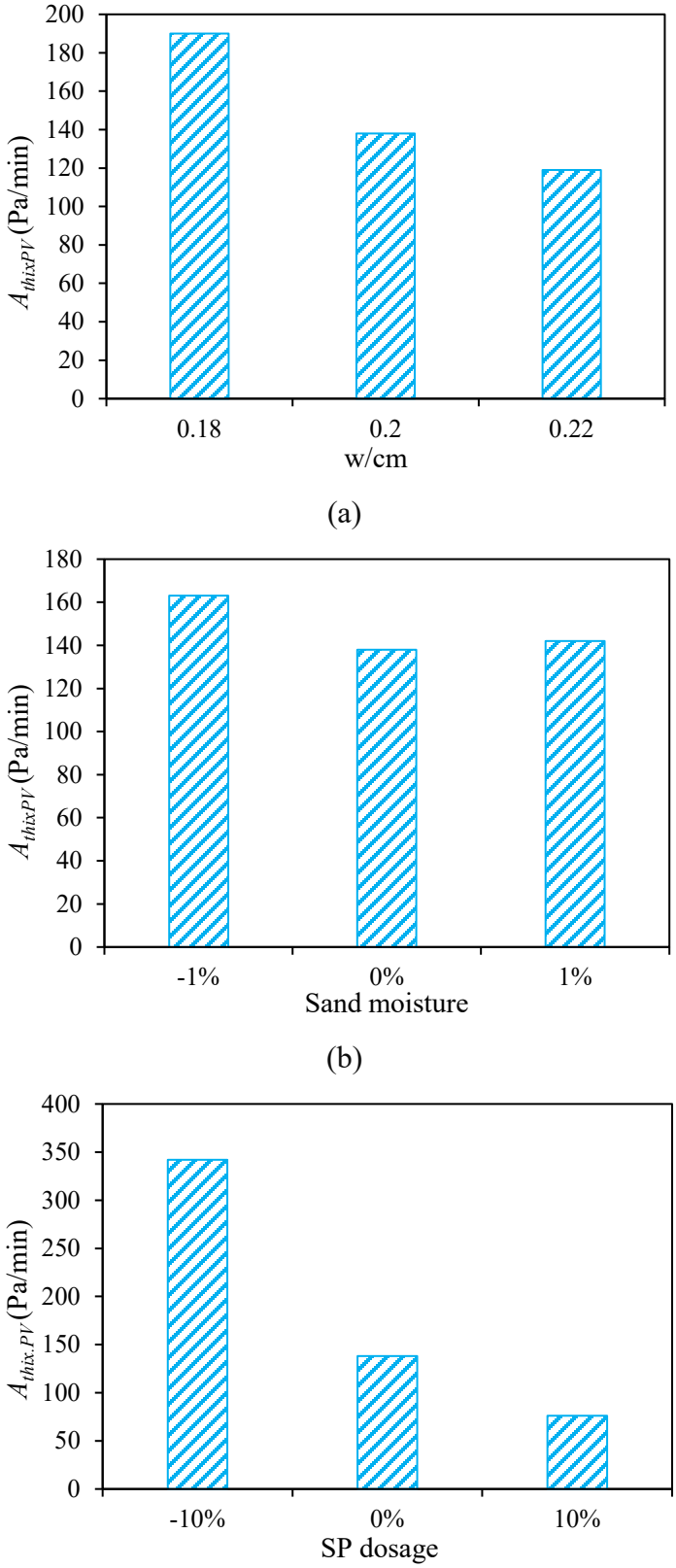

Figure 3.31 Variation of $A_{thix.PV}$ with (a) w/cm, (b) sand moisture, and (c) SP dosage

Table 3-14 shows the variations of undisturbed slump spread (USS) and disturbed slump spread (DSS) of the UHPC with w/cm, sand moisture, and SP dosage. The decreasing rate of USS and DSS values accelerated by reducing w/cm and SP dosage. However, the sand moisture had a limited effect on USS and DSS.

Table 3-14 Variations of USS and DSS with a rest time of UHPC with a variation on w/cm, sand moisture, and SP dosage

Parameters	Variation	USS (in.)				DSS (in.)			
		0 min	5 min	10 min	15 min	0 min	5 min	15 min	30 min
w/cm	0.18	9.5	8.0	6.8	6.5	13.0	8.0	7.5	7.3
	0.20	10.0	7.3	4.5	4.0	10.0	8.7	7.4	7.0
	0.22	11.0	8.3	7.5	6.5	11.0	9.0	9.0	8.5
Sand Moisture	-1%	11.0	8.3	7.0	7.0	11.0	9.5	9.2	8.0
	0	10.0	7.3	4.5	4.0	10.0	8.7	7.4	7.0
	+1%	12.0	8.0	5.2	4.0	12.0	10.	10.3	10.0
SP dosage	-10%	8.5	7.5	7.0	6.5	8.0	7.7	7.0	6.7
	0	10.0	7.3	4.5	4.0	10.0	8.7	7.4	7.0
	+10%	12.0	8.0	5.2	4.0	12.0	10.0	10.3	10.0

The variation of autogenous shrinkage of UHPC with changes in w/cm, sand moisture content, and SP dosage is shown in **Figure 3.32**. The decrease of w/cm from 0.2 to 0.18 reduced 28-d autogenous shrinkage by 20%. The variation in sand moisture and SP dosage had a limited effect on autogenous shrinkage.

The effect of the variation in w/cm, sand moisture, and SP dosage on the shrinkage of UHPC is presented in **Figure 3.33**. The increase in w/cm by 10% increased the 56-d drying shrinkage from -300 to -335 με and in addition the decrease in w/cm resulted in a decrease in 56-d drying shrinkage to -260 με. On the other hand, the variations in sand moisture and SP dosage had a limited effect on drying shrinkage.

As presented in **Figure 3.34**, the variation in w/cm by ±10% and sand moisture by ±1% had limited influence on compressive strength. The compressive strength was reduced by 10% by decreasing SP dosage by 10%. This was associated with the low fluidity that led to difficulty in consolidation.

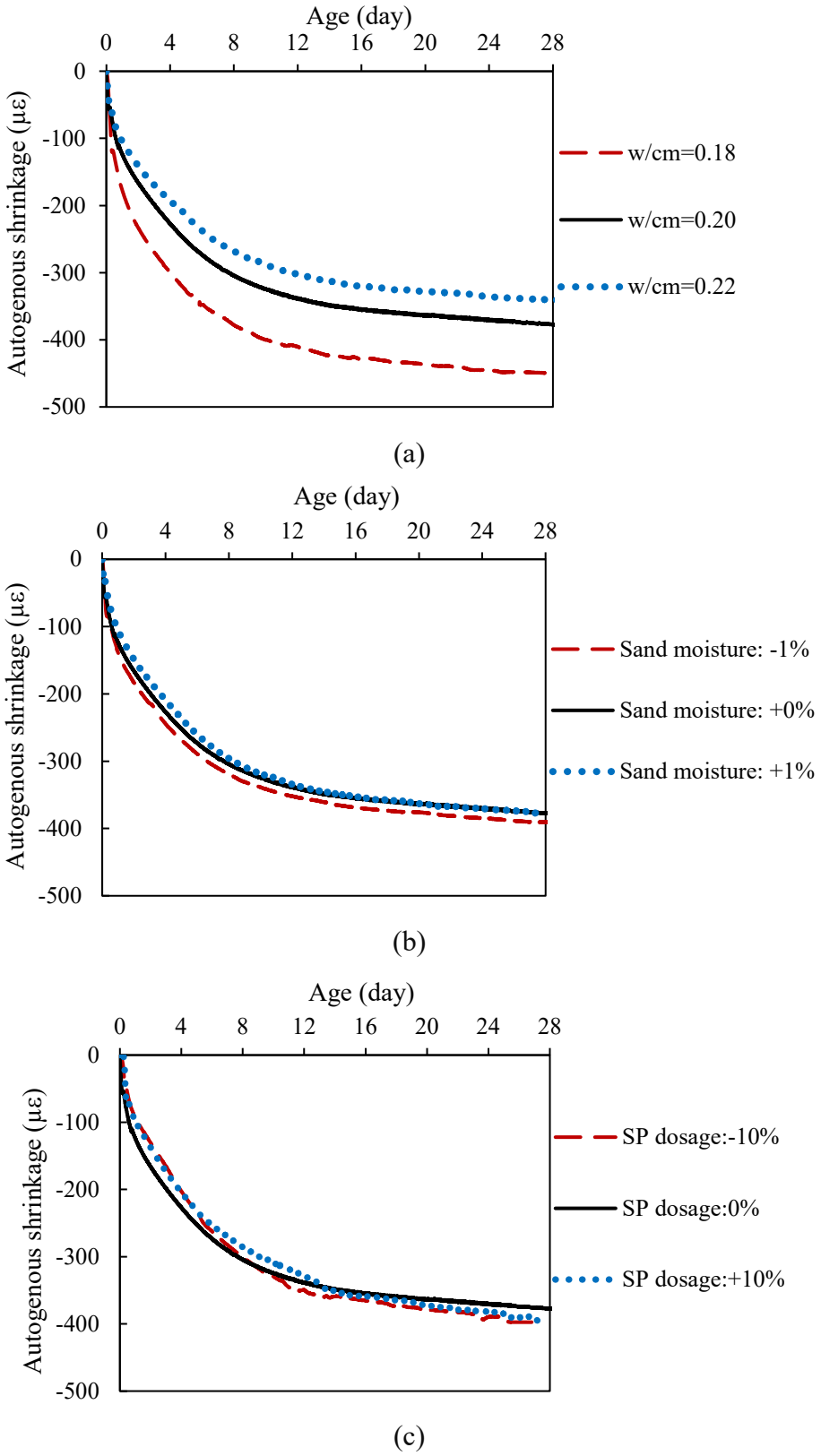

Figure 3.32 Variation of autogenous shrinkage of UHPC with limited changes in (a) w/cm, (b) moisture content of sand, and (c) SP dosage

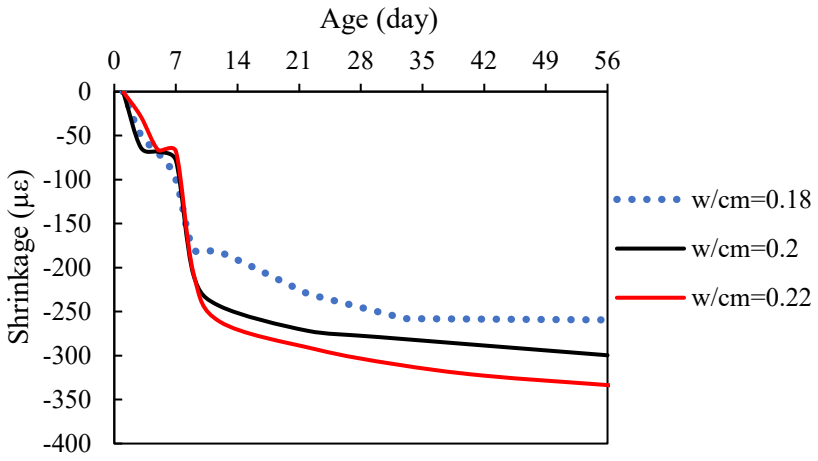

(a)

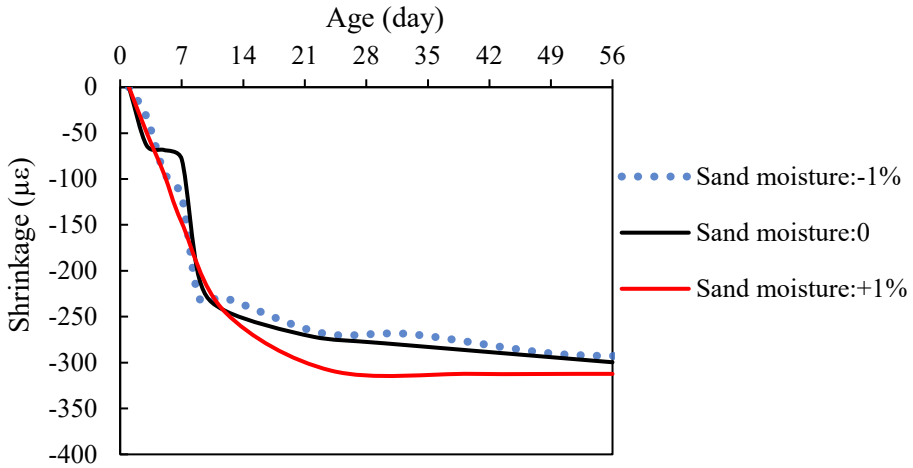

(b)

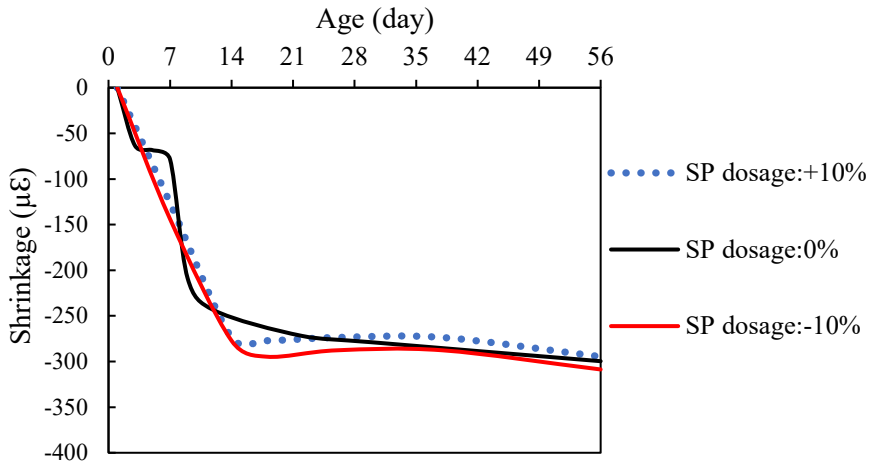

(c)

Figure 3.33 Variation of drying shrinkage of UHPC with limited changes in (a) w/cm, (b) sand moisture, and (c) SP dosage

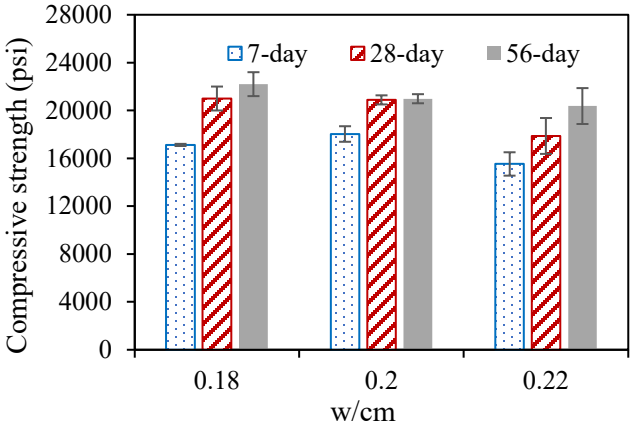

(a)

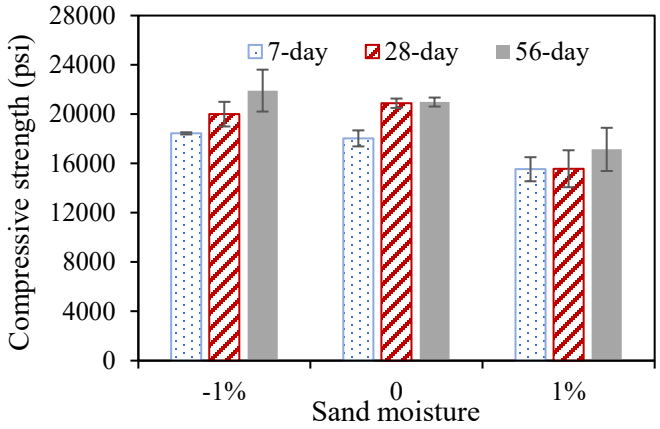

(b)

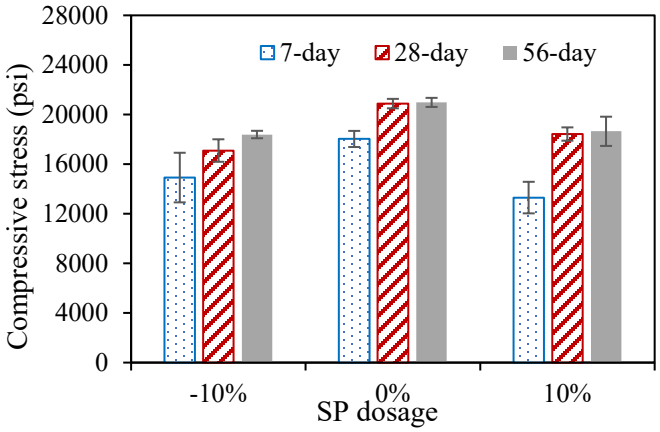

(c)

Figure 3.34 Variation of compressive strength of UHPC with (a) w/cm, (b) sand moisture, and (c) SP dosage

The variations of the 28- and 56-d flexural performance of UHPC with slight changes in w/cm, sand moisture content, and SP dosage are shown in **Figures 3.35-3.37**. Three stages were observed in the load-deflection curves, including the elastic stage (linear increase), deflection-hardening

stage (non-linear increase), and deflection-softening stage (non-linear decrease). The peak flexural tension stress for the mixtures made with 0.2 w/cm exceeded the minimum value specified by NY DOT of 2,000 psi.

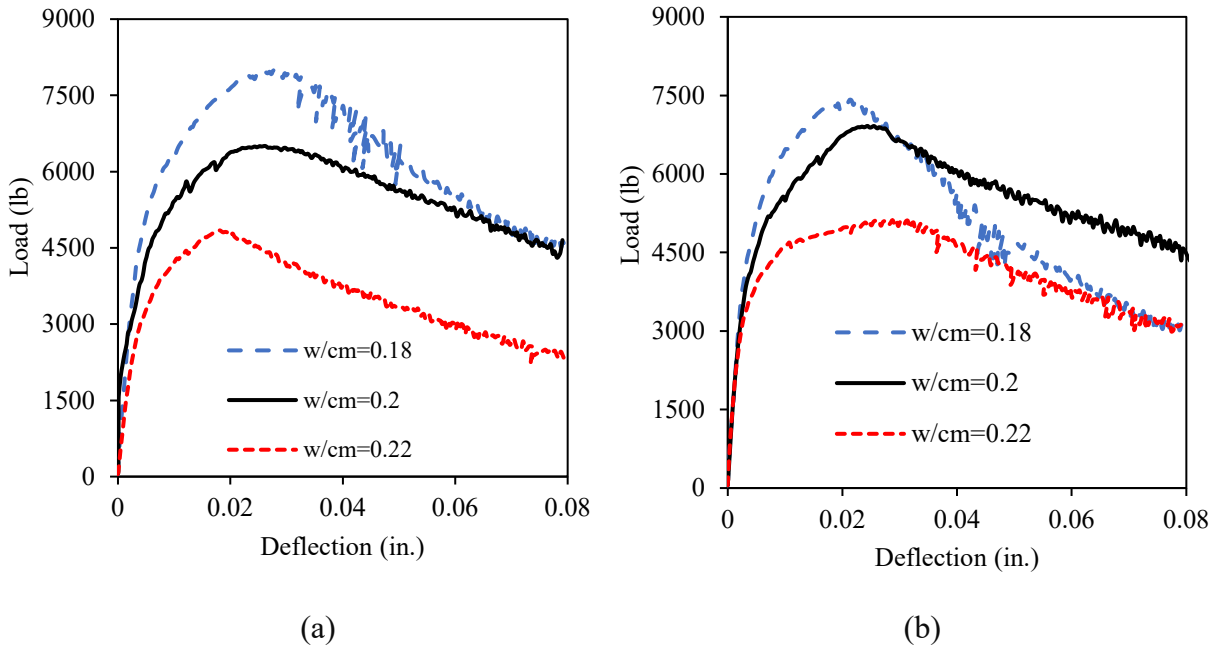

Figure 3.35 Influence of change in w/cm on load-deflection curve of UHPC prismatic specimens at (a) 28 d and (b) 56 d

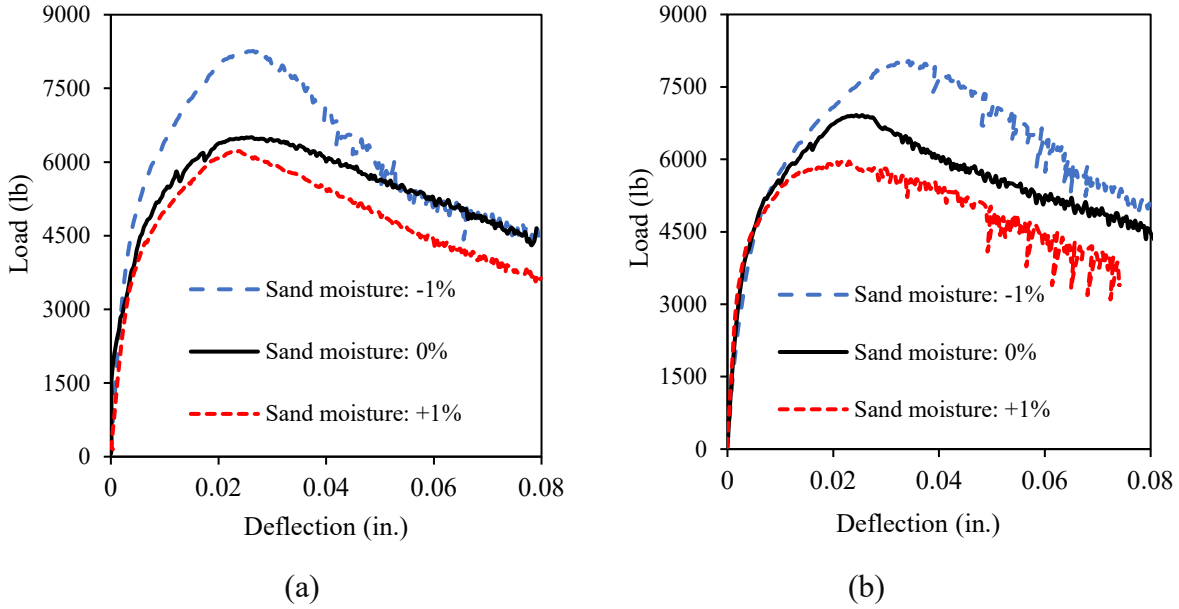

Figure 3.36 Influence of change in sand moisture on load-deflection curve of UHPC prismatic specimens at (a) 28 d and (b) 56 d

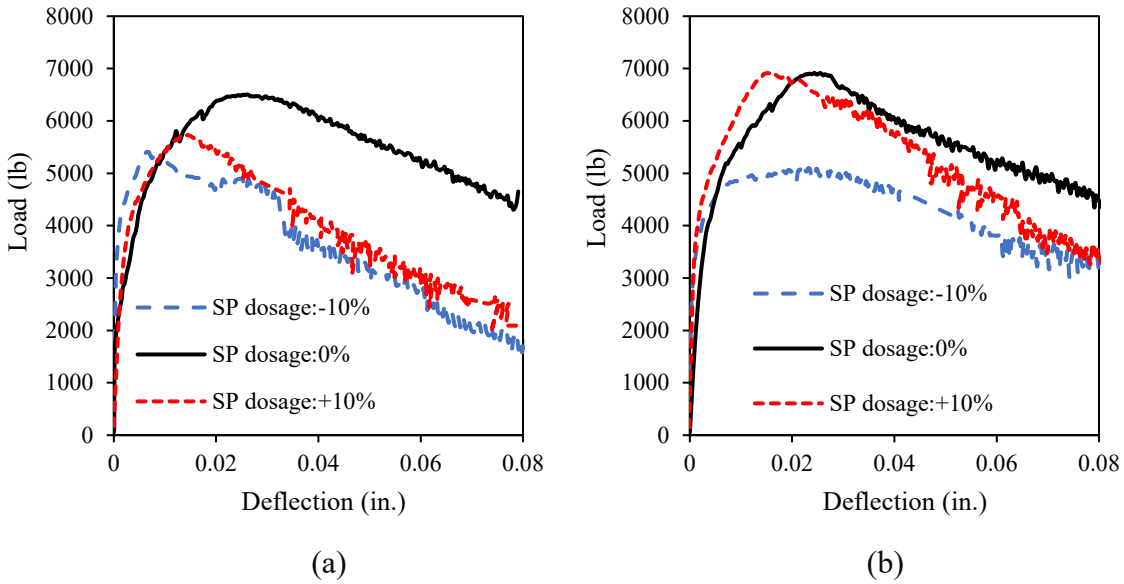

Figure 3.37 Influence of variation in SP dosage on load-deflection curve of UHPC prismatic specimens at (a) 28 d and (b) 56 d

Figures 3.38-3.40 show the variations of flexural strength and toughness of the UHPC mixture with w/cm, sand moisture content, and SP dosage, respectively. The toughness is defined as the area within the flexural load-deflection curve between deflection values of 0 and L/150 (L is the span of the beam and equals 12 in.). The slight decrease in w/cm by 10% reduced the 28-d flexural strength and 28-d toughness by 30% and 40% respectively. Such flexural indices were reduced by 21% and 18%, respectively, by increasing the sand moisture content by 1%. Both the increase and decrease in SP dosage reduced the 28-d flexural strength by 10% and 8%, respectively. This result was in an agreement with the effect of SP dosage on compressive strength.

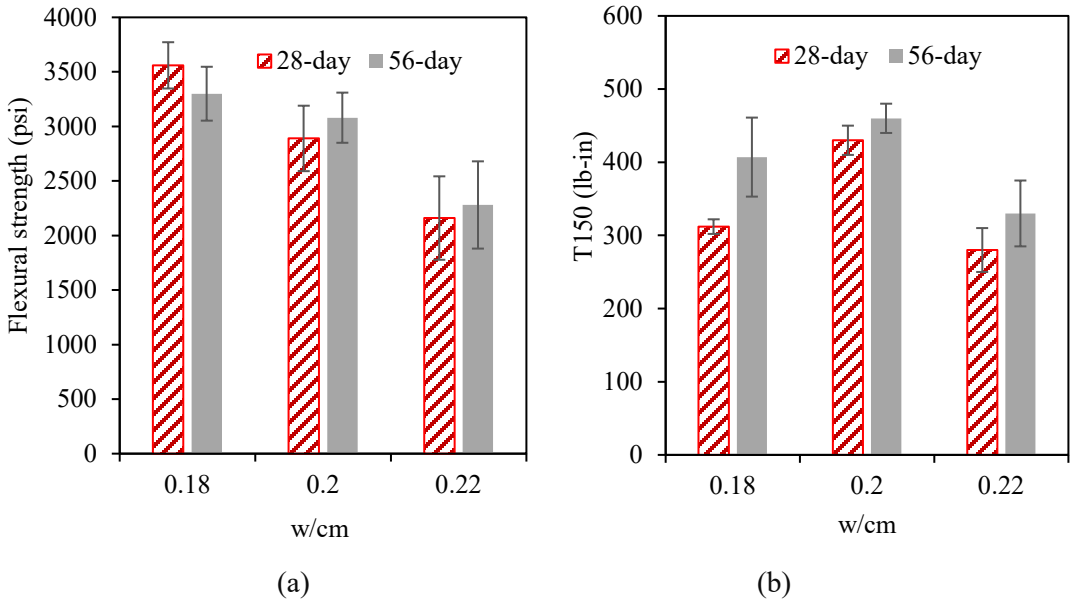

Figure 3.38 Influence of w/cm on (a) flexural strength and (b) T150 of UHPC

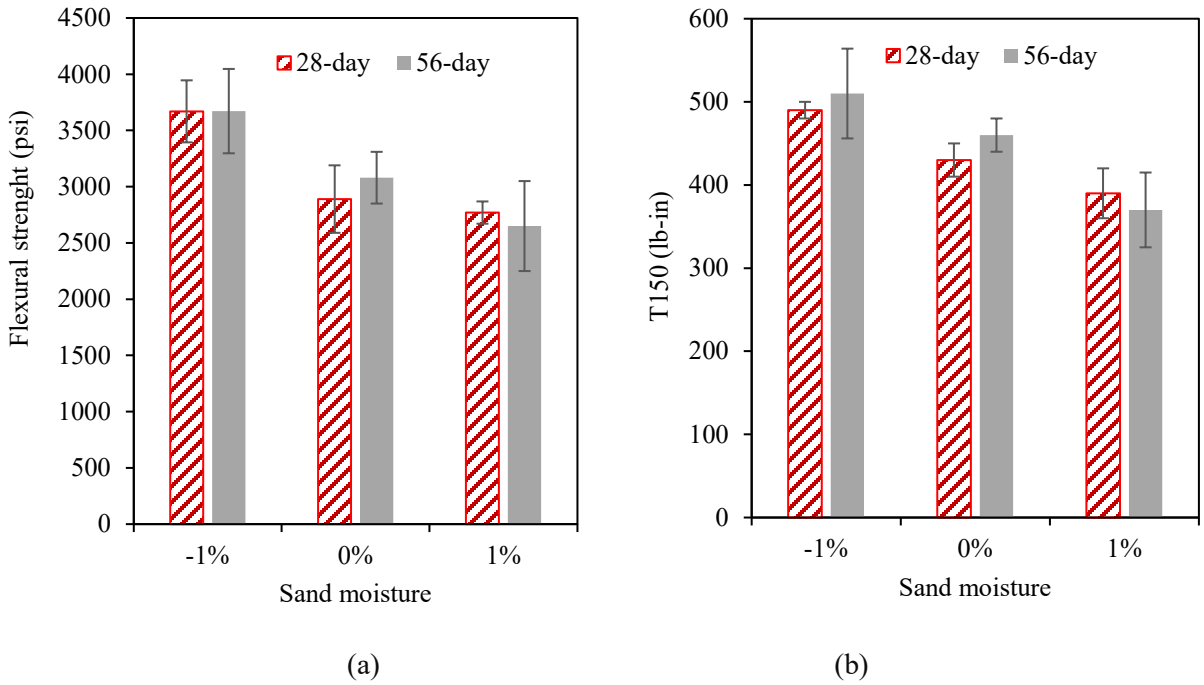

Figure 3.39 Influence of sand moisture on (a) flexural strength and (b) T150 of UHPC

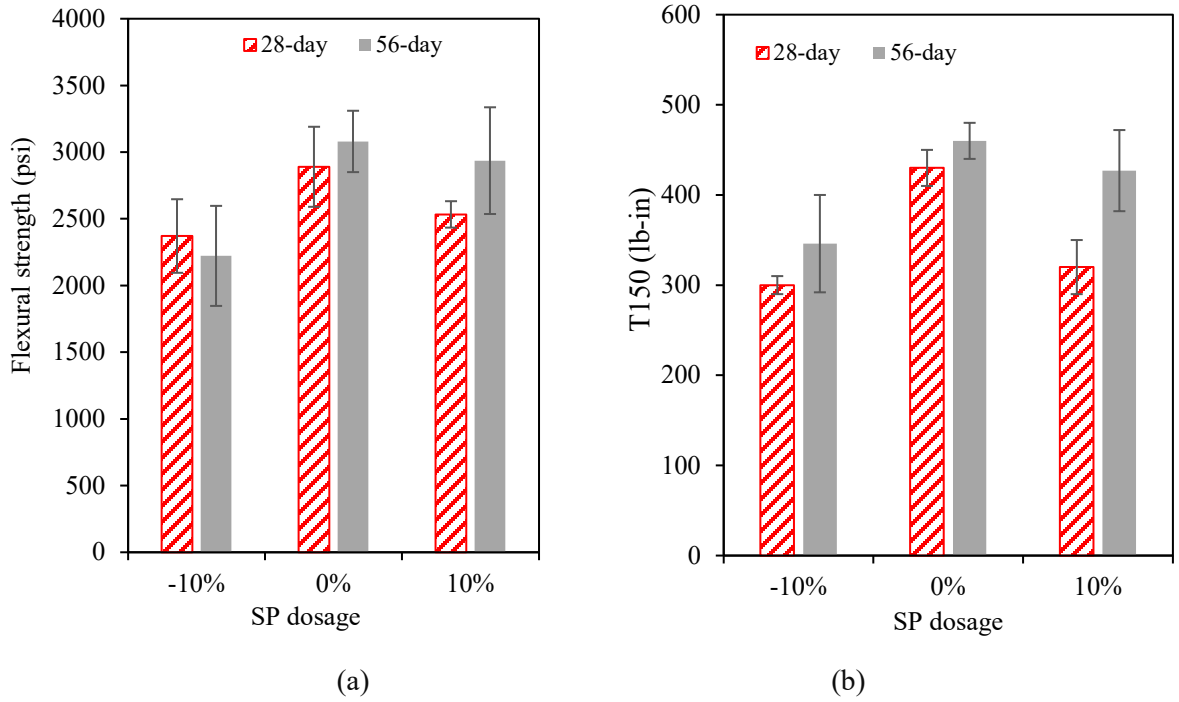

Figure 3.40 Influence of SP dosage on (a) flexural strength and (b) T150 of UHPC

3.4 Summary

The major findings of this task are summarized below.

1. The EUCON ABS was the most effective specialty admixture to enhance the thixotropy of UHPC without compromising SP demand, workability loss, plastic viscosity, compressive strength, and autogenous shrinkage. The optimum content of the EUCON ABS was 0.5%, by mass of binder.

2. Compared to the 17% LWS mixture, the 17% LWS and 1% SRA mixture showed the lowest shrinkage (-350 με at 56 d) and relatively high compressive strength (19,145 psi) The former is also a suitable candidate for thin bonded overlays given its highest compressive strength and thixotropy, as well as relatively low shrinkage.

3. The 7-d moist curing is recommended for field construction of UHPC thin bonded overlay. This duration is required despite the use of saturated LWS for internal curing.

4. The UHPC made with 3.25% fiber volume exhibited higher compressive strength (20,450 psi) and flexural strength (2,930 psi) and lower shrinkage (-300 με initial measurement at 1 d) compared to that of 2% fiber.

5. The variations of w/cm from 0.18 to 0.22 (±10%) and sand moisture content by ±1% did not greatly influence the performance of the LWS17 and SRA1 mixture including rheology, autogenous shrinkage after 28 d, and 28-d compressive and flexural strengths.

Chapter 4: Provisional Performance-Based Specifications

In collaboration with MoDOT, provisional performance-based specifications for the selected non-proprietary thixotropic UHPC for bridge overlay construction were proposed. The specifications included the mixture design of two candidate mixtures for thin bonded UHPC overlay, as shown in **Table 4-1**. The proposed UHPC mixtures are prepared using Type III Portland cement, Class C fly ash, and undensified silica fume. The UHPC makes use of locally available concrete river sand and masonry sand. Pre-saturated LWS is used for internal curing. Both the LWS17 and SRA1 and LWS17 UHPC mixtures presented in Chapter 3 were recommended for field work. The LWS should be saturated for at least 24 hours, and the humidity of the LWS should be determined prior to use. ASTM 1761 recommends the use of a centrifuge to drain excess water from the saturated LWS, thus enabling saturated surface dry conditions. This approach can be adopted on a large scale for field construction.

The mixtures are proportioned with straight micro steel fibers measuring 0.5 in. in length and 0.008 in. in diameter. A polycarboxylate-based SP that can promote early strength gain and the EUCON ABS thixotropic admixture were recommended. This admixture was not available commercially by the company and was replaced by the EUCON AWA P20 which is a thixotropic admixture. A polyether-based air detraining admixture (ADA) was incorporated to reduce the volume of entrapped air.

Table 4-1 Mixture design of two selected non-proprietary thixotropic UHPC mixtures

Raw materials	LWS17	LWS17 and SRA1
Type III cement	1080 lb/yd^3	1080 lb/yd^3
Class C fly ash	675 lb/yd^3	675 lb/yd^3
Silica fume	70 lb/yd^3	70 lb/yd^3
Water	340 lb/yd^3	333 lb/yd^3
River sand	860 lb/yd^3	860 lb/yd^3
Masonry sand	505 lb/yd^3	505 lb/yd^3
Saturated LWS	195 lb/yd^3	195 lb/yd^3
Steel fiber (3.25% by volume)	430 lb/yd^3	430 lb/yd^3
Superplasticizer (PLASTOL 6400)	1.7 gal/yd^3	1.7 gal/yd^3
Thixotropy enhancing admixture (EUCON AWA P20)	1.07 gal/yd^3	1.07 gal/yd^3
Shrinkage reducing admixture (EUCON SRA Floor)	-	2.2 gal/yd^3
Air detraining admixture (EUCON Air Out)	1.2 gal/yd^3	1.2 gal/yd^3

Test methods and performance criteria for workability, mechanical properties, as well as autogenous and drying shrinkage are shown in **Table 4-2**. Autogenous shrinkage is monitored using embedded strain gauges in sealed prismatic specimens.

A high-shear mixer is recommended to secure efficient dispersion and homogeneity. Depending on the ambient temperature, part of the mixing water can be replaced by crushed ice to maintain a UHPC temperature lower than 86 °F at the end of mixing.

Table 4-2 Provisional performance-based specifications for non-proprietary thixotropic UHPC

Property	Test method	Recommended values
Fresh Properties	Unit weight (ASTM C138)	145-155 lb/ft^3
	Air content (ASTM C138)	< 2.5%
	Temperature after mixing	< 86 °F
	Initial slump flow before jolting (ASTM C230)	6.5-8.0 in.
	Initial slump flow after 25 jolts (ASTM C230)	8.0-9.5 in.
	Static yield stress at 5 min (Portable vane)	> 0.1 psi
	Rate of gain of static yield stress from 5 to 30 min (Portable vane)	> 0.01 psi/min
Hardened Properties	1-d compressive strength (ASTM C109)	> 7,700 psi
	7-d compressive strength (ASTM C109)	> 17,400 psi
	28-d compressive strength (ASTM C109)	> 18,700 psi
	7-d flexural strength (ASTM C1609)	> 2,500 psi
	7-d flexural toughness (ASTM C1609)	> 310 lb.in.
	28-d flexural strength (ASTM C1609)	> 2,900 psi
	28-d flexural toughness (ASTM C1609)	> 350 lb.in.
Volume Change	Autogenous shrinkage at 28 d	< -450 με
	Drying shrinkage at 56 d (ASTM C157)	< -500 με
	Restrained shrinkage at 35 d (ASTM C1581)	No cracking

The recommended mixing sequence for the UHPC using a high-shear EIRICH mixer with a capacity of 40 gal (150 L) is as follows:

1. The mixer is prewetted before mixing.
2. The cementitious materials and all three types of sands are added and mixed for 2 min at 1 rps.
3. 90% of the mixing water and 90% SP diluted in the water are added and mixed for 2 min at 6 rps.
4. The rest of the mixing water, SP, and other chemical admixtures (AWA P20, SRA, and ADA) are incorporated and mixed for 4 min at 6 rps.
5. The steel fibers are gradually added over 1 min.
6. The material is mixed for 2 min at 10 rps.

A different mixing duration can be required depending on the selected high-shear mixer for field work. This aspect was required in the provisional performance-based specifications during the mockup testing carried by the contractor.

The concrete discharged from the mixer should be uniform in composition and consistency. The mixing capability should allow for a consistent pace during both the initial and final finishing operations.

It is recommended that the UHPC mixture is delivered from the field mixer by motorized buggies. A vibrating truss screed and hand tools are recommended for the placement and finishing of the UHPC.

The final finishing is recommended to be completed before the formation of a plastic surface film. It is also recommended that a minimum curing temperature of 60 °F be maintained until the initial set of the UHPC. After placement, the UHPC overlay should be coated with a wax-based curing compound and covered with wet burlap and plastic sheet for a minimum of 7 d or the time required to reach a minimum compressive strength of 14,000 psi.

Chapter 5: Field Implementation

5.1 Laboratory Mockup Test

The first of two laboratory mockup tests was conducted at Missouri S&T on June 21, 2022. Representatives from MoDOT and the contractor were present during the mockup test. The UHPC was prepared using a high-shear mixer and the materials that are described earlier for the development of the thixotropic non-proprietary UHPC. The LWS17 and SRA1 mixture was selected as the overlay material for the mockup test. The concrete was cast on a slab measuring 3 × 6 ft and 6 in. in depth that was cast using conventional concrete for the substrate. The surface of the substrate was prepared using texturing and water blasting to enhance bond with the UHPC overlay, as shown in **Figure 5.1**. The substrate surface was covered by wet burlap for one day to ensure saturated surface dry (SSD) condition prior to the casting of the overlay. The substrate slab was placed at a 2% slope.

Figure 5.1 Concrete substrate surface prepared using scarification and water blasting

The mixture proportion of the LWS17 and SRA1 UHPC is shown in **Table 5-1**. The binder included a Type III cement, Class C fly ash, and undensified silica fume. The sand comprised of a concrete river sand, a masonry sand, and a saturated LWS. Steel fiber measuring 0.5-in. in length and 0.008 in. in diameter was used.

A high-shear EIRICH mixer with a capacity of 40 gal (150 L) shown in **Figure 5.2** was employed to prepare the UHPC. The mixer was located in the laboratory, and all of the mixing ingredients

were maintained at approximately 79 °F. The batching sequence was the same as that described in Chapter 4 for the provisional performance-based specifications.

Table 5-1 Mixture design of LWS17 and SRA1-3.25% mixture

Raw material	Unit weight
Type III cement	1080 lb/yd^3
Class C fly ash	675 lb/yd^3
Silica fume	70 lb/yd^3
Water	333 lb/yd^3
River sand	860 lb/yd^3
Masonry sand	505 lb/yd^3
Saturated LWS	195 lb/yd^3
Steel fibers (0.5-in. long, 3.25% by volume)	430 lb/yd^3
SP (Plastol 6400)	1.7 gal/yd^3
Thixotropy enhancing admixture (EUCON AWA P20)	1.07 gal/yd^3
Shrinkage reducing admixture (EUCON SRA Floor)	2.2 gal/yd^3
Air detraining admixture (EUCON Air Out)	1.2 gal/yd^3

Figure 5.2 High-shear EIRICH mixer

The homogeneity of the UHPC material was verified at the end of mixing to ensure that there are no signs of bleeding or segregation. The material temperature, unit weight, and slump flow were determined immediately after the end of mixing, as shown in **Figure 5.3**. The temperature after mixing was 79 °F, which is lower than the upper limit of 86 °F). The initial slump flow test values before and after jolting were 7 and 9 in., respectively.

The mockup casting of 1.5-in. thick UHPC overlay was carried outdoors under an ambient temperature of 87 °F. The concrete was loaded into a container using a forklift for casting the overlay, as shown in **Figure 5.4**. The UHPC flowed readily into place and did not exhibit any risk of segregation or sagging onto the sloped bridge deck. A rake was used to spread the concrete into place before finishing using a hand-held trowel, as shown in **Figure 5.5**. In general, the mixture exhibited excellent workability. Immediately after finishing, the UHPC overlay was cured using wet burlap and plastic sheet for 7 d. No sign of cracking of the overlay was observed after 6 months of outdoor exposure, as shown in **Figure 5.6**.

Figure 5.3 Slump flow test

Figure 5.4 UHPC transport onto conventional concrete substrate using forklift

Figure 5.5 Placement of UHPC overlay

Figure 5.6 Surface of mockup overlay after approximately 8 months of outdoor exposure showing intact surface with no surface cracking

5.2 Field Mockup Test

A field mockup test was conducted on October 10th, 2022, shortly before field implementation to verify the constructability of the UHPC using the materials and equipment selected by the contractor for the placement and finishing of the UHPC. A 1-in. long twisted steel fiber was selected by the contractor for the casting of the UHPC overlay for the bridge deck repair. This was different than the 0.5-in. long micro steel fiber that was used for the mixture development. Given the time constraint before field testing, the research team at Missouri S&T conducted preliminary evaluation of key fresh properties, 1- and 7-d compressive strength and fiber distribution to compare to previous results using the same materials that were employed for the mixture development, in exception of the fiber type. It should be noted that the compressive strength testing was performed on 2-in. cubic specimens instead of 3 x 6 in. cylindrical specimens that is stipulated by ASTM C1856.

Slabs measuring 12 x 12 x 1.5 in. (x, y, and z) were cast with the same UHPC mixture prepared with 1-in. long fibers and 0.5-in. long fibers to investigate the distribution and orientation of fibers in the slabs. The slabs were inclined at a slope of 2%, and the UHPC mixtures were cast without any mechanical consolidation in the direction shown in **Figure 5.7**.

A section measuring 6 x 6 x 1.5 in. was saw cut to observe the fiber distribution. As can be observed in **Figure 5.7**, a lot more fibers (i.e., fiber count) can be observed with the section cast with 0.5-in. long. Enhanced fiber distribution can reduce the risk of cracking and crack propagation. The 1-in. long fibers were predominantly oriented along the x-y plane and less so in the vertical direction. On the other hand, the 0.5-in. long fibers had oriented along all three directions.

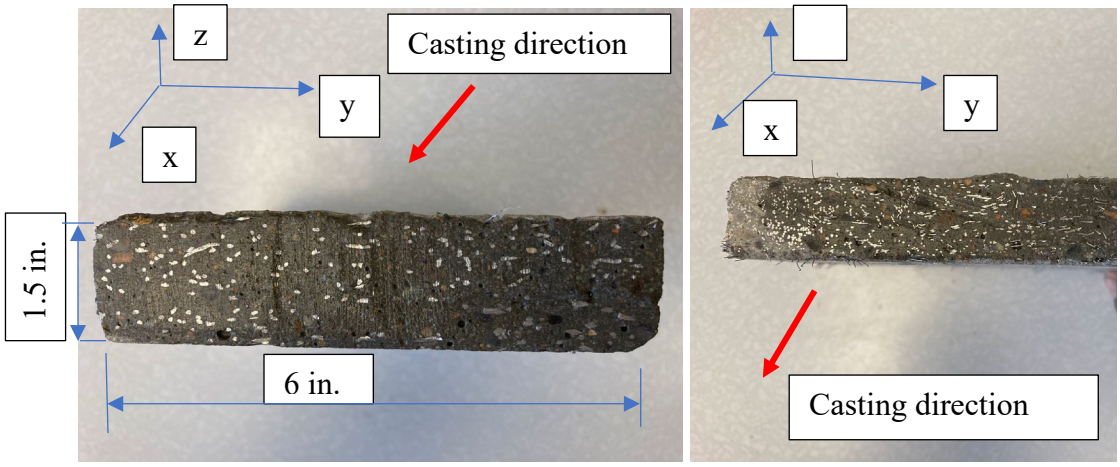

Figure 5.7 Cross section of slabs prepared using (a) 1-in. and (b) 0.5-in. long fibers

Two 12 x 12 ft slabs of different fluidity levels were cast for the mockup. The overlay thickness was 1.5 in. and was cast outdoor on an existing concrete slab in an industrial area. **Figure 5.8-5.13** shows the mixing, slump flow testing, placement, and finishing of the mockup mixtures.

Table 5-2 presents the fresh properties of the mockup mixtures. Both mixtures generated excessive heat due to extended mixing time and adjustments in the batching sequence. The temperature of the fresh concrete at the end of mixing for Mockups A and B were approximately 98 and 113 °F,

which is much higher than the recommended limit of 86 °F. Given the insufficient mixing energy of the selected mixer, the mixing time was extended to secure the desired consistency.

The 2nd mixture (mockup B) had a lower slump of 6 in. after jolting, but was successfully cast, consolidated, and finished compared to the first mixture mockup mixture that had excess water content and showed signs of segregation. Therefore, using a lower limit of slump flow of 6 in. after jolting was proposed for the actual field work. The unit weight, calculated air content, and thixotropy both mockup mixtures met the project requirements.

Figure 5.8 Mixing of UHPC using a skid steer concrete mixer (UHPC with excess water used in mockup A)

Figure 5.9 Slump flow testing of UHPC used in field mockup

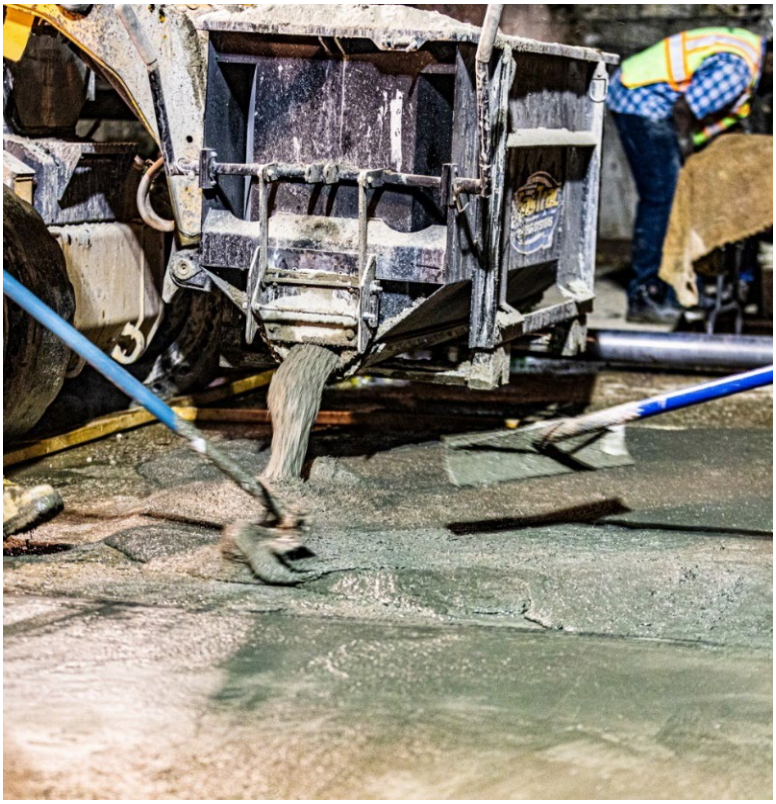

Figure 5.10 Placement of mockup UHPC

Figure 5.11 Spreading of mockup mixtures on existing concrete slab

Figure 5.12 Finishing of mockup mixtures with roller screed

Figure 5.13 Finishing of mockup mixtures with hand-held tools at contractors' property

Table 5-2 Fresh properties of mockup mixtures and lab mixtures using 1-in. long fiber

Property	Specified values	Lab verified mixture	Mockup A	Mockup B
Density (ASTM C138), lb/ft^3	145-155	149	150	150
Air content (ASTM C138), %	< 2.5	2.4	2.0	2.5
Temperature after mixing, °F	< 86	80.6	98.2	113.4
Initial slump flow before jolting (ASTM C230), in.	6.5-8.0	7.0	6.5	4.1
Initial slump flow after jolting (ASTM C230), in.	8.0-9.5	9.0	8.8	6.2
Static yield stress at 5 min, psi	> 0.1	0.26	0.26	0.41
Increase rate of static yield stress from 5 to 30 min, psi/min	> 0.01	0.035	0.036	0.044

Note: 1 psi = 6.89 Pa

The results of the 1- and 7-d compressive strengths of the laboratory verified mixture using the 1-in. long fibers as well as the two mockup mixtures are shown in **Table 5-3**. The 1-d compressive strength results of the laboratory verified, and two mockup mixtures were higher than the specified value. However, this was not the case for the 7-d results where 10% to 15% strength reduction was observed. The mockup B mixture showed a 20% higher 1-d compressive strength compared to the mockup A mixture. The COV of the compressive strength samples taken from the field was higher than that of the concrete sampled on site. The lab mixture made with 0.5-in. long fibers had 20% higher 7-d compressive strength compared to the lab mixture made with 1-in. long fibers.

The results of the 7-d flexural strength and toughness of the two mockup mixtures are compared in **Table 5-4**. The minimum required values are also indicated. Both mockup mixtures met the requirement for the 7-d flexural strength and toughness. The mockup B mixture showed a 15% higher toughness compared to mockup A mixture. The lab mixture made with 0.5-in. long fibers had 13% and 5% higher 7-d flexural strength and toughness, respectively, compared to the lab mixture made with 1-in. long fibers. The 7-d flexural strengths of all samples, including lab mixtures and mockups were higher than the specified NY DOT requirements of 2,000 psi.

The results of the 7-d flexural strength and toughness of the two mockup mixtures are compared in **Table 5-4**. The minimum required values are also indicated. Both mockup mixtures met the requirement for the 7-d flexural strength and toughness. The mockup B mixture showed a 15% higher toughness compared to mockup A mixture. The lab mixture made with 0.5-in. long fibers had 13% and 5% higher 7-d flexural strength and toughness, respectively, compared to the lab mixture made with 1-in. long fibers. The 7-d flexural strengths of all samples, including lab mixtures and mockups, were higher than the specified NY DOT requirements of 2,000 psi.

Table 5-3 Compressive strength of lab mixtures and field mockup trials

Property	Mixture	Average (psi)	COV (%)
1-d compressive strength	Specified values	> 7,700	-
	Lab mixture-0.5 in. fiber	8,410	4.3
	Lab mixture-1 in. fiber	10,490	3.2
	Mockup A-1 in. fiber	9,700	12.1
	Mockup B-1 in. fiber	11,560	5.2
7-d compressive strength	Specified values	> 17,400	-
	Lab mixture-0.5 in. fiber	17,980	1.7
	Lab mixture-1 in. fiber	14,870	3.5
	Mockup A-1 in. fiber	14,760	4.9
	Mockup B-1 in. fiber	15,190	6.8

Note: 1 psi = 6.89 Pa

Table 5-4 Flexural strength and toughness of lab mixtures and field mockup trials

Property	Mixture	Average (psi)	COV (%)
7-d flexural strength	Specified values	> 2,500	-
	Lab mixture-0.5 in. fiber	2,990	4.5
	Lab mixture-1 in. fiber	3,300	4.0
	Mockup A-1 in. fiber	3,350	11.2
	Mockup B-1 in. fiber	3,450	6.8
7-d flexural toughness	Specified values	> 350	-
	Lab mixture-0.5 in. fiber	400	5.4
	Lab mixture-1 in. fiber	420	6.5
	Mockup A-1 in. fiber	410	8.4
	Mockup B-1 in. fiber	480	10.5

Figure 5.14 provides photos of Mockups A and B taken from the field mockup overlays after approximately 5 months of outdoor exposure. Under no traffic conditions, no cracking was observed on mockup A after 5 months of outdoor exposure. 1% of area showed signs of cracking

for mockup B with the crack widths of 0.01 in. The cracking observed on the mockup B can be attributed to the lack of fibers on the surface of the slab as shown in **Figure 5.15 ©.**

(a)

(b)

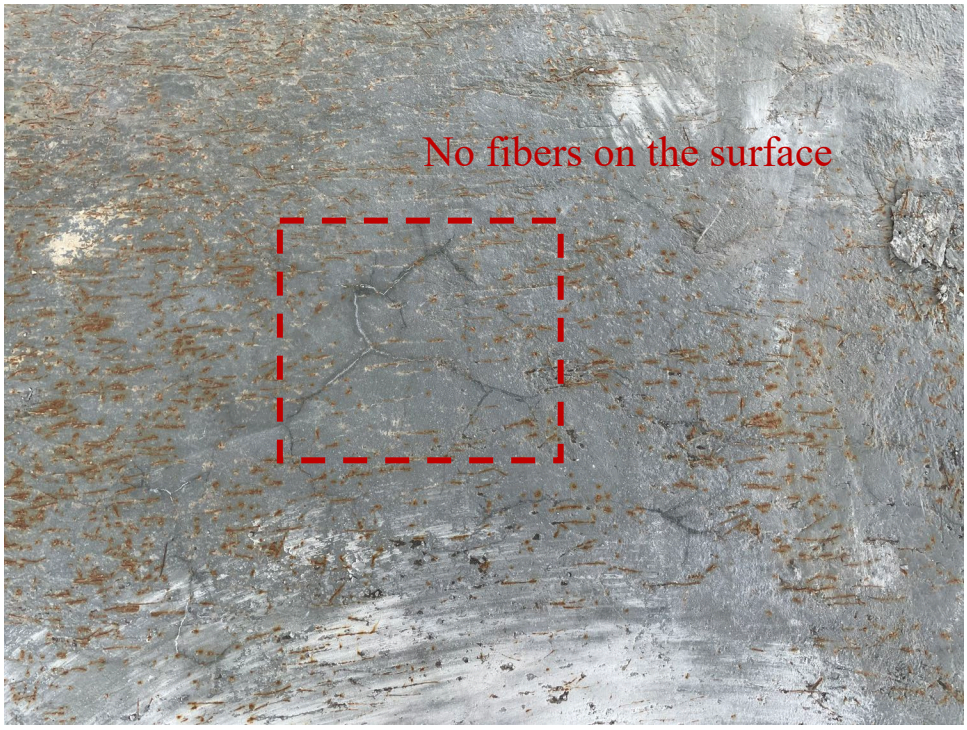

Figure 5.14 Surface of the mockup overlays of (a) mockup A and (b) mockup B after approximately 5 months of outdoor exposure (c) closeup view of cracks on mockup B

5.3 Bridge Deck Construction

The thin bonded overlay bridge deck rehabilitation was carried out on bridges owned by MoDOT. Route Z and M Bridges are located over Interstate 70 approximately 15 and 10 miles west of Boonville, Missouri, respectively. Two continuous-span bridges measuring approximately 200 ft in length were selected. An overview of the Route Z Bridge is shown in **Figure 5.15**. Cross-sections of Route Z and M Bridges are shown in **Figures 5.16** and **5.17**, respectively. The length and width of the roadways are 202 and 204 ft and 22 and 20 ft, respectively.

Figure 5.15 Overview of Route Z Bridge with wet burlap to pre-wet subbase before UHPC casting

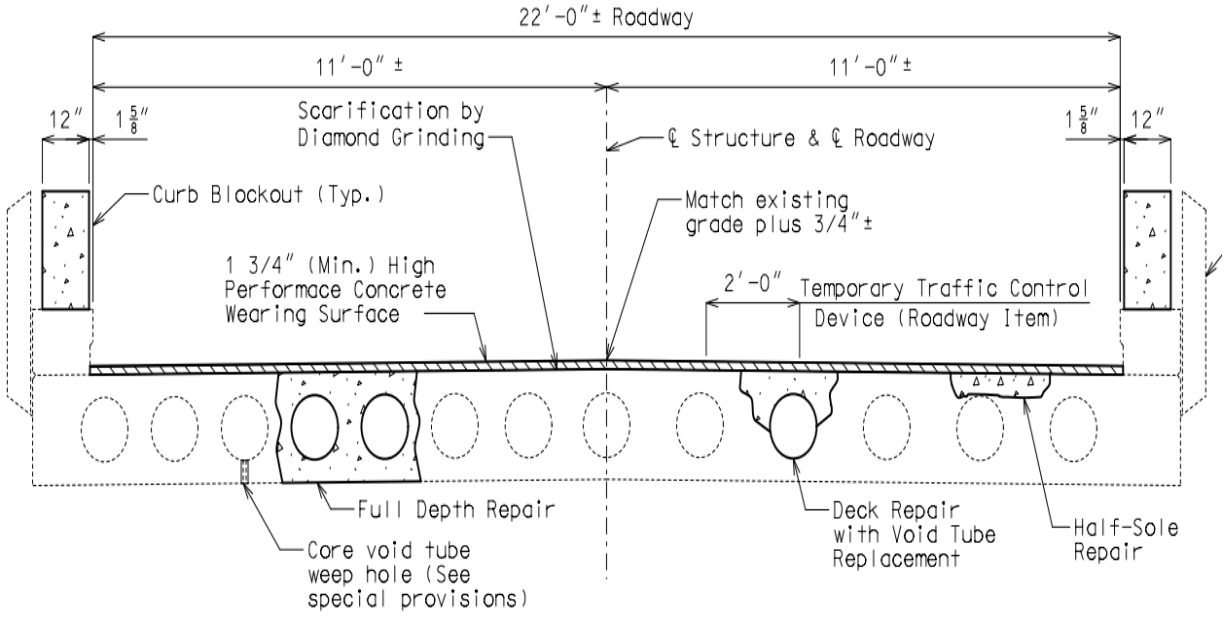

Figure 5.16 Cross section of Route Z Bridge

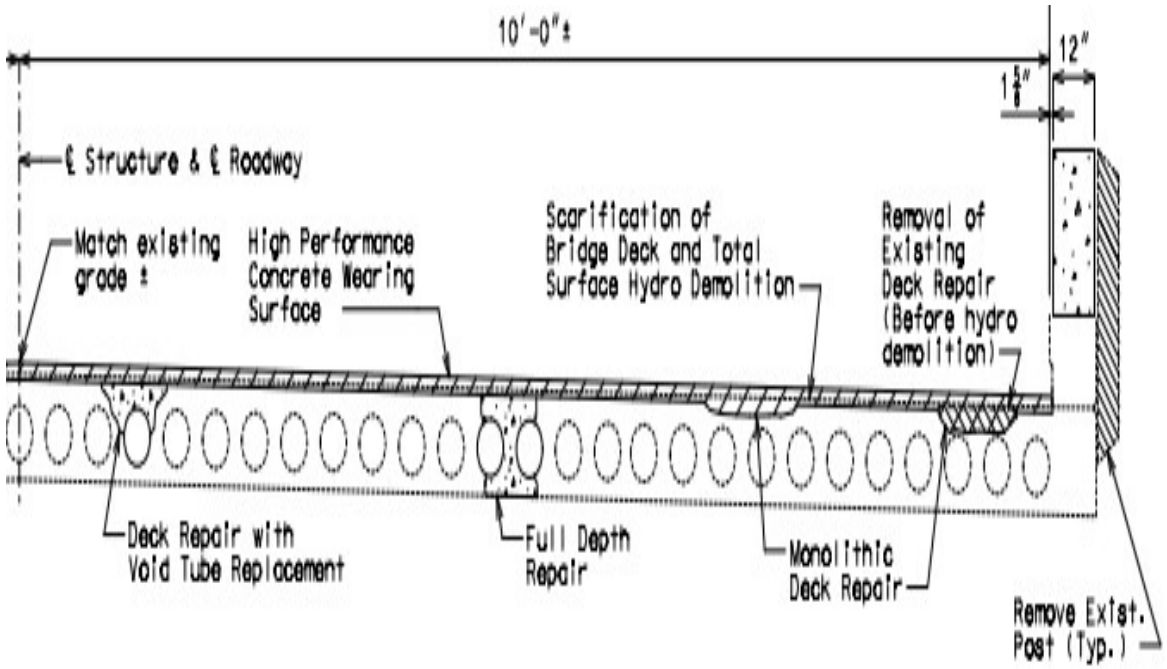

Figure 5.17 Cross section of Route M Bridge

The 60-year-old bridges showed advanced signs of cracking of the bridge deck and signs of corrosion reinforcing bars, as shown in **Figure 5.18** for the Route M Bridge deck. The substrate of Route Z and M Bridges were prepared using diamond grinding and hydrodemolition, respectively. **Figure 5.19** shows the Route Z Bridge deck surface preparation after diamond grinding and the additional surface cleaning just prior to the placement of UHPC overlay. **Figure 5.20** shows the substrate of the Route M Bridge after hydrodemolition. As shown in **Figure 5.21**,

the thickness of the bridge deck overlay for rehabilitation by the UHPC materials was 1.5 in. The bridges were pre-wetted for 1 d to keep the substrate in SSD condition before the placement of the UHPC overlay, as shown in **Figure 5.22**.

(a)

(b)

Figure 5.18 (a) Hydrodemolitioned surface and (b) corrosion of reinforcement and exposed pipes on Route M Bridge

(a)

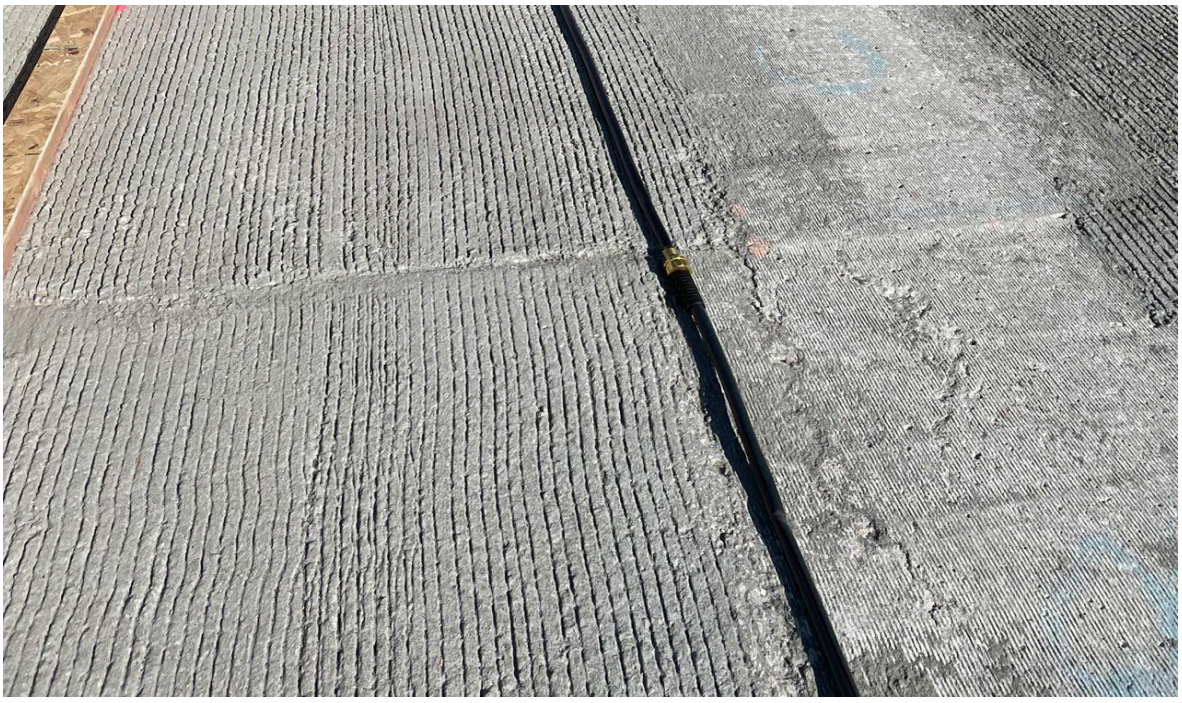

(b)

Figure 5.19 (a) Overview of diamond ground surface for Route Z Bridge (b) close-up view, and (c) cracking of subbase of Route Z Bridge

©

Figure 5.19 (continued) (a) Overview of diamond ground surface for Route Z Bridge (b) close-up view, and (c) cracking of subbase of Route Z Bridge

Figure 5.20 Cleaning up of concrete surface after hydrodemolition of Route M Bridge

Figure 5.21 The thickness of 1.5 in. bridge deck overlay for rehabilitation

Figure 5.22 Pre-wetting of Route Z Bridge concrete substrate before overlay casting

Before casting the UHPC, a comprehensive instrumentation program involving the use of embedded strain gauges, thermocouples, and humidity sensors was employed to monitor deformation, temperature, and internal relative humidity (IRH) in the UHPC overlay, respectively. The sensors were installed near the mid-span of the bridge in the longitudinal direction and were oriented along the direction of traffic. The instrumentation plan for each bridge included 10 embedded strain gauges, two thermocouples, and two humidity sensors, as shown in **Figure 5.23(a)**. The embedded strain gauges are denoted by the symbols S1-S10 and were placed such that strain gauge S1 was located near the curb of the bridge, and strain gauge S10 was located at the middle of the bridge with a spacing of 2 ft between each strain gauge, as shown in **Figure 5.23(b)**.

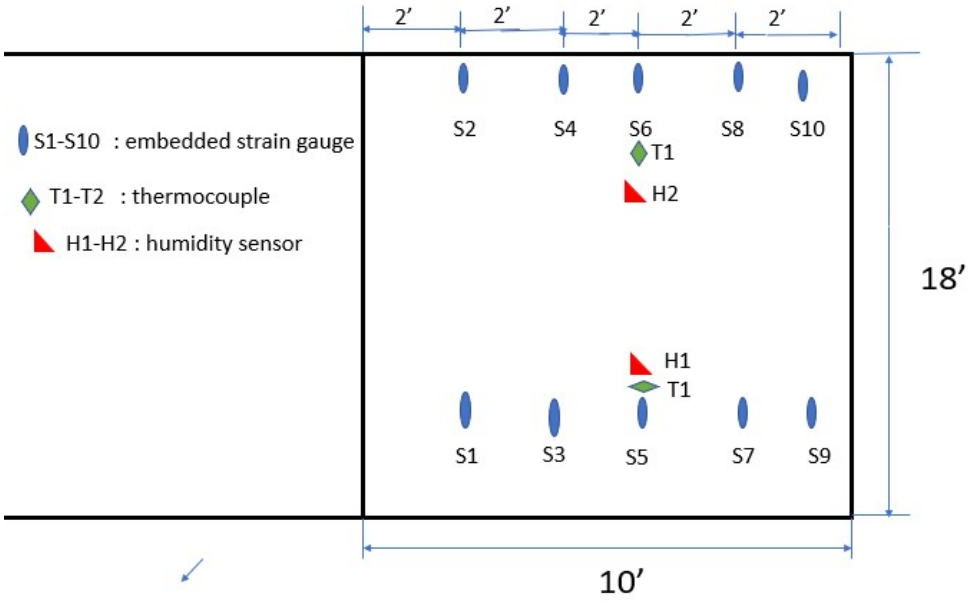

(a)

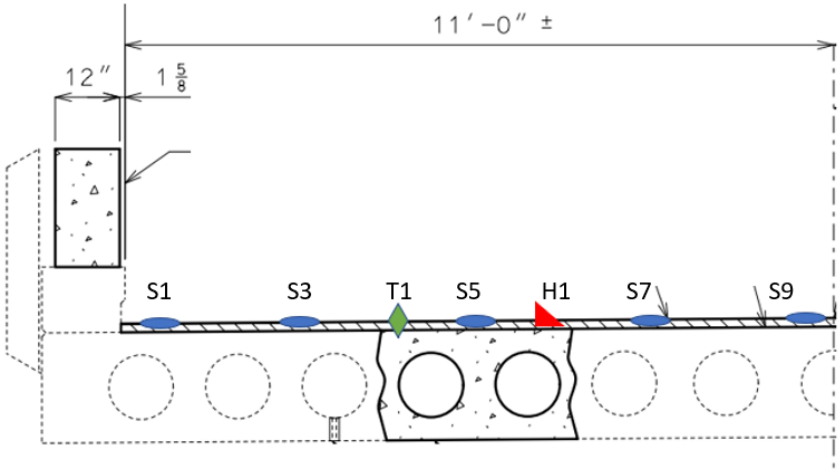

(b)

Figure 5.23 (a) Instrumentation layout in single lane and (b) cross section view of sensor locations

The UHPC mixture employed for the bridge rehabilitation had the same mixture proportioning as that listed in **Table 5-1**, except the 0.5-in. long straight microfiber was replaced with the 1-in. long twisted fiber that is described in **Table 5-5**. The selected silica fume had 95% SiO_2 content which meets the requirements of ASTM C1240. The grain size distribution of the sands used for the UHPC is presented in **Table 5-6**. The grain-size distribution of the concrete river sand and masonry sand were different from the gradation provided in the job special provisions, as shown in **Figures 5.24** and **5.25**, respectively. The river sand and masonry sand provided by the contractor had less uniform distribution, and this can affect the packing density of UHPC.

Table 5-5 Physical properties of twisted steel fibers

Length	1 in.
Diameter	0.02 in.
Tensile strength	260 - 290 ksi

Table 5-6 Particle distribution of sand

Sieve size	% Passing		
	River sand	Masonry sand	Saturated LWS
3 /8-in	-	-	100
No. 4	97.8	-	97.8
No. 8	74.7	-	74.7
No. 16	98	-	44.2
No. 30	18.4	-	26
No. 50	0.4	34.4	16.2
No. 100	-	2.8	10.3
No. 200	-	0.4	7.7

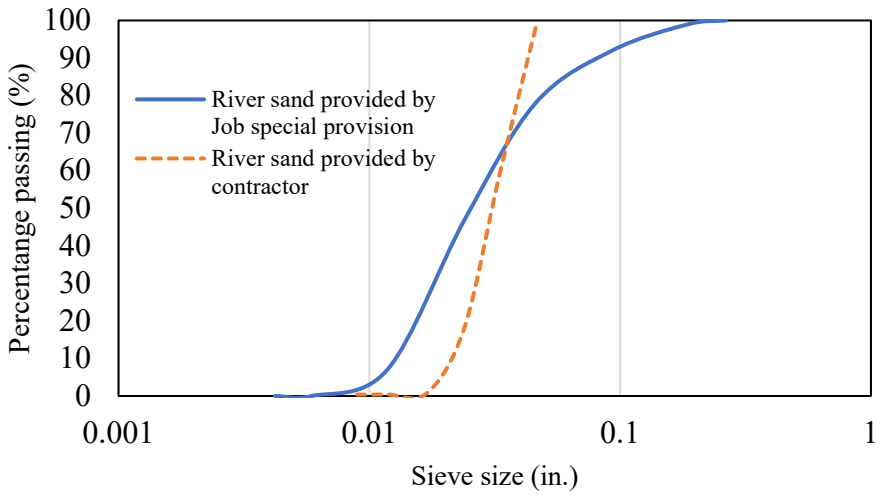

Figure 5.24 Comparison of particle size distribution between concrete river sand provided by contractor and the river sand provided in the job special provision

Figure 5.25 Comparison of particle size distribution between concrete river sand provided by contractor and the river sand provided in the job special provision

The materials were measured out and prepackaged in supersacs to expedite the loading of the dry materials into the mixer, as shown in **Figure 5.26**. The LWS was also packaged in supersacs and saturated for a minimum of 24 hours.

The mixing equipment was a skid steer concrete mixer mounted on a forklift, as depicted in **Figure 5.28**. The mixing was carried out at one end of the bridge, and the mixing time needed to ensure homogeneity was 15 to 20 min. This period was 12 min for the laboratory mixed UHPC using the EIRICH high-shear mixer. The UHPC was transported to the bridge using the forklift-mounted mixer. A total of two mixers were used. The mixing sequence for the UHPC was as follows:

1. A quarter of the mixing water was introduced along with a quarter of the solid materials from the supersacs for the initial mixing for a period of about 3 min. The supersacs contained all the solid materials except the LWS that was added along with the dry materials from buckets, as shown in **Figure 5.27**.
2. The remaining solid materials and LWS were gradually introduced from the supersac hanging using the forklift and mixed with the diluted SP of remaining water for duration of 5 to 8 min.
3. The 1-in. long steel fibers were then gradually introduced after the UHPC had a flowable consistency.
4. The thixotropic admixture was added followed by the SRA and the ADA (all three are liquid-based admixtures), and the UHPC was mixed for 3 min.

At the end of mixing, the UHPC was transported to the casting location and placed onto the bridge deck, as shown earlier in **Figure 5.10**. The UHPC was spread into place using a rake and was finished with a circular rotating roller screed, as shown in **Figure 5.29**.

Figure 5.26 Dry materials in supersacs

Figure 5.27 Saturated LWS

Figure 5.28 Loading of materials into mixer and UHPC mixing

(a)

Figure 5.29 UHPC overlay construction(a) placement of UHPC and (b) placement of sensors and gauges at the bottom of the overlay

(b)

Figure 5.29 (continued) UHPC overlay construction(a) placement of UHPC and (b) placement of sensors and gauges at the bottom of the overlay

Immediately after finishing, the surface of the UHPC was sprayed with an evaporation retardant (Eucobar), as shown in **Figure 5.30**. The surface was then covered with wet burlap and plastic, as indicated in **Figure 5.31**. However, in some cases, non-proper curing was observed. **Figure 5.32** shows some of the improper curing where the North Bound lane overlay surface was no longer moist cured 2 d after casting, and the South bound lane surface had non-uniform moist curing shortly after casting.

Figure 5.30 Application of evaporation retardant at conclusion of finishing of UHPC

Figure 5.31 Curing of UHPC with evaporation retardant, wet burlap, and plastic sheet

Figure 5.32 North Bound lane overlay surface with improper most curing dry 2 d after casting (left) and South bound lane surface shortly after casting with non-uniform moist curing (right)

5.4 Sample Preparation and Test Methods

UHPC samples needed to evaluate fresh and hardened properties were taken immediately after the end mixing. The slump flow was measured according to ASTM C230. The UHPC was cast in the mini slump cone in one lift and consolidated by rodding. The initial slump spread before and after 25 jolts was determined. The unit weight was measured and used to determine the air content according to ASTM C138 using 25 in^3 cylindrical container where the material was consolidated onto a vibrating table for 60 seconds.

Static yield stress was evaluated using the portable vane test that is described earlier (**Figure 3.2**). The static yield stress was measured after 5, 15, and 30 min of rest. The vane was rotated slowly during 10 to 15 s, and the maximum torque T (N·m) was determined according to the procedure described in Section 3.2.

Field samples for hardened properties were taken from four UHPC batches from Route Z and two batches from Route M. The samples included 2-in. cubes for testing compressive strength, 16 × 3 × 3 in. prismatic samples for determining flexural strength, and 3 × 3 × 12 in. prismatic samples to monitor drying shrinkage. All samples were cast in one lift and then consolidated onto a vibrating table for 60 sec. The samples were covered with wet burlap and plastic sheet for 2 d before transporting them to the Clayco Advanced Construction and Materials Laboratory at Missouri S&T. The samples were maintained in wet conditions during transport and were de-molded and cured in lime-saturated water at 70 ± 2 °F for an additional 5 d (7 d of age) followed by air curing at 73 ± 3°F and 50% ± 4% relative humidity until the time of testing. The 2-d ± 2 hr compressive strength was determined after demolding.

Figure 5.33 shows the compressive strength test setup. The compressive strength was determined at 1, 7, and 28 d according to ASTM C109. The loading rate was controlled at 50 psi/sec.

Figure 5.33 Compressive strength test

The flexural strength testing was conducted at 7 and 28 d in accordance with ASTM C1609, as shown in **Figure 5.34**. The loading rate was maintained at a controlled displacement of 0.0035

in./min until failure and the test was performed on a span length of 12 in. The flexural strength was calculated as follows:

$$F = PL/bd^2$$

where F is the flexural strength (psi); P is the load (lbf), L is the span (in.), b is the average width of the sample (in.), and d is the average depth of the sample (in.).

Figure 5.34 Test setup for flexural strength

Drying shrinkage was determined according to ASTM C157. A digital-type extensometer was used to measure length change, as shown in **Figure 5.35**. The specimens were subjected to initial 7-d moist curing in lime-saturated water at 70 ± 2 °F followed by air curing at 73 ± 3°F and 50% ± 4% relative humidity. Shrinkage measurements started immediately after demolding at 1 d, and then on daily basis for the first week and on weekly basis until the age of 56 d.

Figure 5.35 Digital-type extensometer for drying shrinkage

The UHPC overlays for Route Z and Route M Bridges were cast between October 20 and 22, 2022 and November 4 and 6, 2022, respectively. The results of the fresh properties of samples obtained from Route M and Route Z Bridges are reported in **Table 5-7**.

Table 5-7 Fresh properties

Bridge No.	Lane	Location (time)	Ambient / concrete temp. (°F)	Slump flow before jolts (in.)	Slump flow after jolting (in.)	Unit weight (lb/ft^3)	Static yield stress at 5 min (psi)	A_{thix} (psi/min)	Calculated air content (%)
Route Z	North bound	Middle (12:30)	66 / 95	4.0	6.2	151	x	x	1.8
		Middle (13:30)	68 / 98	4.2	6.9	150	0.66	0.06	2.0
		End (15:00)	73 / 96	5.0	7.5	149	x	x	2.5
		End (16:00)	74 / 99	4.2	6.5	150	x	x	1.9
	South bound	Start (12:00)	80 / 90	4.1	6.5	150	0.71	0.08	2.1
		Middle (14:00)	82 / 93	4.5	7.4	149	0.72	0.08	2.4
Route M	South bound	Middle (12:30)	78 / 95	4.2	6.3	150	x	x	2.0
		Middle (13:30)	79 / 96	4.5	7.0	151	0.74	0.04	1.8

The slump flow, air content, and variation of static yield stress with rest time met the performance specifications. However, the temperature of the fresh UHPC at the end of mixing ranged from 90 to 99 °F, which is much higher than the specified value of 86 °F. One factor which caused the elevated temperatures was the degradation of the mixer used, which hampered mixing. It is important to set the specified temperature of fresh UHPC because the high temperature of UHPC contributes to expanding the concrete and increases the risk of cracking.

The compressive strength, flexural strength and toughness, and drying shrinkage of the UHPC sampled from Route Z and M Bridge overlays are shown in **Table 5-8**. These samples were obtained from the different batches that were placed in different locations. In the general, the COV of samples taken from Route Z Bridge ranged from 1% to 8% are comparable to those from Route M Bridge, 2% and 5%. These values are acceptable for field-sampled specimens. The two sets of samples taken from the South bound lane of Route Z Bridge exhibited much higher compressive strength than those from the two sets of samples secured from the North bound lane that were cast 2 days apart. For instance, the 2-, 7-, and 28-d compressive strengths of two sets of samples taken from the South bound lane were 10,580, 14,470, and 18,030 psi, respectively, compared to 7,680, 13,510, and 15,070 psi, respectively, for two sets of samples taken from the North bound lane.

Table 5-8 Hardened properties for Route Z and Route M Bridges

Bridge No.	Lanes	Location	Compressive strength (psi) (COV, %)			Flexural strength (psi)		Drying shrinkage (μm/m)
			2 d ± 2 hr	7 d	28 d	7 d	28 d	56 d
Route Z	North bound	Middle	8,320 (5.1)	14,030 (1.3)	15,820 (5.0)	2,150	x	x
		Middle	7,030 (0.6)	12,980 (5.9)	14,310 (6.0)	2,380	2,780	x
		End	x	x	x	x	x	-450
	South bound	Start	x	x	x	x	x	x
		Start	9,860 (7.8)	14,440 (5.8)	18,540 (2.5)	2,780	3,560	x
		Middle	11,300 (8.5)	14,500 (4.7)	17,520 (3.2)	2,650	x	x
		Middle	x	x	x	x	x	x
Route M	South bound	Middle	11,220 (2.0)	14,280 (4.6)	15,800 (2.6)	x	x	x
		Middle	8,210 (2.1)	11,940 (1.8)	14,800 (3.6)	x	x	x
		End	x	x	x	x	x	-395
		End	x	x	x	x	x	-340

The 2-, 7-, and 28-d compressive strengths of samples taken from the North bound lane were 38%, 7%, and 24%, respectively, lower than those from the South bound lane. The reduction of 7- and 28-d compressive strengths ranged from 17% to 25% and 5% to 19%, compared to the specified values of 17,400 and 18,700 psi, respectively.

Furthermore, samples taken from two successive batches along the same lane of Route Z Bridge exhibited some variation in compressive strength. For example, the 2-, 7-, and 28-d compressive strength results of samples taken from the North bound lane were 18%, 8%, and 11%, respectively. Lower variations of 15%, 1%, and 6%, respectively, were obtained for samples taken from the South bound lane. The high variations of compressive strength between different UHPC batches taken from Route Z Bridge can be attributed to material quality control. Excess water was observed in some cases where the saturated LWS in the lower parts of the supersacs was not properly drained before use, hence increasing the effective w/cm and resulting in erratic variations in strength. As shown in **Figure 3.35 (b)** and **3.40 (a)**, an increase of 1% of sand moisture content can lead to 18%, 14%, and 19% reduction in the 56-d compressive strength, flexural strength, and flexural toughness, respectively, for the proposed LWS17 and SRA1 mixture.

Similar results were obtained for flexural strength. The 7- and 28-d flexural strengths of samples taken from the South bound lane for Route Z Bridge were approximately 400 and 800 psi higher sampled than those from the North bound lane, respectively. The flexural strength obtained exceed the specified requirement from NY DOT of 2,000 psi at 28 d.

These results are lower than the minimum specified values of 2,500 and 2,900 psi, respectively. The 56-d drying shrinkage of samples taken both Route Z and M Bridges were similar ranging from -350 to -440 με, as indicated in **Table 5.7**. These results meet the upper limit of -500 με.

5.5 Instrumentation

Figure 5.36 presents the connection to DAQ box for (a) Route Z Bridge and (b) Route M Bridge, respectively. Temperature/internal relative humidity (IRH) sensors and in-situ strain gauges were placed in a selected section of 10 × 18 ft near the midspan of the bridge overlay. The embedded strain gauges denoted by the symbols S1-S10 were placed such that strain gauge S1 was located near the curb of the bridge and strain gauge S10 was located at the middle of the bridge with a spacing of 2 ft between each strain gauge (shown in **Figure 5.23(b)**). The temperature together with IRH and in-situ strain gauges started to be recorded 4 hours after casting both bridge deck overlays. The connection of the wiring from the sensors to the DAQ box was delayed preventing damage during construction operations.

Figure 5.36 Connection to DAQ box for Route Z Bridge (left) and Route M Bridge (right)

The variations of temperatures in Route Z and M Bridge overlays are reported in **Figures 5.37** and **5.38**, respectively. For both overlays, there was a slight increase in temperature from 73 to 77 °F during the first 5 hours after the start of recording (corresponding to 9 hours of age), which is attributed to the rapid hydration of the UHPC.

A sharp decrease in temperature from 73 to 22 °F in the first 3 d was observed for the Route M Bridge overlay compared to 77 to 45 °F for the Route Z Bridge. The in-situ temperature from the bridge overlays varied with the ambient temperatures including a temperature as low as 35 °F in the first 28 d of age.

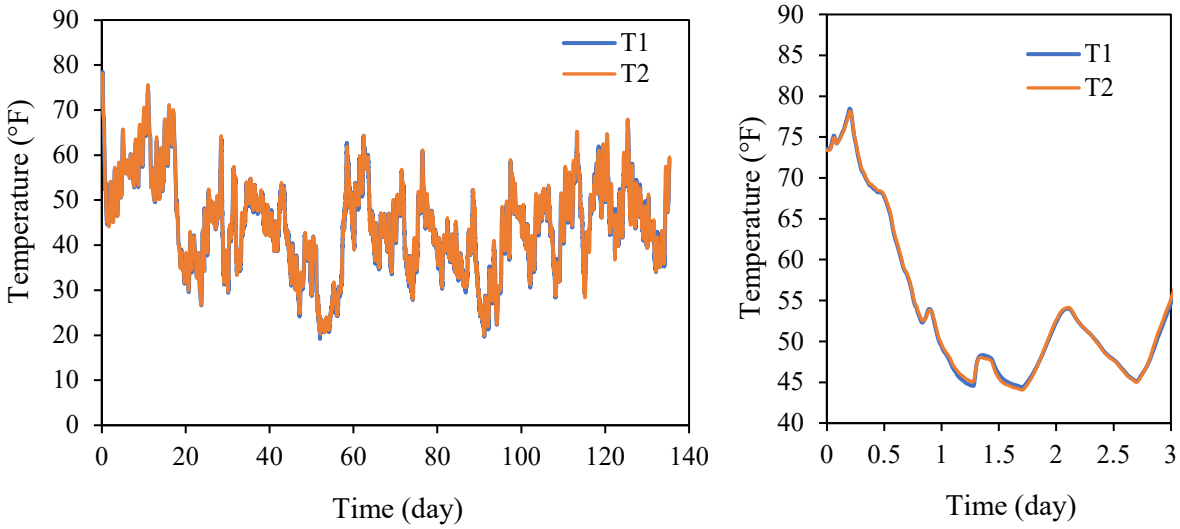

Figure 5.37 Temperature variation in Route Z UHPC overlay with time

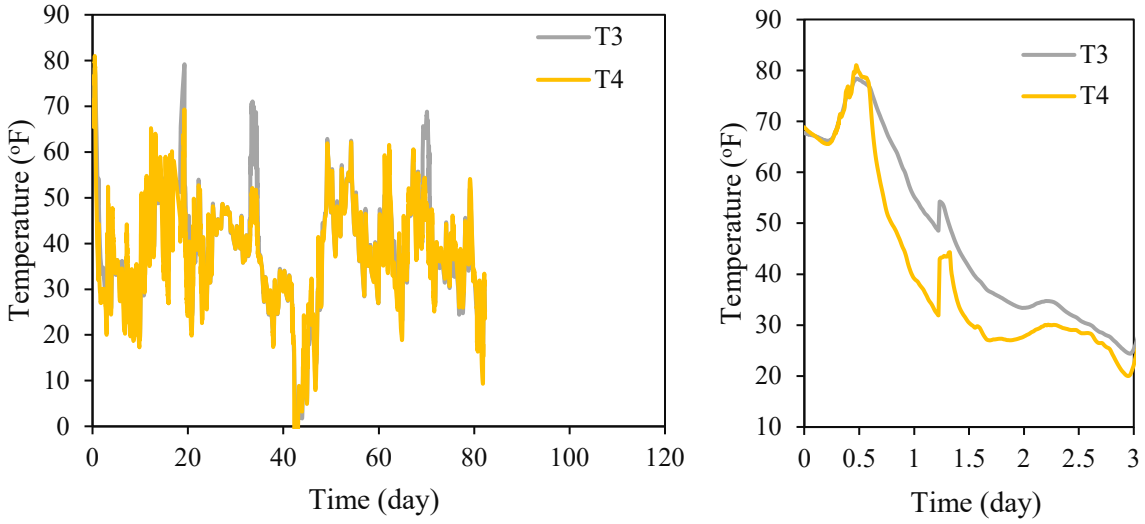

Figure 5.38 Temperature variation in Route M UHPC overlay with time

The variations of IRH in the Route Z and M UHPC overlays are shown in **Figures 5.39** and **5.40**, respectively. The IRH dropped gradually from 100% to approximately 75% after 40 d.

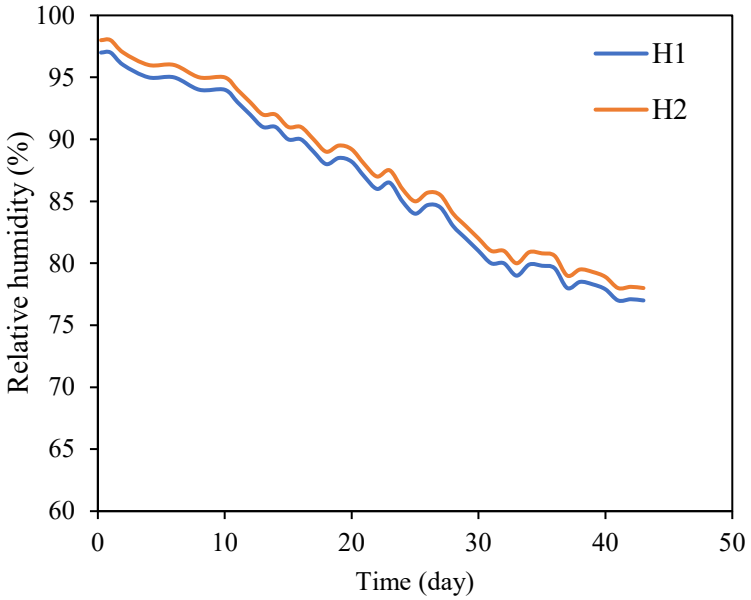

Figure 5.39 Variation of relative humidity in Route Z UHPC overlay with time

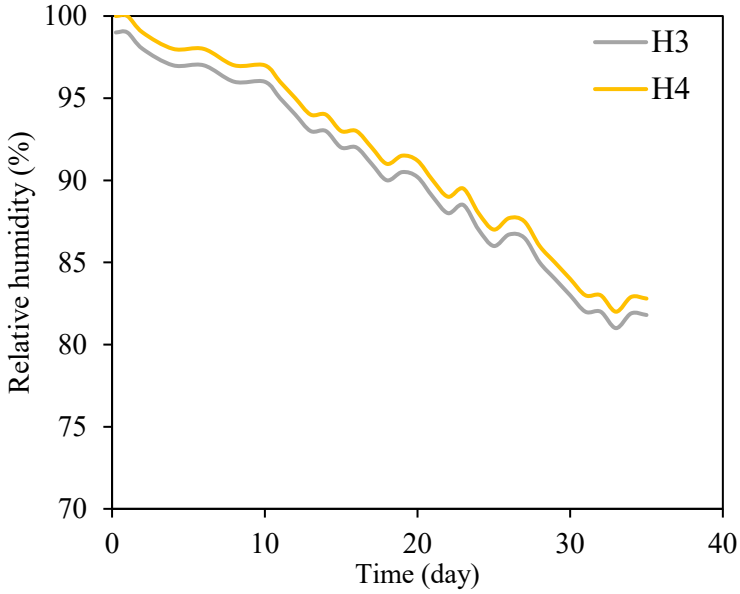

Figure 5.40 Variation of relative humidity in Route M UHPC overlay with time

The variations of in-situ strains of the Route Z and M UHPC overlays of sensors located at the bottom of the overlays are shown in **Figures 5.41** and **5.42**, respectively. Negative values indicate compressive strain, and positive values indicate tensile strain. For the strain gauges located near the curb of Route Z Bridge (S1 to S6 strain gauges), strains lower than -600 με were noted. Sensors located near the curbs (S1 and S2 strain gauges) were almost null. However, strain values higher than -2,000 με were recorded for sensors located at the middle of the cross section in the transverse direction of the Route Z Bridge (S9 and S10 strain gauges). The high compressive strains at the

center of Route Z Bridge resulted in a high risk of cracking. Similar results can be found for the variations of in-situ strain in Route M UHPC overlay.

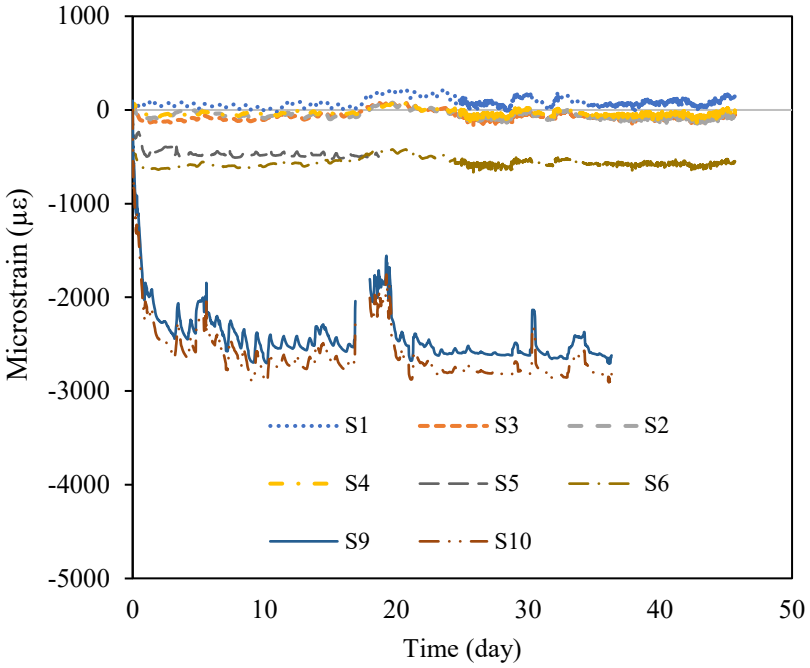

Figure 5.41 Variations of in-situ strain of Route Z UHPC overlay with time

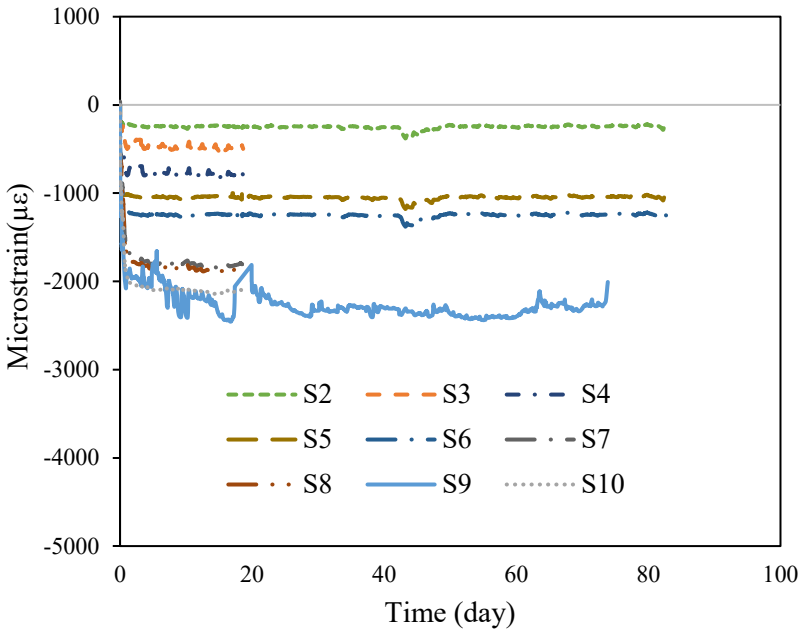

Figure 5.42 Variation of in-situ strain of Route M UHPC overlay

5.6. Field Inspection

A bridge inspection was carried out one week after the construction of Route Z Bridge; Bridge M was covered by snow after 7 days. Route Z and M Bridges were inspected after 96 and 81 days, respectively. The purpose of the inspection was to examine and document any signs of cracking or deterioration on the bridge overlays.

Figure 5.43 shows a photo of Route Z Bridge taken one week after the end of the bridge deck rehabilitation. No cracking was observed on either lane. On the other hand, **Figures 5.44** and **5.45** indicate a considerable amount of cracking that was observed on the North bound lane of Route Z Bridge after 96 days; however, no cracking occurred in the South bound lane. The cracks in the North bound lane were located at approximately 56 ft from both sides of the central region of the North bound lane, as shown in **Figures 5.45**. The total area of the bridge deck that exhibited cracking for the Route Z Bridge was 1120 ft^2, which corresponds to approximately 27% of the bridge deck surface. The crack opening at the upper surface ranged between 0.01 and 0.04 in. (0.25 to 1 mm) with an average width of 0.02 in., as shown in **Figure 5.46** The average crack length was 9 in. with average spacing of 5 in. (**Figure 5.47**).

The visual inspection of the South bound lane of Route Z Bridge indicated sound surface condition without cracks compared to the North bound lane. As indicated earlier, a large variation of compressive strength was noted from field-sampled specimens that were taken from both lanes with those from the North bound lane showing 7,030, 13,000, and 14,310 psi after 2, 7, and 28 d, respectively, compared to 11,300, 14,500, and 17,520 psi, respectively, for samples taken from the South bound lane. This indicates that the UHPC used for the rehabilitation of the South bound lane had better performance than that on the North bound lane.

Figure 5.43 Route Z Bridge inspection 7 days after placement indicating no cracking on both North bound and South bound lanes

Figure 5.44 Route Z Bridge inspection 96 days after placement showing significant cracking in the North bound lane and no cracking on the South bound lane

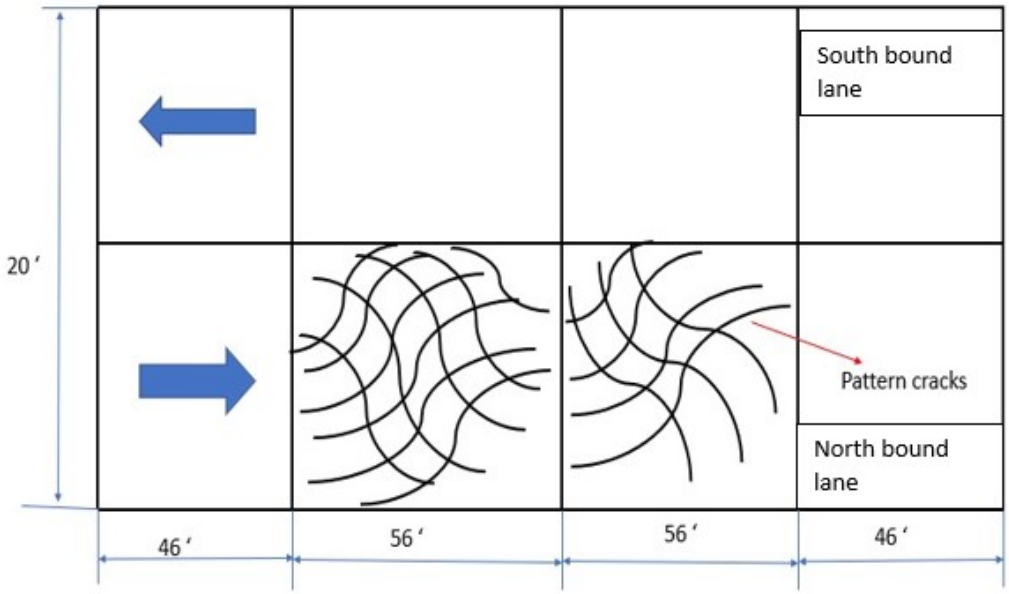

Figure 5.45 Illustration of cracks for Route Z Bridge after 96 days

Figure 5.46 Measurement of crack width for Route Z Bridge

Figure 5.47 Measurement of crack spacing for Route Z Bridge

Figure 5.48 shows the overall cracking of the Route M Bridge that was carried out 81 days after casting. Cracks were observed for both lanes, as illustrated in **Figure 5.49**. The crack widths ranged between 0.005 and 0.040 in. with an average crack width of 0.02 in. The density of the cracking was higher along the central line of the bridge where the maximum moment is expected. The total crack area for Route M Bridge was 2100 ft^2, which corresponds to approximately 46% of the bridge deck surface.

In the case of the Route M Bridge that was rehabilitated in November, 2022, a sharp drop in temperature from 73 to 22 °F was observed in the first 3 d. A decrease in temperature at early age for the UHPC can reduce strength due to the reduction in the hydration kinetics of the binder and pozzolanic activity (Liu et al., 2014). Valipour et al., 2020 showed that a drop in curing temperature from 73 to 50 °F can reduce the 1-d compressive strength of UHPC proportioned with 0.20 w/cm by 60%. This suggests that the compressive strength results determined from samples taken from the field and cured in lime-saturated water at room temperature would be higher than the in-situ strength.

Given the sharp drop in temperature at early age for Rout M overlay, it is believed that the UHPC had not gained sufficient strength to resist cracking. Furthermore, as indicated earlier in **Figures 5.41** and **5.42**, compressive strain values of -3,000 and -2,400 με were recorded in the South bound lane of Route Z and North bound lane of Route M overlays, respectively. These strains were obtained from strain gauges S9 and S10 are located at the middle of the bridge corresponding to the highest moment across the bridge deck. High concentration of cracking was observed at the central line of Route M Bridge in the longitudinal direction (shown in **Figure 5.48**). Such high strain values coupled with microcracking that can take place at early age can contribute significantly to cracking.

As indicated earlier, the specified 7-d continuous moist curing under wet burlap and plastic sheet was not respected. As shown in **Figure 5.32 (**right), the wet burlap used to cover the UHPC shortly after placement in the central part of the Z Bridge dried quickly because of strong winds encountered at the bridge site leaving the surface with non-uniform moist curing. The North bound lane portion on the left side after 2 days of casting did not have any burlap cover. The lack of continuously wet burlap can hinder strength development despite the use of LWS. **Figure 5.39** shows the drop starting shortly after casting in the IRH measured in the Route Z Bridge (the sensors were connected to the DAQ box after approximately 4 hours.

It is recommended to carry out another field inspection and drill cores to determine the pull-off bond strength at various places on both bridges and take core sample to investigate crack depths and fiber distribution across the thickness of the overlays. The latter should be done in areas that are intact, which can allow better comparison between the surface preparation of the substrate using diamond grinding versus hydrodemolition.

(a)

(b)

Figure 5.48 Cracking of the Route M Bridge overlay after 81 days (a) cracking concentrated in central line of the longitudinal direction and (b) transverse cracks

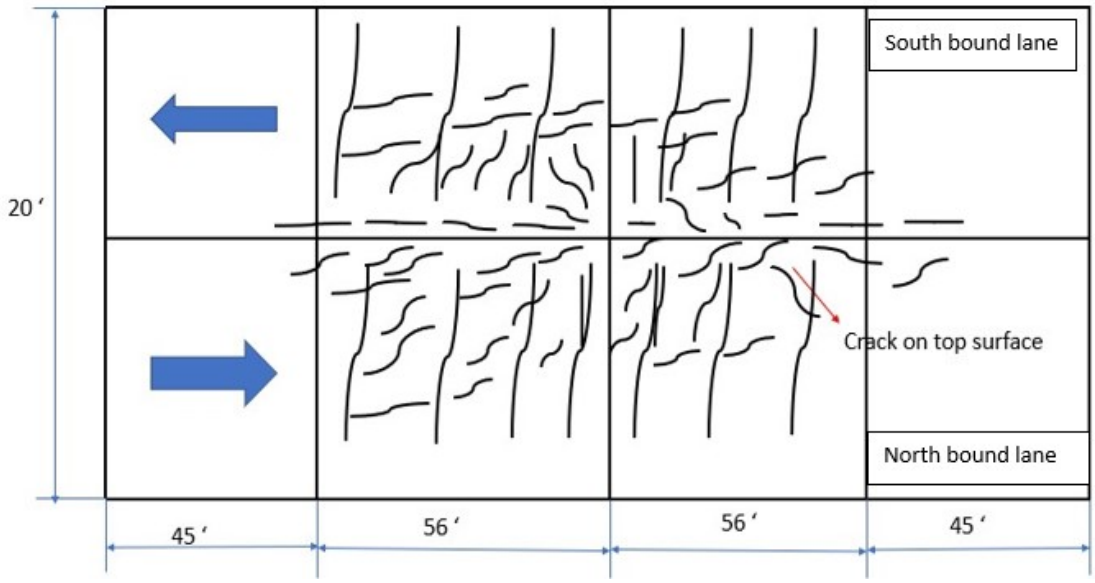

Figure 5.49 Illustration of cracks on Route M Bridge

5.7 Fine-tuning of Performance-based Specifications

Based on the field observations, the performance-based specifications of the thixotropic UHPC that was reported in **Table 4-1** can be maintained except for the initial slump flow before and after jolting that can be reduced to 4 to 6 in. and 6 to 7 in., respectively, as indicated in **Table 5-9**.

Table 5-9 Performance-based specifications of non-proprietary thixotropic UHPC

Test methods	Range
Initial slump flow before jolting (ASTM C230)	4-6 in.
Initial slump flow after 25 cycles of jolting (ASTM C230)	6-7 in.
Air content (ASTM C138)	< 2.5%
UHPC temperature after mixing	< 86 °F
Static yield stress at 5 min (Portable vane)	> 0.1 psi
Increase rate of static yield stress from 5 to 30 min	> 0.01 psi/min
1-d compressive strength (ASTM C109)	> 7,700 psi
7-d compressive strength (ASTM C109)	> 17,400 psi
Minimum period of moist curing	7 d or time to reach 14 ksi
Strength at bridge opening	> 14,000 psi
28-d compressive strength (ASTM C109)	> 18,700 psi
28-d flexural strength (ASTM C1609)	> 2900 psi
28-d flexural tension ratio (peak to first crack)	> 1.25
28-d flexural toughness (ASTM C1609)	> 350 lb.in.
28-d tensile strength	> 720 psi
28-d autogenous shrinkage	< 450 με
56-d drying shrinkage after 7-d of moist curing (ASTM C157)	< 500 με

It is recommended that for thin bonded UHPC overlays a thickness of 1.5 or 2 in. and a maximum fiber length of 0.5 in. should be used. The specimen size to evaluate compressive and flexural strengths of such UHPC should be 3 x 6 in. cylindrical specimens and 3 x 3 x 14 in. prismatic specimens, respectively, in accordance with ASTM C1856.

The selected mixture should be robust to tolerate small variations in water content, SP dosage, and temperature. High shear mixers such as the EIRICH mixer should be used for batching the UHPC.

The LWS should be used under SSD condition by allowing the supersacs to properly drain. Any additional humidity from the LWS should be taken into consideration. ASTM 1761 recommends the use of a centrifuge to drain excess water from the saturated LWS, thus enabling saturated surface dry conditions. This approach can be adopted on a large scale for field construction. t It is important to ensure a minimum of 7 d of continuous moist curing of the UHPC overlay.

Chapter 6: Conclusion

The main objective of this research is to evaluate the constructability and performance of non-proprietary thixotropic UHPC for thin bonded bridge deck overlay construction. The UHPC was designed to have low autogenous shrinkage by incorporating saturated LWS and SRA, while exhibiting excellent mechanical properties. A modified UHPC using 1-in. long fibers instead of 0.5-in. long fibers was used for field implementation of Route Z and M Bridge deck overlays. Based on the results presented in this report, the following conclusions can be drawn:

i. The investigated non-proprietary UHPC mixtures exhibited no cracking after approximately 2.5 years of outdoor exposure without mechanical loading regardless of the fiber content and overlay thickness. The use of 3.25% microfiber measuring 0.5 in. in length and overlay thicknesses of 1.5 and 2 in. were recommended for the rehabilitation of thin bonded bridge deck overlays. The incorporation of saturated LWS in the UHPC mixtures was shown to maintain IRH compared to the mixtures made without any LWS. The thickness of 1.5 in. UHPC overlay slabs made with 3.25% microfiber exhibited 95% and 270% higher flexural load and toughness, respectively, compared to the LMC overlay slabs.

ii. The LWS17 and LWS17 and SRA1 mixtures prepared with 0.5-in. long fiber were recommended for thin bonded overlays given their highest compressive strength and thixotropy and relatively low shrinkage. The content of 0.5% EUCON ABS, by mass of binder, was recommended to enhance thixotropy of UHPC without compromising the workability, mechanical properties, and shrinkage. A 7-d moist curing duration was recommended for field construction. The variation of w/cm by ±10% and sand moisture content by ±1% did not exhibit a significant influence on the performance of the LWS17 and SRA1 mixture. This included rheology, autogenous shrinkage, and compressive and flexural strengths.

iii. Provisional performance-based specifications were developed for non-proprietary thixotropic UHPC. These mixtures are prepared with using Type III Portland cement, Class C fly ash, undensified silica fume, concrete river sand, masonry sand, pre-saturated LWS, and straight micro steel fibers, as well as a polycarboxylate-based SP, EUCON thixotropic admixture, and ADA.

iv. A high-shear mixer is recommended to secure efficient dispersion and homogeneity. Specialized test methods and performance criteria for workability, mechanical properties, autogenous and drying shrinkage were recommended. A wax-based curing compound is recommended to be applied immediately after the end of placement, followed by wet curing using a wet burlap and plastic sheet for a minimum of 7 d.

v. Two mockup tests were conducted on concrete slabs measuring 3 × 6 ft for the lab mockup and 12 x 12 ft for the field mockup before field implementation to verify the constructability of the UHPC. The LWS17 and SRA1 mixture with 0.5-in. long fibers was selected for the first mockup test carried out at Missouri S&T using the proposed mixture, and high shear mixer. No sign of cracking of the overlay was observed after 6 months of outdoor exposure. The second mockup was carried out by the contractor using a 1-in. long twisted steel fiber that

was selected for field implementation. A lower slump flow of 6 in. after jolting was proposed to ensure successful casting and finishing for field work. The skid steer mixer necessitated prolonged mixing and led to excessive heat generation.

vi. The thin bonded overlay deck rehabilitation was carried out on Route Z and M Bridges over highway 70 in Missouri. The UHPC samples were taken from six locations on Route Z Bridge and two locations on Route M Bridge. The slump flow, air content, and variation of static yield stress with rest time met the performance specifications for the UHPC. However, the temperature of the fresh UHPC at the end of mixing ranged between 90 and 99 °F, which is higher than the specified value of 86 °F. Two sets of samples taken from the South bound lane of Route Z Bridge exhibited much higher compressive strengths of 14,470 and 18,030 psi at 7 and 28 d compared to strength values of 13,510, 15,070 psi from the North bound lane cast 2 days apart. All strength results were consistently lower than the minimum specified values of 17,400 and 18,700 psi at 7 and 28 d, respectively. The 7- and 28-d compressive strengths of samples taken from the North bound lane are 7% and 24% lower, respectively, than those from the South bound lane. The high variations of compressive strength between different UHPC samples taken from different batches from the Z Bridge can be attributed to the variation in moisture content of LWS.

vii. Field inspection was carried out after 7 and 96 d of construction on Route Z Bridge, and 81 d on Route M Bridge, respectively. No signs of cracking were observed on Route Z Bridge after 7 d. However, signs of cracking were observed after 96 d on the North bound lane of Route Z bridge while no cracking was observed on the South bound lane. The cracks observed on the North bound lane of Route Z Bridge represented 27% of the total bridge deck area and the crack widths ranged between 0.01 and 0.04 in. Cracks were observed for both lanes Route M Bridge after 81 d. The crack widths ranged between 0.005 and 0.040 in. with the total crack area being approximately 46% of the total bridge deck area for Route M Bridge. The crack development can be attributed to the decrease in ambient temperature and lack of proper moist curing.

viii. The performance-based specifications and recommendations developed initially were fine-tuned following the experience from the bridge overlay construction. Recommendations including using a maximum length of 0.5 in steel fibers and ensuring proper moist curing were made for future UHPC overlay construction.

References

Brühwiler, Eugen, Malena Bastien-Masse, Hartmut Mühlberg, Bernard Houriet, Blaise Fleury, Stéphane Cuennet, Philippe Schär, Frédéric Boudry, and Marco Maurer. 2015. "Strengthening the Chillon Viaducts Deck Slabs with Reinforced UHPFRC." In *IABSE Conference, Geneva 2015: Structural Engineering: Providing Solutions to Global Challenges - Report*, 1171–78. International Association for Bridge and Structural Engineering (IABSE). https://doi.org/10.2749/222137815818358457.

Engineering Center at Iowa State University, Bridge. 2018. "Use of Ultra-High-Performance Concrete for Bridge Deck Overlays Final Report Iowa Department of Transportation (InTrans Projects 16-573 and 16-574) Federal Highway Administration." www.intrans.iastate.edu.

Haber, Zachary B, and Benjamin Allen Graybeal. n.d. "Field Testing of an Ultra-High Performance Concrete Overlay." https://www.researchgate.net/publication/323971644.

Khayat, Kamal H, and P Eng. 2018. "Final Report Prepared for Missouri Department of Transportation Design and Performance of Cost-Effective Ultra High Performance Concrete for Bridge Deck Overlays." https://orcid.org/0000-0002-0739-0211.

Khayat, Kamal H, P Eng, Weina Meng, and Matthew Hopkins. 2018. "Final Report Prepared for Missouri Department of Transportation Use of Lightweight Sand for Internal Curing to Improve Performance of Concrete Infrastructure." https://orcid.org/0000-0002-0739-0211.

Liu, Jun, Yao Li, Yuanquan Yang, and Yunpeng Cui. 2014. "Effect of Low Temperature on Hydration Performance of the Complex Binder of Silica Fume-Portland Cement." *Journal Wuhan University of Technology, Materials Science Edition* 29 (1): 75–81. https://doi.org/10.1007/s11595-014-0870-2.

Meng, Weina, Mahdi Valipour, and Kamal Henri Khayat. 2017. "Optimization and Performance of Cost-Effective Ultra-High Performance Concrete." *Materials and Structures/Materiaux et Constructions* 50 (1): 1–16. https://doi.org/10.1617/s11527-016-0896-3.

Omran, Ahmed F, Siwar Naji, and Kamal H Khayat. 2009. "Portable Vane Test to Assess Structural Buildup at Rest of Self-Consolidating Concrete."

Sritharan, Sri, Gaston Doiron, Dean Bierwagen, Brian Keierleber, and Ahmad Abu-Hawash. 2018. "First Application of UHPC Bridge Deck Overlay in North America." *Transportation Research Record* 2672 (26): 40–47. https://doi.org/10.1177/0361198118755665.

Teng, Le, and Kamal H. Khayat. 2022. "Effect of Overlay Thickness, Fiber Volume, and Shrinkage Mitigation on Flexural Behavior of Thin Bonded Ultra-High-Performance Concrete Overlay Slab." *Cement and Concrete Composites* 134 (November). https://doi.org/10.1016/j.cemconcomp.2022.104752.

"Ultra-High Performance Concrete for Bridge Deck Overlays." n.d. www.fhwa.dot.gov/research.

Valipour, Mahdi, and Kamal H. Khayat. 2020. “Robustness of Ultra-High-Performance Concrete to Changes in Material Temperature.” *ACI Materials Journal* 117 (4): 47–56. https://doi.org/10.14359/51724613.

Wibowo, Hartanto, and Sri Sritharan. 2018. *Use of Ultra-High-Performance Concrete for Bridge Deck Overlays*.